

*Digital Comprehensive Summaries of Uppsala Dissertations
from the Faculty of Science and Technology 2650*

Exploring phosphonic acids for metallo- β -lactamase inhibition

*In search of new strategies to fight antibiotic
resistance*

KINGA VIRÁG GULYÁS



ACTA UNIVERSITATIS
UPSALIENSIS
2026



UPPSALA
UNIVERSITET

Dissertation presented at Uppsala University to be publicly examined in BMC A1:11 1a, Husargatan 3, Uppsala, Friday, 8 May 2026 at 08:30 for the degree of Doctor of Philosophy. The examination will be conducted in English. Faculty examiner: Professor Fredrik Almqvist (Department of Chemistry and Department of Clinical Microbiology, Umeå universitet).

Abstract

Gulyás, K. V. 2026. Exploring phosphonic acids for metallo- β -lactamase inhibition. *In search of new strategies to fight antibiotic resistance. Digital Comprehensive Summaries of Uppsala Dissertations from the Faculty of Science and Technology* 2650. 116 pp. Uppsala: Acta Universitatis Upsaliensis. ISBN 978-91-513-2777-8.

The Global Antibiotic Research & Development Partnership (GARDP) estimates that antibiotic resistance claims one life in every 6 seconds. It is currently associated with 5 million deaths annually, a number that continues to rise. A major challenge in combating antibiotic resistance is the emergence of metallo- β -lactamase enzymes that degrade our most used antibiotics, the β -lactams. Combination therapy, which involves administering an enzyme inhibitor alongside an existing β -lactam antibiotic, presents a viable strategy to address this issue. However, no metallo- β -lactamase inhibitors are currently available on the market, underscoring the urgent need for their development.

This work describes the development of new phosphonic acid-based metallo- β -lactamase inhibitors and studies their binding to the target metallo- β -lactamase enzymes. Phosphorous-containing molecules are promising inhibitor candidates, which act as transition state analogues that bind to the zinc ions essential for the metallo- β -lactamase activity. The synthesis and bioactivities of three sets of phosphonic acid-type inhibitors are described. These compounds proved to be active on purified metallo- β -lactamases (micromolar to nanomolar IC_{50}) as well as on living bacteria, they were Gram-negative membrane permeable and not cytotoxic to human cells. Their binding event was evaluated by solution NMR spectroscopy, X-ray crystallography, molecular docking and molecular dynamics studies. The key interaction between the phosphonic acid core and the enzymes' zinc ions was determined. These findings are expected to contribute to the development of clinically applicable metallo- β -lactamase inhibitors.

Keywords: antibiotic resistance, phosphonic acids, metallo- β -lactamase inhibitors, NMR binding studies

Kinga Virág Gulyás, Department of Chemistry for Life Sciences, Organic Chemistry, Box 576, Uppsala University, SE-75123 Uppsala, Sweden.

© Kinga Virág Gulyás 2026

ISSN 1651-6214

ISBN 978-91-513-2777-8

URN urn:nbn:se:uu:diva-582535 (<http://urn.kb.se/resolve?urn=urn:nbn:se:uu:diva-582535>)

*“Akár azt hiszed, képes vagy rá,
akár azt, hogy nem, igazad lesz.”*

*“Whether you believe you can do
a thing or not, you are right.”*

- Henry Ford

List of Papers

This thesis is based on the following papers, which are referred to in the text by their Roman numerals.

- I. Gulyás, K. V., Zhou, L., Salamonsen, D., Prester, A., Bartels, K., Bosman, R., Haffke, P., Tamási, V., Thoma, J., Andersson Rasmussen, A., Csala, M., Schroder Leiros, H.-K., Xu, Z., Rohde, H., Schulz, E. C., Zhu, W., Erdélyi, M. (2024) Dynamically chiral phosphonic acid-type metallo- β -lactamase inhibitors. *Commun. Chem.*, 8:119.
- II. Gulyás, K. V., Li, B., Bartels, K., Kaur, G., Thoma, J., Palczert, Z., Tamási, V., Tapia, K. C., Andersson Rasmussen, A., Kräutle, R. V., Simon, M., Adorján, Á., Csala, M., Schofield, C. J., Zhu, W., Schulz, E. C. and Erdélyi, M. Phosphonic acid inhibitors of metallo- β -lactamases. *Manuscript*.
- III. Gulyás, K. V., Bartels, K., Kaur, G., Thoma, J., Palczert, Z., Tamási, V., Tapia, K. C., Andersson Rasmussen, A., Simon, M., Csala, M., Schofield, C. J., Schulz, E. C. and Erdélyi, M. Discovery of an α -aminophosphonic acid VIM-2 inhibitor. *Manuscript*.
- IV. Gulyás, K. V., Jansa V., Bartels, K., Thoma, J., Palczert, Z., Tamási, V., Andersson Rasmussen, A., Csala, M., Fröhlich, C., Schulz, E. C. and Erdélyi, M. Exploring α -aminophosphonic acids for metallo- β -lactamase inhibition. *Manuscript*.

Reprints were made with permission from the respective publishers.

Parts of this thesis are based on and have been previously published as the author's licentiate thesis entitled "Development of novel phosphonic acid-type metallo- β -lactamase inhibitors" (Uppsala University, 2024).

Contributions

Contribution from the author to the listed papers.

- I. Synthesis, purification, analysis and characterization of all compounds, NMR titration experiments and data analysis, competitive inhibition assays, ADME property prediction and analysis, contribution to the protein expression and purification and to the docking simulations, writing of the first version of the manuscript and SI and contribution to its improvements.
- II. Design and conceptualization of the project, design of the synthesis and purification of the pyridine-containing compounds, analysis and characterization of the intermediates and final pyridine-compounds. Supervision of Erasmus student Rebekka Kräutle and master thesis student Máté Simon who carried out the synthesis and purification of the pyridine-containing compounds. Contribution to the design and synthesis of the thiazole and carboxylic acid-containing compounds, and supervision of master thesis student Áron Adorján who initially started the thiazole synthesis. ADME property prediction and analysis, NMR titration studies and data analysis, contribution to the protein expression and purification of the protein used for NMR titration, writing of the first version the manuscript and SI and contribution to its improvements.
- III. Design and conceptualization of the project, design of the synthesis and purification of the compounds, supervision of master thesis student Máté Simon who carried out the synthesis and purification of the pyridine-containing compound, synthesis and purification of the other compounds, analysis and characterization of all the compounds, NMR binding studies and data analysis, ADME property prediction and analysis, contribution to the protein expression and purification of the protein used for NMR titration, writing of the first version the manuscript and SI and contribution to its improvements.

- IV. Design and conceptualization of the project, design of the synthesis and purification of the intermediates and final compounds, carried out of the synthesis and purification of the final compounds and the starting material, analysis and characterization of all the intermediates and final compounds, NMR titration experiments and data analysis, contribution to the protein expression and purification of the protein used for NMR titration, ADME property prediction and analysis, IC_{50} and MIC measurements, GIM-1 NMR backbone assignment, supervision of Erasmus student Vojtech Jansa, who carried out the synthesis of the intermediates. Writing of the first version the manuscript and SI and contribution to its improvements.

The following papers are not included in the thesis.

Zhang, J., Gulyás, K. V., Li, J., Ma, M., Zhou, L., Wu, L., Xiong, R., Erdélyi, M., Zhu, W., Xu, Z. (2024) Unexpected effect of halogenation on the water solubility of small organic compounds. *Comput. Biol. Med.*, 108209.

Salamonsen, D., Buda, K., Wang, D., Gulyás, K. V., van de Kamp, M. W., Fröhlich, C. (2026) Mechanistic origins and evolutionary erosion of collateral sensitivity in a β -lactamase. *Submitted*.

This thesis was written by the author alone and without content generation using generative artificial intelligence (AI) tools.

Contents

| | |
|---|----|
| 1. Introduction..... | 15 |
| 1.1 The multidisciplinary problem of antibiotic resistance | 17 |
| 1.2 β -Lactam antibiotics | 18 |
| 1.3 β -Lactamase enzymes and their resistance mechanism | 22 |
| 1.4 β -Lactamase inhibitors..... | 27 |
| 1.5 The scientific gap: Metallo- β -lactamase inhibitors | 27 |
| 1.6 The advantage of phosphonic acids for metallo- β -lactamase inhibition..... | 29 |
| 1.7 Aim of the thesis..... | 31 |
| 2. Outline of experimental methods..... | 32 |
| 2.1 Activity measurements | 32 |
| 2.2 NMR titration | 34 |
| 2.3 Protein expression and purification | 36 |
| 2.4 Molecular docking simulations..... | 37 |
| 2.5 ADME predictions and drug-likeness..... | 39 |
| 3. Dynamically chiral phosphonic acids as broad-spectrum inhibitors (Paper I) | 41 |
| 3.1 Design of dynamically chiral phosphonic acid inhibitors..... | 41 |
| 3.2 Synthesis of phosphonic acids | 42 |
| 3.3 Assessment of the phosphonic acids as metallo- β -lactamase inhibitors | 44 |
| 3.4 Phosphonic acid inhibitors with favourable ADME properties | 49 |
| 4. The effect of structural modifications on inhibitory activity (Paper II and III) | 51 |
| 4.1 Design of the new core scaffolds..... | 51 |
| 4.2 Synthesis of the pyridinyl compounds..... | 53 |
| 4.3 Evaluation of the impact of core-changes on bioactivity..... | 55 |
| 4.4 ADME predictions..... | 61 |

| | |
|--|----|
| 5. α -Aminophosphonic acids for improved inhibitory potency (Paper IV)..... | 64 |
| 5.1 Design and predicted properties of α -aminophosphonic acids | 64 |
| 5.2 α -Aminophosphonic acid synthesis | 66 |
| 5.3 Inhibition of VIM-2 and GIM-1 | 68 |
| 5.4 NMR backbone resonance assignment of German- imipenemase 1 | 72 |
| 6. Peptidic phosphonic acids for IMP-1 inhibition | 76 |
| 6.1 Design introducing natural amino acids | 76 |
| 6.2 Docking simulations | 77 |
| 6.3 Synthesis of the peptidic inhibitors..... | 80 |
| 6.4 Enzyme inhibitory activities | 81 |
| 6.5 ADME property predictions | 82 |
| 7. Halogenated arylphosphonic acids inhibit VIM-2 | 84 |
| 7.1 Design of the inhibitors | 84 |
| 7.2 Microwave synthesis | 84 |
| 7.3 Activity and binding studies | 87 |
| 8. Concluding remarks | 91 |
| 9. Sammanfattning på svenska..... | 93 |
| 10. Acknowledgement | 95 |
| 11. References..... | 98 |

Abbreviations

| | |
|----------------|---|
| μ W | Microwave |
| ADME/T | Absorption, distribution, metabolism, excretion, toxicity |
| Ala/A | Alanine |
| Arg/R | Arginine |
| Asn/N | Asparagine |
| Asp/D | Aspartic acid |
| BBB | Blood-brain barrier |
| Boc | <i>Tert</i> -butoxycarbonyl |
| CC_{50} | 50 % cytotoxic concentration |
| CphA | Carbapenemase from <i>Aeromonas</i> |
| CSP | Chemical shift perturbation |
| Cys/C | Cysteine |
| DCM | Dichloromethane |
| DIPEA | <i>N,N</i> -diisopropylethylamine |
| DMF | Dimethylformamide |
| DNA | Deoxyribonucleic acid |
| DS | Docking score |
| <i>E. coli</i> | <i>Escherichia coli</i> |
| EDTA | Ethylenediaminetetraacetic acid |
| EtOAc | Ethyl acetate |
| EtOH | Ethanol |
| Fmoc | Fluorenylmethoxycarbonyl |
| GARDP | Global antibiotic research & development partnership |
| GI | Gastrointestinal |
| GIM | German-imipenemase |
| Gln/Q | Glutamine |
| Glu/E | Glutamic acid |
| Gly/G | Glycine |
| HATU | Hexafluorophosphate azabenzotriazole tetramethyl uronium |
| HBA | Hydrogen bond acceptor |
| HBD | Hydrogen bond donor |
| HEPES | 4-(2-Hydroxyethyl)-1-piperazineethanesulfonic acid |
| HepG2 | Human hepatocellular carcinoma G2 |

| | |
|-------------------------|---|
| HFIP | Hexafluoroisopropanol |
| HIA | Human intestinal absorption |
| His/H | Histidine |
| HPLC | High performance liquid chromatography |
| HSQC | Heteronuclear single quantum coherence |
| <i>IC</i> ₅₀ | Half-maximal inhibitory concentration |
| Ile/I | Isoleucine |
| IMAC | Immobilized metal affinity chromatography |
| IMP | Imipenemase |
| IPTG | Isopropyl thiogalactoside |
| LC-MS | Liquid chromatography–mass spectrometry |
| LE | Ligand efficiency |
| Leu/L | Leucine |
| LogP | Logarithm of the water-octanol partition coefficient |
| Lys/K | Lysine |
| MBL | Metallo-β-lactamase |
| MBLI | Metallo-β-lactamase inhibitor |
| MDCK | Madin-Darby canine kidney |
| mRNA | Messenger ribonucleic acid |
| MW | Molecular weight |
| NBS | N-bromosuccinimide |
| NCS | N-chlorosuccinimide |
| NDM | New-Delhi metallo-β-lactamase |
| NMR | Nuclear magnetic resonance |
| Nr. | Number |
| OD ₆₀₀ | Optical density at 600 nm |
| OMV | Outer membrane vesicle |
| PBP | Penicillin binding protein |
| PDB | Protein data bank |
| Pd/C | Palladium on carbon |
| Pgp | P-glycoprotein 1 |
| Phe/F | Phenylalanine |
| PPB | Plasma protein binding |
| Ro5 | Rule of five |
| RP | Reversed-phase |
| SBL | Serine-β-lactamase |
| SBLI | Serine-β-lactamase inhibitor |
| SDS-PAGE | Sodium dodecyl-sulfate polyacrylamide gel electrophoresis |
| Ser/S | Serine |
| SI | Selectivity index |

| | |
|-------|---|
| SP | Standard precision |
| TEV | Tobacco etch virus |
| THF | Tetrahydrofuran |
| Thr/T | Threonine |
| TMS | Tetramethylsilane |
| TPSA | Topological polar surface area |
| Tris | Tris(hydroxymethyl)aminomethane |
| Trp/W | Tryptophan |
| Trt | Trityl/triphenylmethyl |
| Tyr/Y | Tyrosine |
| Val/V | Valine |
| VIM | Verona-integron encoded/borne metallo- β -lactamase |
| WHO | World health organization |

1. Introduction

The aim of this work is to develop and evaluate new metallo- β -lactamase inhibitors to contribute to the fight against the increasing global challenge of antibiotic resistance.

Antibiotics have been fundamental for modern medicine, providing treatment for bacterial infections and saving countless lives since their discovery.¹ Our healthcare system highly relies on antibiotics from basic medical procedures to modern cancer treatments (**Figure 1.1**).^{2,3} Without effective antibiotics e.g. a simple wound infection, which is easily treatable for more than 80 years, could be deadly again as it was in the pre-antibiotic era.

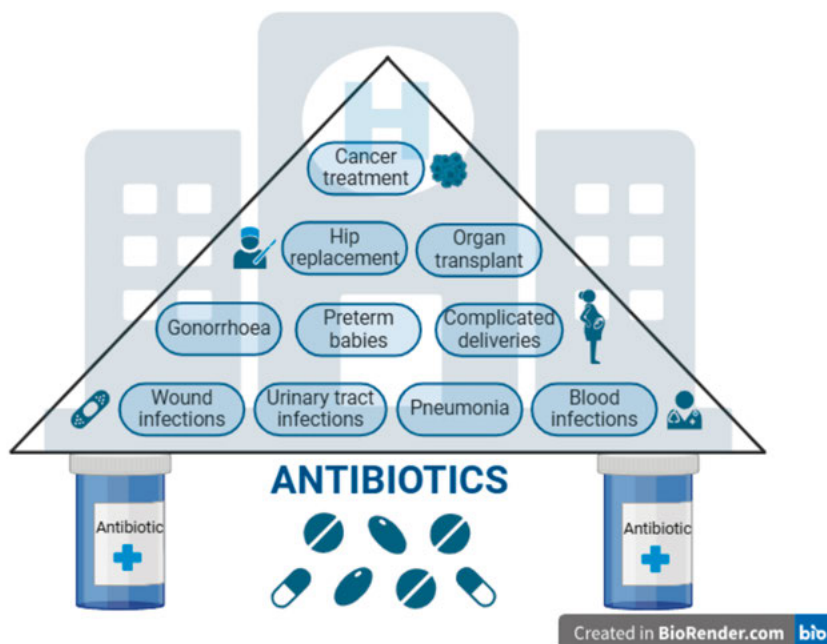


Figure 1.1. Effective antibiotics are the basis for a working healthcare system.² Created with BioRender.com.

The emergence of antibiotic resistance poses a significant threat to public health⁴, as bacteria evolve mechanisms to evade the effects of these life-saving

drugs.⁵ It was estimated that antibiotic-resistant infections were directly related to 700,000 - 1.27 million deaths in 2019.^{4,6,7} If current trends continue, this number could rise up to 10 million per year by 2050, which reaches the number of deaths caused by cancer (**Figure 1.2**).^{4,6,7} One especially challenging resistance mechanism involves metallo- β -lactamases (MBLs), enzymes that degrade β -lactam antibiotics, rendering them ineffective.⁸⁻¹⁰ They are able to dismantle even our last-resort carbapenems, which leaves us very limited options to treat difficult infections, often including agents with serious side effects like e.g. nephrotoxicity, neurotoxicity or anaphylaxis.¹¹⁻¹⁵ Metallo- β -lactamases endanger the application of our most commonly prescribed and worldwide used β -lactam antibiotics.¹⁶

β -Lactams are one of the most important group of antibiotics due to their broad spectrum activity against a wide range of bacterial infections combined with relatively low toxicity.¹⁷ They are extensively used in clinical settings worldwide and it is crucial to preserve them for future generations. To counter the problem caused by metallo- β -lactamases, the development of metallo- β -lactamase inhibitors (MBLIs) offers a viable strategy for restoring the efficacy of β -lactam antibiotics.¹⁸⁻²⁰

Despite the urgent need, the development of new antibiotics and inhibitors is not an attractive venture for pharmaceutical companies, primarily due to high costs and low financial returns.²¹⁻²³

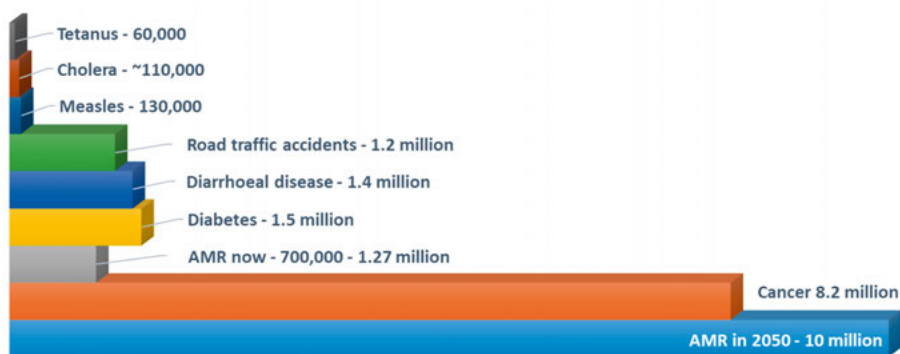


Figure 1.2. Number of deaths attributed to antimicrobial resistance is estimated to exceed the number of deaths caused by cancer by 2050.^{6,7}

1.1 The multidisciplinary problem of antibiotic resistance

Antibiotic resistance is a complex, multidisciplinary problem that poses a severe threat to global health and requires coordinated efforts across various fields to be addressed effectively. It does not only affect healthcare, but also animal care, food production, and economics.^{24,25} Antibiotic resistance is a significant financial burden, costing the global healthcare system an estimated \$20 billion in direct costs annually, with additional costs of \$35 billion due to lost productivity.²⁶ Antibiotic resistant infections are difficult to treat, leading to longer hospital stays, extended intensive care, the need for more complex treatment and higher mortality rates.^{4,27-32} It causes productivity loss due to prolonged sickness and absence from work.^{33,34} Many modern medical procedures, such as surgeries, chemotherapy, and organ transplantations rely on effective antibiotics to prevent and treat infections and lower the risks of severe complications.^{4,35} Antibiotic resistance jeopardizes the safety and success of these procedures.³⁶ Without effective antibiotics, common infections and minor injuries can become life-threatening again.

It may seem like antibiotic resistance is not a major problem for developed countries. Currently, the burden of antibiotic resistance disproportionately affects low- and middle-income countries, where access to healthcare and antibiotics is limited.^{37,38} However, antibiotic resistance does not recognize borders. Resistant bacteria can quickly spread between individuals, communities, and countries through international travelling and trading, making it a global health issue.^{4,39,40}

The rise of resistant bacteria is driven by factors such as overuse and misuse of antibiotics in human medicine and agriculture, insufficient infection control measures, and inadequate sanitation practices.^{3,4,41,42} While resistance occurs naturally and cannot be completely eliminated,^{43,44} it is important to realize the need for more rational use of antibiotics to avoid the resistance acceleration. Immediate action is necessary to prevent the next major global health crisis of the modern era.

Currently, the pipeline for new antibiotics is limited, and resistance is outpacing the development of new drugs.^{21,45} This means that fewer treatment options are available for resistant infections and that we increasingly rely on last-resort antibiotics. The overuse and misuse of antibiotics accelerated the development of resistance, which lead to the need for new types of antibiotics, that might have more severe side effects and might be less accessible.^{46,47} Research estimates that already 5.7 million people die every year due to lack of access to effective antimicrobials.⁴⁸ Antibiotic resistance is a significant prob-

lem across various classes of antibiotics, but the most pressing issues are observed for β -lactams, which account for more than 65 % of all antibiotic prescriptions and are available even in low- and middle-income countries.^{18,49,50}

1.2 β -Lactam antibiotics

There are 12 main classes of antibiotics, the β -lactams, the sulfonamides, the aminoglycosides, the tetracyclines, chloramphenicol, the macrolides, the glycopeptides, the ansamycins, the quinolones, the streptogramins, the oxazolidinones and the lipopeptides, all having been discovered around the 1930's - 1990's (**Figure 1.3**).⁵¹⁻⁵³ Although, there were some new discoveries since,^{51,54} they still remain our main antibiotic arsenal. They operate through various mechanisms to target and kill bacteria or inhibit their growth.^{17,55,56}

β -Lactam antibiotics inhibit cell wall synthesis by binding to penicillin-binding proteins (PBPs), preventing the cross-linking of peptidoglycan chains, which are crucial for bacterial cell wall integrity. Glycopeptide antibiotics, as vancomycin, also disrupt cell wall synthesis but by binding directly to the peptidoglycan precursors. Macrolides (such as erythromycin), tetracyclines (e.g. doxycycline), chloramphenicol and oxazolidinones all inhibit protein synthesis by binding to bacterial ribosomes, preventing the translation of essential proteins. Aminoglycosides, such as gentamicin, also interfere with protein synthesis by causing misreading of mRNA. Fluoroquinolones, including ciprofloxacin, target bacterial DNA gyrase and topoisomerase IV, enzymes essential for DNA replication and transcription. Lastly, lipopeptides as the polymyxins bind to the bacterial cell membrane and disrupt its integrity.

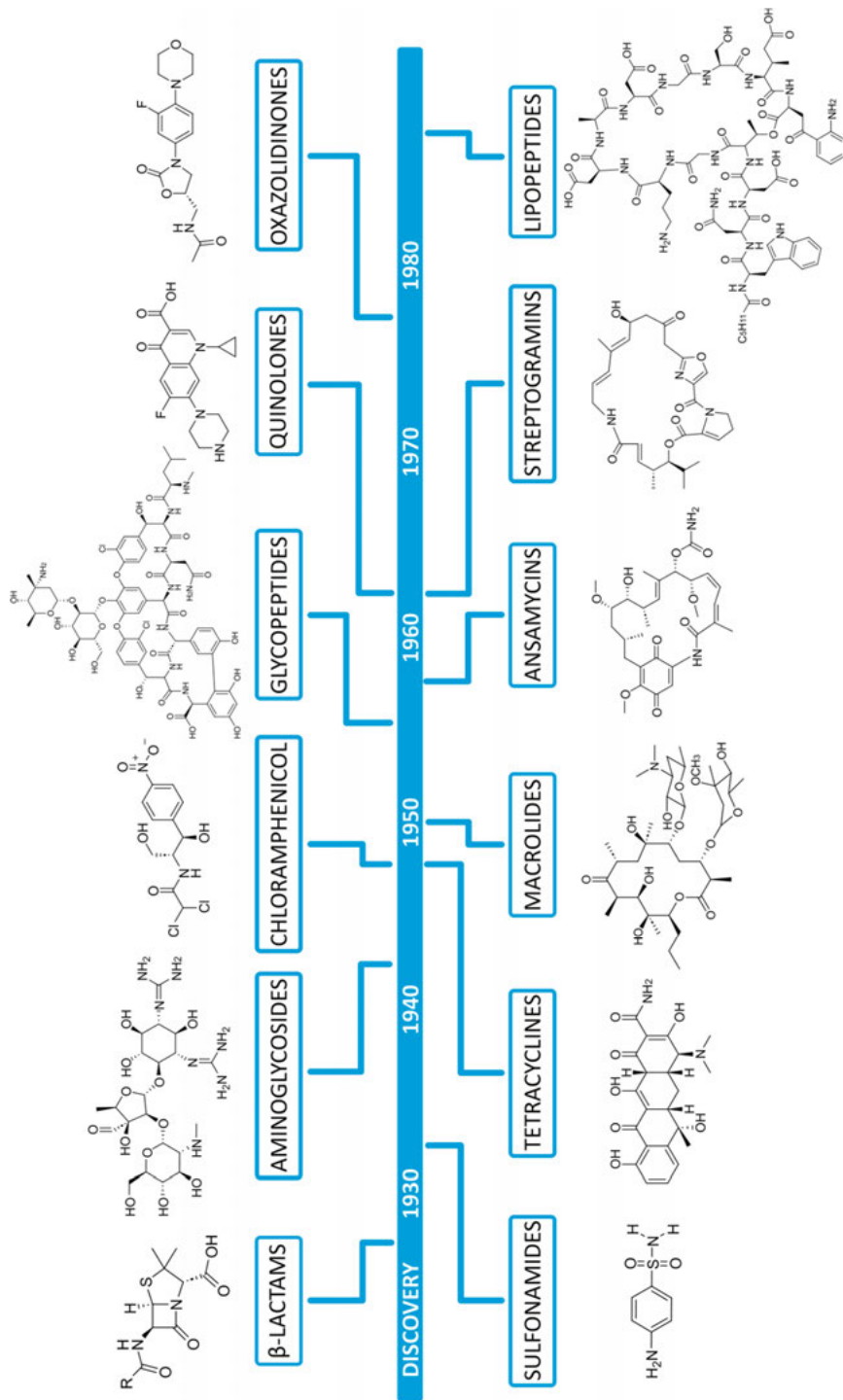


Figure 1.3. The 12 main antibiotic classes.⁵¹⁻⁵³

The first discovered β -lactams became a very successful class, as they are still the most prescribed antibiotics worldwide, they are cheap and also available in low- and middle income countries, and nevertheless they have very few side effects.^{17,57} They also have a broad spectrum of antibacterial activity,^{58,59} including both Gram-positive and Gram-negative pathogens such as *Staphylococcus aureus*, *Streptococcus pneumoniae*, *Escherichia coli*, and *Pseudomonas aeruginosa*.⁵⁶ Their importance is highlighted by the World Health Organization (WHO) that published the Model List of Essential Medicines, where half of the key access antibiotics come only from the β -lactam group (**Table 1.1**).⁶⁰

Table 1.1. Essential antibiotics according to the WHO Model List of Essential Medicines.⁶⁰

| β -LACTAM MEDICINES | | OTHER ANTIMICROBIALS | |
|-------------------------------|----------------------------|----------------------|---------------------------------|
| amoxicillin | cefalexin | amikacin | metronidazole |
| amoxicillin + clavulanic acid | cefazolin | chloramphenicol | nitrofurantoin |
| ampicillin | cloxacillin | clindamycin | spectinomycin |
| benzathine benzylpenicillin | phenoxymethylpenicillin | doxycycline | sulfamethoxazole + trimethoprim |
| benzylpenicillin | procaine benzyl penicillin | gentamicin | trimethoprim |

Antibiotic resistance is endangering this important class of medicines as well. The WHO Bacterial Priority Pathogens List displays the pathogens that pose the greatest threat to human health. On this list, in total 8 out of the 13 bacterial families, and all from the critical group are resistant to β -lactam antibiotics (**Table 1.2**).⁶¹ This highlights the importance of this class of antibiotics and demonstrates why the resistance problem against β -lactams needs to be addressed.

Table 1.2. The WHO Bacterial Priority Pathogens List.⁵⁴ The β -lactam resistant pathogens are highlighted in blue.

| Priority 1: CRITICAL | Priority 2: HIGH | Priority 3: MEDIUM |
|--|--|---|
| <i>Acinetobacter baumannii</i> , carbapenem-resistant | <i>Salmonella Typhi</i> , fluoroquinolone-resistant | Group A <i>Streptococci</i> , macrolide-resistant |
| <i>Enterobacterales</i> , 3 rd generation cephalosporin-resistant | <i>Shigella spp.</i> , fluoroquinolone-resistant | <i>Streptococcus pneumoniae</i> , macrolide-resistant |
| <i>Enterobacterales</i> , carbapenem-resistant | <i>Enterococcus faecium</i> , vancomycin-resistant | <i>Haemophilus influenzae</i> , ampicillin-resistant |
| | <i>Pseudomonas aeruginosa</i> , carbapenem-resistant | Group B <i>Streptococci</i> , penicillin-resistant |
| | <i>Non-typhoidal salmonella</i> , fluoroquinolone-resistant | |
| | <i>Neisseria gonorrhoeae</i> , 3 rd generation cephalosporin-resistant, fluoroquinolone-resistant | |
| | <i>Staphylococcus aureus</i> , methicillin-resistant | |

The β -lactam class consists of hundreds of molecules, all having the four-membered β -lactam ring as a key element in the structure, which is essential for their activity (**Figure 1.4**).^{16,18,62} Their history started in 1928 when Sir Alexander Fleming discovered penicillin, which shortly became a life-saving medicine.⁶³ It was called the miracle drug during the second World War and is estimated to have saved over 200 millions of lives up to date.⁶⁴ Researchers repeatedly modified the original structure to improve efficacy, ADME properties or toxicity, which lead to the subclasses of penams/penicillins, oxa- and carbapenams, penems, oxa- and carbapenems, cepheems/cephalosporins, oxa- and carbacephems and monobactams.^{18,62,64} Important to note that carbapenems are considered as last-resort drugs that should be saved for difficult to treat, life threatening infections caused by multidrug-resistant bacteria, where no other treatment options are effective.⁶⁵⁻⁶⁸ Unfortunately, resistance exists against all β -lactam subclasses.^{67,69}

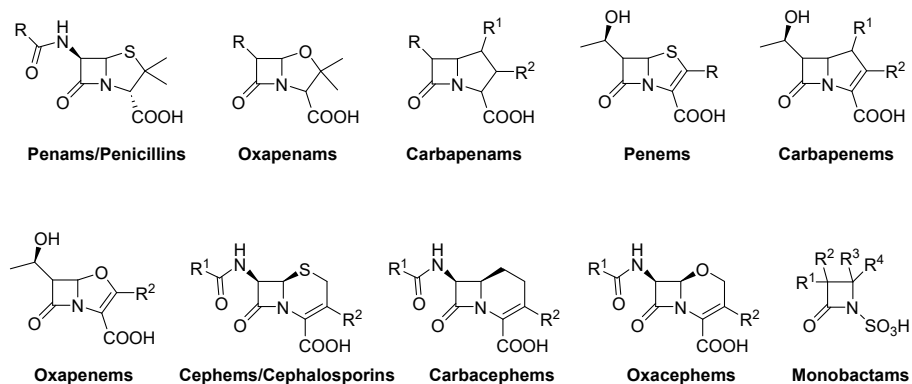


Figure 1.4. The subclasses of the β -lactam antibiotics.^{16,55,57} Their key structural element, the four-membered β -lactam ring is highlighted with blue.

β -Lactams target and disrupt bacterial cell wall synthesis, which is crucial for bacterial survival and proliferation. They mimic the D-Ala-D-Ala motif so they are recognised as substrates and bind to penicillin-binding proteins (PBPs), which belong to the group of transpeptidase enzymes. The β -lactams are covalent inhibitors of PBPs that form an acyl-enzyme complex with the enzyme's active site serine. The enzyme therewith becomes sterically blocked, which prevents the cross-linking of peptidoglycan chains, weakening the cell wall and leading to cell lysis and death.^{16,62}

1.3 β -Lactamase enzymes and their resistance mechanism

In response to the use of β -lactam antibiotics, bacteria have evolved defence mechanisms to resist the lethal effects of these drugs (**Figure 1.5**).⁷⁰ This includes the alteration of PBPs, so β -lactams cannot bind to them anymore. Bacteria also developed efflux pumps that can expel β -lactam antibiotics from the cell, decreasing the intracellular concentration of the drug. Another way bacteria defend themselves is by reducing the cell membrane permeability, which results in decreased uptake of β -lactam antibiotics. However, by far the most widely spread and clinically most important way of defence is the production of β -lactamase enzymes, which are able to hydrolyse the β -lactam ring, rendering the antibiotic ineffective.^{62,71-73}

Resistance Mechanisms to β -lactam antibiotics

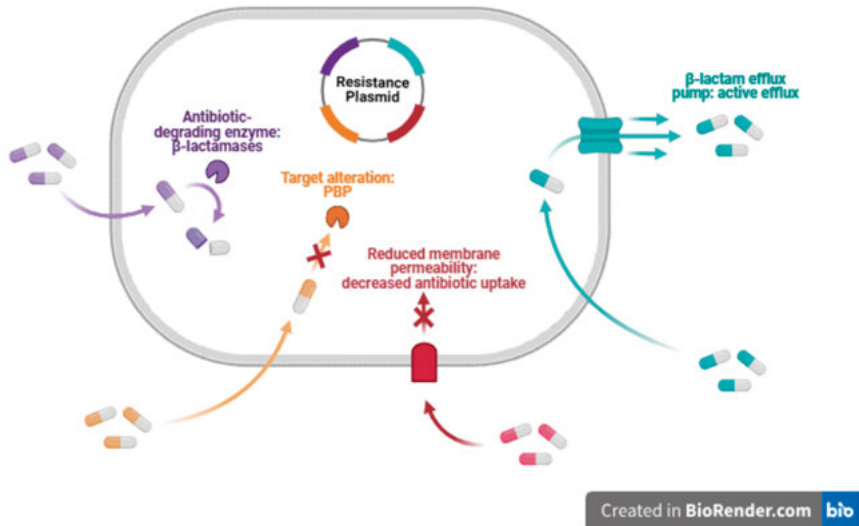


Figure 1.5. The most common resistance mechanisms against β -lactam antibiotics.⁷⁰ Created with BioRender.com.

Different types of β -lactamase enzymes can degrade various β -lactam antibiotics. The two main types of β -lactamases are the serine- and the metallo- β -lactamases that differ in their mechanism of hydrolysing the β -lactam ring. The most commonly used Ambler classification categorizes these enzymes based on their amino acid sequences and structural mechanisms into four main classes (A, B, C and D).^{74,75} Class A, C, and D enzymes are serine- β -lactamases (SBLs) that use a serine residue in their active site to perform the hydrolysis, while class B β -lactamases are known as metallo- β -lactamases (MBLs) that require zinc ion(s) for their catalytic activity.^{74,76-78}

Hydrolysis by SBLs begins with the enzyme binding to the antibiotic's β -lactam ring. The serine hydroxy group attacks the carbonyl carbon of the β -lactam ring, forming a covalent acyl-enzyme intermediate and breaking the β -lactam ring open. This reaction deactivates the antibiotic, rendering it unable to inhibit the penicillin-binding proteins essential for bacterial cell wall synthesis. The acyl-enzyme intermediate is then hydrolysed, releasing the inactivated antibiotic and regenerating the active enzyme for further catalytic cycles.^{73,76-78} This process relies on one or two zinc ions and a coordinating water molecule in the case of metallo- β -lactamases (**Figure 1.6**).⁷⁴ First, the zinc ions coordinate with the β -lactam ring. This coordination activates a water molecule, facilitating its nucleophilic attack on the carbonyl carbon of the

β -lactam ring. The water molecule hydrolyses the ring, again breaking it open and inactivating the antibiotic.^{66,76-78}

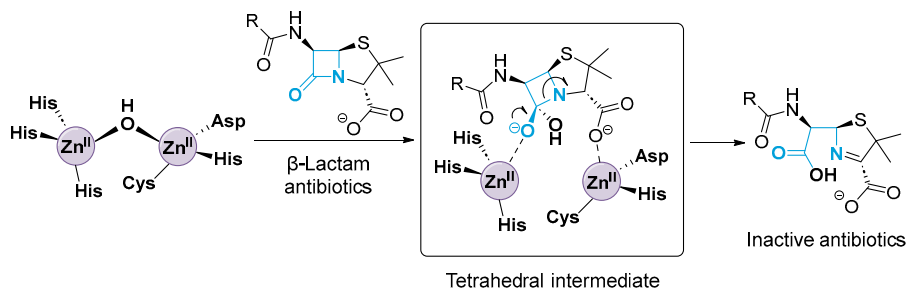


Figure 1.6. The proposed general β -lactam antibiotic hydrolysis mechanism by metallo- β -lactamases on the example of a penicillin.^{59,69-71}

The MBLs are divided into subclasses B1, B2, and B3, each with distinct characteristics.^{16,62,79-81} Subclass B1 MBLs, such as Imipenemases (IMP), Verona-integron-encoded enzymes (VIM), and New-Delhi metallo- β -lactamases (NDM), are the most widespread and clinically most relevant. They typically require two zinc ions for full activity.^{82,83} They exhibit broad-spectrum activity against almost all classes of β -lactams, including penicillins, cephalosporins, and carbapenems, but not monobactams.⁸⁴ It was found that the sulfonate group of monobactams replace the bridging catalytic water between the two active site zinc ions which is essential for the nucleophilic attack on the β -lactam carbonyl carbon of the antibiotic.^{16,85} Subclass B2 MBLs, such as carbapenemase from *Aeromonas* (CphA), primarily target carbapenems and are unique in that they require only one zinc ion for activity.⁷⁴ Subclass B3 MBLs, like the L1 enzyme, also utilize two zinc ions and have a broad substrate profile similar to B1 enzymes, however this class is less clinically relevant.^{74,86}

My work targets enzymes belonging to the B1 subclass, namely Verona integron-encoded metallo- β -lactamase 1 and 2 (VIM-1/VIM-2), New Delhi metallo- β -lactamase 1 (NDM-1), Imipenemase 1 and 26 (IMP-1/IMP-26) and German-imipenemase 1 (GIM-1) (**Figure 1.7**). Rapid evolution of mutants is characteristic to these enzymes,⁸⁷ currently (22 December, 2025) there are 1026 metallo- β -lactamases, from which 688 are members of the B1 subfamily.⁸⁸ VIM-2, NDM-1 and IMP-1 are the clinically most relevant enzymes of all MBLs and they present a particular challenge in clinical settings not only in low- and middle income countries but also in developed countries.^{9,89}

IMP-1 is one the earliest discovered B1 MBL, but still has the least number of developed inhibitors. It is most widespread in Asia-Pacific region in *Pseudomonas aeruginosa* but rapidly spreads to different Gram-negative species

due to horizontal gene transfer and quickly appeared in Europe as well.⁹⁰⁻⁹² IMP-1 is among the most challenging clinically relevant MBLs to inhibit, owing to narrower and slightly more rigid active site and distinct zinc coordination environment.^{58,93-95} Of the bicyclic boronates, the most successful MBLs, only xeruborbactam has been reported to show activity against IMP-type enzymes, while taniborbactam is ineffective.⁹⁴ IMP-26 is an emerging variant, increasingly detected in clinical isolates, reported mainly in East-Asia (China and Japan). Due to a single amino acid mutation of Val67Phe, IMP-26 already shows 10-fold lower sensitivity to xeruborbactam compared to IMP-1.^{94,96} They contribute to high carbapenem resistance in Asia.⁹⁰⁻⁹²

VIM-2 was first reported in 1996 and is now a widespread enzyme found in various Gram-negative bacteria, particularly *Pseudomonas aeruginosa* and *Enterobacteriaceae*.⁹⁷⁻⁹⁹ It is one of the most studied and characterized and the globally most prevalent member of the B1 family. VIM-1 is closely related to VIM-2, having high structural similarity (93 %).^{97,100,101} VIM-1 was the first VIM-type enzyme detected in clinical isolates and is more common in Southern Europe e.g. Italy.^{100,101} Amino acid mutations in loop-10 of VIM-1 and VIM-2 have been reported to lead to functional significance. VIM-2, for example, has higher affinity for carbapenems and some penicillins (e.g. benzylpenicillin, ampicillin, piperacillin), generally lower hydrolytic efficiency for cephalosporins (e.g. cefepime) except for e.g. nitrocefim¹⁰⁰ and is much more successful in resistance development. VIM-2 is easier to be inactivated by chelators indicating more loosely bound zinc ions compared to VIM-1.

NDM-1 appeared much later, in 2008, but has rapidly spread globally and nowadays it is the most widespread and epidemiologically threatening MBL worldwide.^{102,103} It is predominantly present in *Enterobacteriaceae* such as *Klebsiella pneumoniae* and *Escherichia coli*.¹⁰³

GIM-1, although geographically more restricted to Germany,¹⁰⁴⁻¹⁰⁶ is also a potentially good target to study, especially for broad-spectrum inhibition, as it has the most unique active site pocket and amino acid sequence within the B1 subfamily.^{107,108} The GIM-1 binding pocket is somewhat narrower and contains aromatic residues (228W and 233Y) in positions where other MBLs have hydrophilic ones.¹⁰⁷

All of these enzymes require two zinc ions for their full activity, share a common catalytic mechanism based on the zinc ions, they are similar in size (~30 kDa, 260-270 amino acids) and they have two zinc coordination sites, one with three histidine residues (Zn1 site) and another one with an aspartic acid, a cysteine and a histidine residue (Zn2 site).^{16,74} They exhibit a characteristic $\alpha\beta/\beta\alpha$ sandwich fold.^{16,62} They utilize several flexible loops to have a broad β -lactam substrate profile.^{16,69,77,109} Although they belong to the same

subfamily, have a conserved mechanistic framework and similar active site architecture, the overall sequence similarity between IMP-, VIM-, NDM- and GIM-type enzymes is only ~30%.¹¹⁰ Due to the flexibility and structural diversity, different loop dynamics, zinc coordination geometry, and active-site electrostatics of these β -lactamases, it has been proven difficult to develop a molecule that inhibits several members of the family.^{82,111} It is often seen in the literature that a candidate structure has good activity against e.g. VIM-2 but is inactive against NDM-1.¹¹²

Overall, the diversity, flexibility and adaptability of metallo- β -lactamases and the rapid evolution of new mutants via horizontal gene transfer significantly contribute to antibiotic resistance, challenges the development of clinically useful inhibitors, complicating treatment and necessitating continuously ongoing research for novel inhibitors that overcome the aforementioned issues.

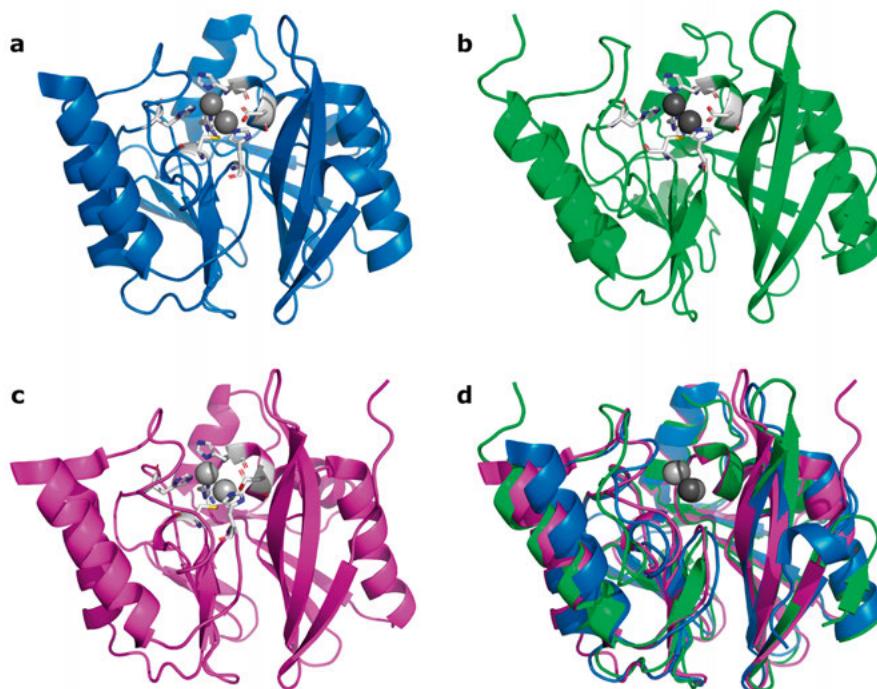


Figure 1.7. The secondary structure of the apo-proteins of selected MBLs with the two zinc binding sites highlighted in grey. (a) VIM-2 (blue, PDB ID: 4NQ2). (b) NDM-1 (green, PDB ID: 3SPU). (c) GIM-1 (magenta, PDB ID: 2YNT). (d) Overlay of the secondary structures of VIM-2, NDM-1 and GIM-1.

1.4 β -Lactamase inhibitors

The development of new antibiotics with novel mode of action has been challenging.¹¹³ Another way to address resistance than developing new antibiotics is to restore the initial activity of existing antibiotics. This can be achieved by administering β -lactams together with a β -lactamase inhibitor, in combination therapy. Such combinations have been successfully utilized since the 1980's.^{70,114-116} For example, Augmentin, which contains amoxicillin as the β -lactam antibiotic and clavulanic acid as the β -lactamase inhibitor, became one of the most selling antibiotics worldwide.^{117,118} However, only serine- β -lactamase inhibitors (SBLIs) exist on the market, whereas no MBL inhibitors (MBLIs) are available for clinical treatment.^{72,119,120} The existing SBL inhibitors either have a β -lactam-like structure (e.g. clavulanic acid, sulbactam, tazobactam, enmetazobactam) or a completely new structure, e.g. the diazabicyclooctane type avibactam, relebactam or durlobactam which are among the newest approved inhibitors on the market (**Figure 1.8**).^{72,121}

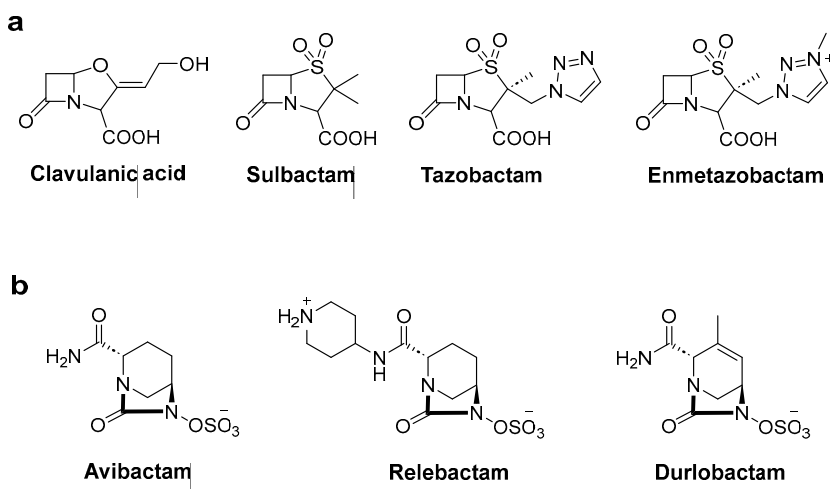


Figure 1.8. Examples of the marketed serine- β -lactamase inhibitors. (a) SBLIs possessing a β -lactam-like structure. (b) SBLIs with novel diazabicyclooctane structure.^{72,121}

1.5 The scientific gap: Metallo- β -lactamase inhibitors

The use of serine- β -lactamase inhibitors made it possible to effectively target bacterial resistance mediated by serine- β -lactamases. This led to an evolutionary pressure favouring the selection of bacteria with metallo- β -lactamases, making these pathogens an increasing clinical challenge. The latter are able to

destroy all subclasses of β -lactam antibiotics (including the last-resort carbapenems), except the monobactams.^{72,120,121} Nevertheless, MBLs often co-exist with SBLs which can significantly enhance the bacterial resistance profile, making the treatment of infections caused by such bacteria particularly challenging.^{72,122,123} The presence of both types of β -lactamases allows the bacteria to hydrolyse all subclasses of β -lactam antibiotics. The co-expression of these enzymes is facilitated by mobile genetic elements like plasmids, integrons and transposons, which can carry multiple resistance genes and spread rapidly among bacterial populations, exacerbating the problem of antibiotic resistance.¹²⁴⁻¹²⁷

Hitherto, developing MBL inhibitors has been difficult. Although a lot of different structures have been proposed for promising MBL inhibition, it has been a great challenge to compare the results from different research groups. No standard protocols are used in this field and the difficulty of comparing results also delays the successful inhibitor development.¹²⁸

The most general MBL inhibitor designs include zinc-dependent strategies, mimicking the structure of β -lactam antibiotics, or developing transition state analogues.^{72,89,129} As all MBLs have zinc ion(s) in their active site, which is essential for their activity, chelating these ions by the inhibitors seems to be a viable strategy. Examples include EDTA, aspergillomarasmine A and other chelating agents, although these must be specific to avoid off-target effects.^{72,129-133} It is also important to keep in mind that there are essential metalloenzymes in the human body, many of them using zinc ion as a co-factor, which participate in e.g. antioxidant defence, anti-inflammatory actions, immune responses.¹³⁴ An interesting, specific zinc chelator example is Zn148, containing three pyridine rings for zinc-sequestering, that shows no off-target effects most probably due to its aliphatic polyalcohol side chain.¹³²

After discovering that captopril (**Figure 1.9**) is a potent inhibitor of MBLs, several research groups focused on developing thiol-containing compounds due to the known affinity of zinc to thiol. These compounds work by the displacement of the active site water molecule responsible for the nucleophilic attack in the β -lactam hydrolysis. Although captopril was a promising MBLI candidate, its primary target is the angiotensin converting enzyme and has a blood pressure lowering effect.¹³⁵ The most advanced compounds *in vitro* however, never reached clinical trials due to limited Gram-negative membrane permeability and accumulation in the periplasm where MBLs are located.^{133,136,137}

Another zinc-targeting group is carboxylic acid containing compounds originating from dipicolinic acid as a promising lead. The result of a lead optimization campaign of dipicolinic acid is ANT2681 (**Figure 1.9**), a thiazole

carboxylate compound that is in the preclinical phase.^{138,139} Among the carboxylate class, indole-2-carboxylates (**Figure 1.9**) were identified with a new mechanism of action. They are locking but not replacing the zinc-complexed water molecule thus still preventing β -lactam antibiotic hydrolysis.^{68,133,140}

Up to date, the most successful MBLI examples are the bicyclic boronates e.g. taniborbactam, xeruborbactam and the most recent KSP-1007 (**Figure 1.9**) that have reached clinical trials.^{20,89,120} They are covalent inhibitors that mimic the tetrahedral transition state of the β -lactam hydrolysis and coordinate to the active site zinc ions.^{20,78,119} Unfortunately, resistance has already been observed for taniborbactam before even reaching the market.^{82,141,142}

To withstand rapid resistance development, new inhibitor structures need to be developed. A promising direction is utilizing a phosphorous atom in the inhibitor design as those compounds may bind to MBLs in an analogous manner as the bicyclic boronates. There are currently no β -lactam antibiotics or inhibitors in clinical use that have phosphorus atom in their structure. Their potential to be used as next generation MBL inhibitors is therefore worth to explore.

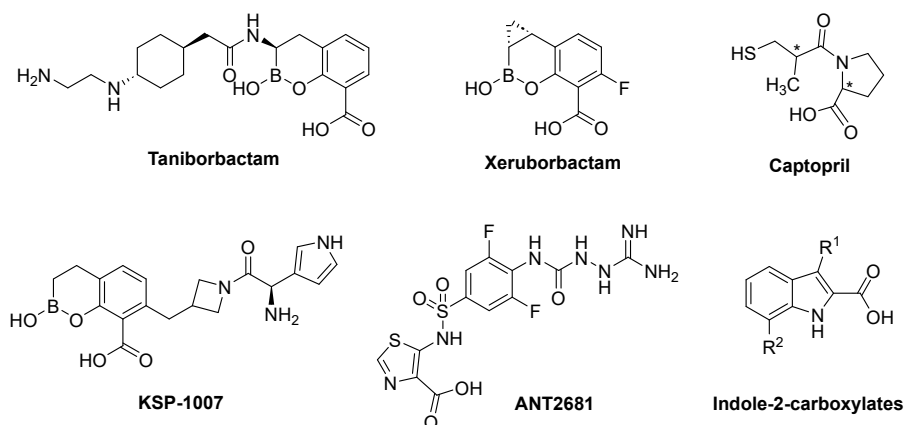


Figure 1.9. The structures of the most successful MBL inhibitors.

1.6 The advantage of phosphonic acids for metallo- β -lactamase inhibition

Although phosphorous is a relatively rarely used heteroatom in approved drugs, it still plays an important role in medicinal chemistry when specific mechanistic requirements need to be addressed. Phosphorous is often used in prodrug strategies or in phosphonic acids as bioisosters of carboxylic acids.¹⁴³ However, there are also drugs where phosphorous atom is important for the biological activity like in nucleotide analogues, transition state inhibitors or in

the bisphosphonate drugs used to treat osteoporosis.¹⁴⁴ Phosphorous-containing compounds (**Figure 1.10**) recently became potential MBL inhibitor candidates,^{109,110,145,146} however, they often show low potency, have solubility and stability issues and are generally difficult to synthesise and purify.^{62,65,69,103,109,147-149} In metallo- β -lactamase inhibition, however, their potential as a transition state analogue has not yet been exploited despite its advantageous characteristics. Transition state analogue enzyme inhibitor design is a successful, often used strategy as a compound that mimics the transition state of an enzyme-substrate complex should have higher affinity and bind more tightly to the enzyme's active site than its natural substrate.¹⁵⁰ For transition state analogue inhibitor design, knowledge of the enzymatic reaction is essential. The hydrolysis of β -lactam antibiotics by metallo- β -lactamases is proposed to proceed via a tetrahedral transition state. Phosphorous-containing molecules can mimic the tetrahedral intermediate of β -lactam hydrolysis catalysed by metallo- β -lactamases, enabling the binding to the active site without undergoing further hydrolysis by the enzymes. This strategy has already been utilized and proven successful in the example of the previously mentioned bicyclic boronates. The hydrolysis mechanism also relies on the zinc ions of the metallo- β -lactamase active site. Phosphonic acids have been reported to strongly bind to zinc ions creating different binding motifs, such as bidentate coordination to one zinc ion or bridging two zinc ions. Phosphonic acids can integrate the transition state analogue strategy with zinc-binding capability and provide a new, so far unused structural motif for MBL inhibition. In this work, all inhibitor design is based on a central, zinc coordinating phosphonic acid moiety adopting a tetrahedral geometry. The core structure of the designed inhibitors mimics the hydrolysis product of β -lactam antibiotics by metallo- β -lactamases. However, these structures are not further hydrolysed but expected to bind to the active site of the enzymes. Although phosphorous containing compounds can be associated with synthetic and pharmacokinetic challenges, e.g. their inherently high polarity, they exhibit attractive mechanistic features for specific biological targets and allow structural modifications to optimize their potentially unfavourable properties.

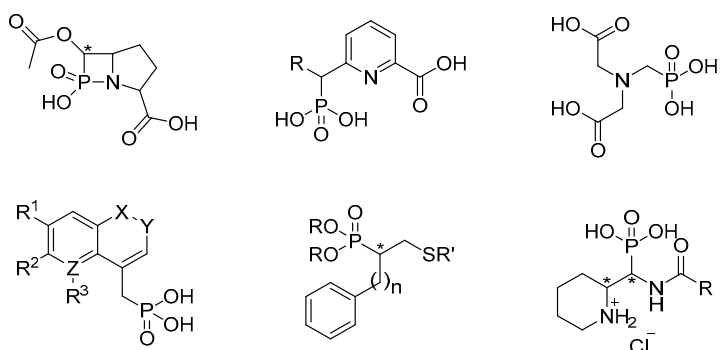


Figure 1.10. The most promising phosphorous-containing MBL inhibitor structures.^{109,110,145-148}

1.7 Aim of the thesis

The overall purpose of this thesis work is to contribute to the discovery of a clinically applicable metallo- β -lactamase inhibitor for combination therapy with β -lactam antibiotics. This, in the long run, will contribute to addressing antibiotic resistance globally.

I aim to evaluate the potential of phosphonic acids as possible MBL inhibitors by designing and synthesising a series of compounds with favourable predicted properties, determine their activity against a variety of metallo- β -lactamases, study their binding event and to use the obtained knowledge to further improve the compounds. I wish to gain understanding on the molecular basis of the inhibitory activity and the binding of phosphonic acids, and evaluate their potency to be developed into broad spectrum or selective metallo- β -lactamase inhibitors.

2. Outline of experimental methods

2.1 Activity measurements

Half-maximal inhibitory concentration (IC_{50}) measurements were used to identify compounds active on purified metallo- β -lactamases. IC_{50} measurements are widely used to determine the concentration needed to reduce an enzyme's activity by 50 % under defined assay conditions.¹⁵¹ This measurement serves as a simple and quick initial tool to identify promising hits and guide optimization efforts. They are, however, often carried out under not standardized assay conditions and they do not take into account the mechanism of inhibition. Thereto, the IC_{50} of irreversible inhibitors is time dependent, and therefore a single value cannot be used for correctly describing a compound's potency.¹²⁸ IC_{50} values alone are accordingly not sufficient for comparison of inhibitors, but are useful for initial identification of compounds with promising MBL inhibitory activity (low micromolar).¹²⁸

To obtain the IC_{50} values of inhibitors, the MBL mediated hydrolysis of a chromogenic reporter substrate (**Figure 2.1**) in the presence of an inhibitor was followed by measuring UV-Vis absorbance in 96-well assay plates. Nitrocefin hydrolysis by VIM-2 and IMP-26 at 482 nm, imipenem or meropenem hydrolysis by NDM-1 at 300 nm was monitored on a SpectraMax M4 spectrophotometer or an Epoch 2 plate reader. The inhibitor concentrations ranged between 0-1500 μ M and the reactions were monitored after 5 min incubation time. All measurements were performed at least in triplicates at 25 °C. The time-dependence of the inhibition was assessed by measuring the IC_{50} values with 5, 30 and 60 min incubation times. The initial velocities at each inhibitor concentration were fitted to dose-response curves (log[inhibitor] vs normalized response) by nonlinear regression to determine IC_{50} values (**Figure 2.2a**).

Another method for assessing IC_{50} values of the inhibitors is utilizing fluorogenic substrates. These substrate structures possess a probe that is released during hydrolysis, resulting in an increase or decrease of fluorescence signal, depending on the exact substrate structure. The IC_{50} values measured at the University of Oxford, UK, employed substrate FC5 liberating 7-hydroxycoumarin that gives an increased signal as the result of substrate hydrolysis.¹⁵²

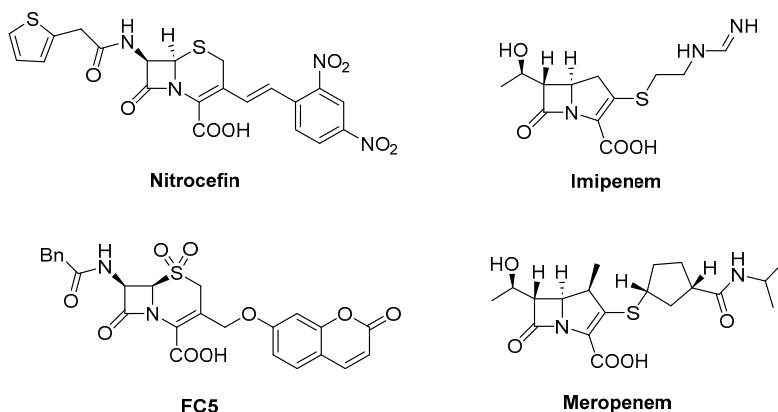


Figure 2.1. The substrate structures used for the inhibitory activity assessment of the phosphonic acids developed for metallo- β -lactamase inhibition.

Enzyme kinetics were also utilized to gain understanding on the inhibition mechanism. To determine whether the compounds act by competitive inhibition, the VIM-2 mediated hydrolysis of reporter substrate nitrocefin with eight different concentrations was tested without inhibitor and with two different inhibitor concentrations. The enzyme activity was followed by measuring the absorbance at 482 nm on a 96-well assay plate using a SpectraMax 190 plate reader. Michaelis-Menten kinetics were employed to fit nitrocefin concentration dependence of the initial reaction velocities. The kinetic parameters were calculated using the Michaelis-Menten equation (**Figure 2.2b**). The data can be visualised on a double reciprocal plot showing that for competitive inhibition the apparent Michaelis-Menten constant ($K'_M = y$ -intercept) increases with increasing inhibitor concentration ($[I]$) while the maximum rate of the reaction ($V_{max} = x$ -intercept) does not change (**Figure 2.2b**).

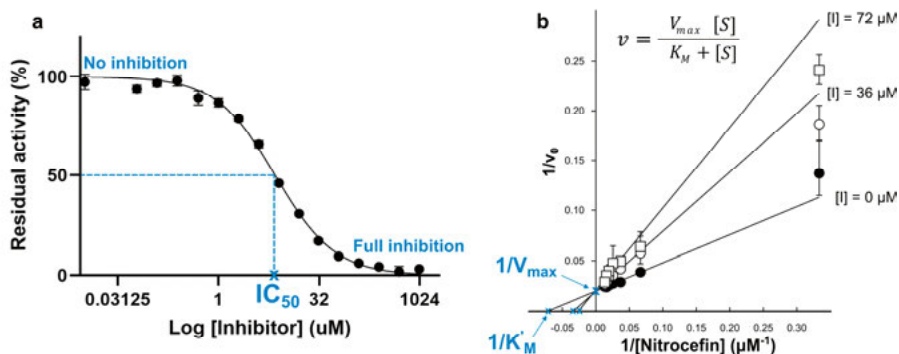


Figure 2.2. (a) The dose-response curve of compound **18p**, a selected example. (b) The double reciprocal Michaelis-Menten plot on the example compound **6g** and the Michaelis-Menten equation. Here, $[I]$ is inhibitor concentration and $[S]$ substrate (nitrocefin) concentration.

It is important to confirm the binding of the inhibitor to its selected target, however, one also needs to ensure that the inhibitor reaches its target and acts as a synergist in combination with a β -lactam antibiotic. To assess the activity of the inhibitors in a cellular context, minimal inhibitory concentrations (MIC) of meropenem were determined using a VIM-2 expressing *E. coli* strain.¹⁵³⁻¹⁵⁵ The MIC value of an antibiotic is the lowest concentration required to prevent visible growth of a microorganism after a defined incubation period.^{156,157} The MIC measurement is widely used in antibiotic research to quantify inhibitor potency and allows comparison of the activities of compounds, strains and treatment combinations. The MIC value of meropenem was determined using the broth microdilution method.^{156,158} Serial two-fold dilutions of meropenem in a 96-well assay plate together with fixed concentration (500 μM) of the inhibitors were inoculated with the bacterial suspension and incubated for 16 hours at 37 $^{\circ}\text{C}$. The turbidity of the plate was evaluated with an Epoch 2 plate reader measuring absorbance endpoint at 600 nm, and the lowest concentration showing no visible bacterial growth was determined as the MIC of meropenem.

2.2 NMR titration

The overall aim of this work is to gain understanding necessary for the design of phosphonic acid-based inhibitors of metallo- β -lactamases. Studying the binding event of inhibitors is essential to reach this goal. Solution NMR spectroscopy offers a powerful and versatile approach for elucidating the molecular details of enzyme-ligand interactions at near-physiological conditions in solution, preserving the native state of the enzymes.^{159,160} It

enables the confirmation of ligand binding, estimation of binding affinities, determination of binding sites and it also offers insight into binding kinetics and interaction modes.¹⁶¹ It can be especially valuable when obtaining enzyme-ligand co-crystals is not possible. NMR titration experiments allow the identification of amino acid residues important for binding together with capturing dynamic aspects of binding events, including changes in protein dynamics and conformational fluctuations, which might be critical for understanding the binding mechanism.^{162,163} The two-dimensional ¹H, ¹⁵N HSQC spectrum of a selected ¹⁵N-labeled enzyme is measured in a D₂O containing buffer. In this spectrum, every backbone amino acid residue has at least one corresponding cross peak (except prolines). Upon incremental addition of the ligand to the enzyme solution, the movement and intensity changes of these cross peaks can be followed and it gives information about the exchange rate between the free and the bound form of the studied enzyme.^{164,165} This exchange can be identified as slow, intermediate or fast relative to the NMR timescale (**Figure 2.3**).^{149,161,162}

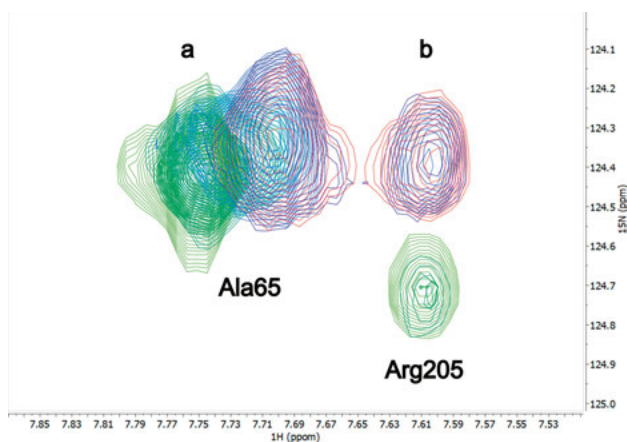


Figure 2.3. (a) Fast exchange and (b) slow exchange on the example of VIM-2.

In slow exchange, the cross peaks of the free enzyme weaken and start disappearing upon the first addition of the ligand, and a new peak corresponding to the ligand bound protein starts appearing. The intensities of the free and bound forms of the protein change during the titration. This typically indicates tight binding and slow dissociation (low k_{off}) and can be associated with longer residence time of the ligand. During fast exchange, only a single peak is visible and its gradual chemical shift change can be followed as the ligand concentration is increased. Fast exchange happens when the affinity of a ligand is moderate or weak, and the binding kinetics is

rapid. Intermediate exchange can be described as the mixture of the previous two, and may suggest conformational rearrangements and dynamic processes accompanying the binding. The weighted average of the individual chemical shift changes in the ^1H and ^{15}N dimensions are called chemical shift perturbations (CSP or $\Delta\delta_{\text{NH}}$) and can be calculated using **Equation 2.1** where R_{scale} is a scaling factor accounting for the chemical shift range differences of the two nuclei.¹⁶⁶ The chemical shift perturbations are considered significant above the population mean plus at least one standard deviation.^{167,168}

$$\Delta\delta_{\text{NH}} = \sqrt{\Delta\delta_{\text{H}}^2 + \left(\frac{\Delta\delta_{\text{N}}}{R_{\text{scale}}}\right)^2}; R_{\text{scale}} = 6.5$$

Equation 2.1. Chemical shift perturbation values (CSP, $\Delta\delta_{\text{NH}}$) are calculated as the weighted average of the chemical shift changes in f1 ($\Delta\delta_{\text{N}}$) and f2 ($\Delta\delta_{\text{H}}$) dimensions.

2.3 Protein expression and purification

The ^{15}N -labeled protein used for NMR titrations was expressed and purified^{111,169} with the help of Anna Andersson Rasmussen at the Lund Protein Production Platform (Lund University) managed by Wolfgang Knecht. The *bla*_{VIM-2} gene was previously transformed into *E. coli* and the resulting strain was used for the expression of VIM-2. ^{15}N -labeled VIM-2 was expressed in ^{15}N -labeled ammonium chloride containing M9 minimal media supplemented with ampicillin. The cells were grown at 30 °C until an optical density at 600 nm (OD_{600}) reached ~0.6, after they were further incubated at 18 °C. Isopropyl- β -d-thiogalactopyranoside (IPTG) was used for induction at 1.2 OD_{600} when also zinc chloride was added to the culture as it was seen previously to improve yield. IPTG is a commonly used inducer of gene expression for *E. coli*.¹⁷⁰ After 19 h, the cells were harvested by centrifugation and lysed with a French Pressure Cell. The soluble extract containing the His-tagged VIM-2 was collected for purification. The protein was first purified using immobilized metal affinity chromatography (IMAC) with a HisTrap HP column and a gradient of imidazole containing buffer. The fractions containing VIM-2 determined by SDS-PAGE were digested using Tobacco Etch Virus (TEV) protease in the presence of dithiothreitol (DTT) to cleave the His-tag from VIM-2. The TEV protease, His-tag and any remaining uncleaved VIM-2 was separated from the cleaved enzyme with reverse IMAC using the previous column and buffer. The wash and flow-through fractions were analysed with SDS-PAGE and the fractions containing the cleaved VIM-2 were dialysed for the last anion exchange chromatography (ACE) purification step. A HiTrap HP Q column and gradient of NaCl in tris(hydroxymethyl)aminomethane (Tris) buffer was used for the ACE purification of VIM-2. Pure VIM-2 fractions were collected, dialysed to the final buffer and concentrated to 13 mg/ml final

concentration. The final enzyme purity was assessed by SDS-PAGE (Figure 2.4). The expression of VIM-2 from 6 L M9 media yielded in 138 mg (23 mg per 1 L culture) purified uniformly ^{15}N -labeled enzyme.

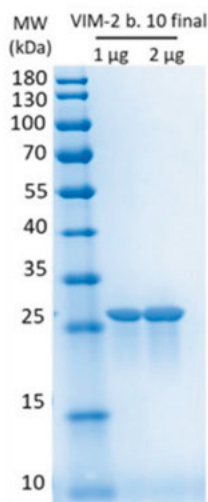


Figure 2.4. The final purity of the uniformly ^{15}N -labeled VIM-2 was assessed by SDS-PAGE gel analysis.

2.4 Molecular docking simulations

Computational simulations can help when experiments are not possible or are too demanding at a very early stage of a drug discovery project. Molecular docking is a quick and cheap method to help planning and designing new drug candidates.^{171,172} Docking is extensively used e.g. during *in silico* virtual high-throughput screening, when the target is known and rapid prioritization of compounds is needed before synthesis and biological testing.^{173,174} Docking can predict how a molecule could bind to a target and propose preferred binding modes, orientations and key interactions based on energy calculations and geometric fitting.^{171,174} It is most often used to assess molecules prior to synthesis,¹⁷⁵ however it can be also useful to complement experimental data or when no experimental data is possible to obtain.

In this work, we aimed to develop and validate docking methods starting from experimental co-crystal structures, and use it to predict binding affinities and binding modes of our inhibitors to target enzymes where our experimental data was limited. Our docking methods were developed from X-ray co-crystal structures of VIM-2 with different phosphonic acid MBL inhibitor candidates, and used for predictions with the target enzymes where no X-ray or NMR

binding studies could be carried out. The results, where possible, were compared to the experimental NMR binding data, to validate that the method that was developed from VIM-2 co-crystals, could reproduce the binding on e.g. NDM-1. Molecular docking was used as a complementary tool to experimental data which enabled the comparison of binding modes and relative affinities across related enzymes within the B1 MBL family.

Docking was done using Schrödinger software primarily using the Glide module in the Maestro interface. The protein as well as the ligand structures were energy optimized at a selected pH prior to docking. All possible protonation states and stereoisomers were generated and used for flexible docking. Flexible docking was selected due to the active-site plasticity of metallo- β -lactamases where rigid docking is often insufficient to account for ligand binding induced loop adjustments. The receptor grid was generated using either amino acid residues or the ligand in the crystal structure to determine center of mass, and water molecules important for binding were kept in the pocket. The three best-ranked docking poses for each ligand were retained for subsequent analysis.

It is important to note, however, that simulations often perform poorly for metalloproteases.¹⁷⁶ It has been proven to be difficult to computationally model the geometry, polarization effects and interactions of the metal centers of MBLs, which, however, is crucial for understanding their catalytic activity.¹²⁸ In addition, MBL active sites are highly flexible, with mobile loop regions (e.g. loop 3 and loop 10) that can adopt different conformations upon ligand binding, whereas most docking approaches treat the protein as largely rigid or only partially flexible.^{171,177,178} The presence of structurally and catalytically important water molecules, including the bridging hydroxide between the zinc ions, further complicates modelling, as these are often treated simplistically despite playing a key role in binding. Moreover, small differences in active-site architecture between closely related enzymes can lead to substantial differences in inhibitor potency that docking methods frequently fail to capture.^{171,178,179} Consequently, while docking can provide useful qualitative insights into possible binding modes, its predictive power for metallo- β -lactamase inhibitor design remains limited, and results should be interpreted cautiously and complemented with experimental validation. Relying on docking for MBLI design therefore can be often misleading and should be used with care. In order to achieve reasonable reliability of the computations, the docking protocol was developed based on experimental data (X-ray, NMR) of closely related compounds to those predicted, on the same class of MBL enzymes.

2.5 ADME predictions and drug-likeness

For a successful drug discovery project, the pharmacokinetic properties and the toxicity profile of a drug are just as important as its potency. Research showed that between 2010 and 2017, poor absorption, distribution, metabolism, excretion, and toxicity (ADME/T) were responsible for ~40-45 % of compounds failing in clinical trials.¹⁸⁰⁻¹⁸² Although not a must, it is advantageous to pay attention to these properties early in the compound design. Promising ADME properties, obtained by computation, already at an early stage can significantly reduce the drug development time and costs.¹⁸³⁻¹⁸⁶ There are several webservers and software that are quick and easy to use for predicting whether a compound could potentially become a viable drug candidate,¹⁸⁷⁻¹⁸⁹ of which we used the PreADMET^{190,191} and the SwissADME¹⁹² webservers. While keeping in mind their limitations, they were used as complementary decision-support tools guiding structural optimization and to assess drug-likeness for low-cost and time. These webservers calculate molecular descriptors and apply statistical models trained on large experimental datasets of existing compounds with known properties, and apply empirical rules to estimate the properties of the new compounds.^{192,193} Physicochemical parameters such as molecular weight (MW), topological polar surface area (TPSA), molar refractivity, number of (aromatic) heteroatoms, hydrogen bond acceptors (HBA) and donors (HBD) and rotatable bonds were calculated. These are all important properties taken into consideration when predicting whether a molecule could be potentially drug-like (**Table 2.1**). In addition, water solubility, logP, cell permeability, blood-brain barrier (BBB) penetration, gastrointestinal absorption, P-glycoprotein-, CYP-enzyme and plasma protein binding were estimated.

For our metallo- β -lactamase inhibitors, the balance between water solubility and lipophilicity is important as the compounds need to be able to cross the Gram-negative outer membrane but also be water soluble and accumulate in the periplasmic space, where the MBLs reside. Molar refractivity means the polarizability of a mole of a substance, which in drug design is used to estimate molecular bulk and electronic polarizability and to help understanding how molecular shape and electronic properties affect ligand-receptor binding. The limitation of the number of rotatable bonds aims to balance the flexibility of a compound needed to adapt to the binding site and rigidity that is often required for higher binding affinity. The compounds should avoid blood-brain barrier penetration, P-glycoprotein-, CYP-enzyme and plasma protein binding. P-glycoprotein inhibition often results in drug-drug interactions and increases the risk of toxicity. The CYP-enzyme family (cytochrome P450) is important for drug metabolism. Among the members,

CYP3A4 is estimated to play a role in ~50 % of marketed drugs, therefore its inhibition is undesirable.¹⁹⁴ Plasma protein binding shows how much of a drug is available for action. Both too low and too high plasma protein binding is disadvantageous as very low binding may result in rapid clearance and short duration of action, while too high binding limits the free, pharmacologically active drug fraction.

Table 2.1. Criteria for molecule's oral bioavailability according to the Lipinski's Rule of Five¹⁹⁵, CMC-like rule (or Ghose filter)¹⁹⁶, Muegge filter¹⁹⁷, Veber (GSK) filter¹⁹⁸ and Egan rule¹⁹⁹.

| | Lipinski Ro5 | CMC-like rule | Muegge rule | Veber filter | Egan rule |
|-----------------------------------|-------------------------|--------------------------|------------------------|-------------------------|----------------------|
| MW [g/mol] | ≤ 500 | 160 to 480 | 200 to 600 | - | - |
| LogP | ≤ 5 | -0.4 to 5.6 | -2 to 5 | - | ≤ 5.88 |
| Nr. of HBA | ≤ 10 | - | ≤ 10 | - | - |
| Nr. of HBD | ≤ 5 | - | ≤ 5 | - | - |
| Total nr. of atoms | - | 20 to 70 | - | - | - |
| Molar refractivity | - | 40 to 130 | - | - | - |
| TPSA [Å²] | - | - | ≤ 150 | ≤ 140 | ≤ 131.6 |
| Nr. of rotatable bonds | - | - | ≤ 15 | ≤ 10 | - |
| Nr. of carbons | - | - | > 4 | - | - |
| Nr. of heteroatoms | - | - | > 1 | - | - |
| Nr. of rings | - | - | ≤ 7 | - | - |

3. Dynamically chiral phosphonic acids as broad-spectrum inhibitors (Paper I)

3.1 Design of dynamically chiral phosphonic acid inhibitors

To overcome the challenges with previously reported phosphorous-containing MBL inhibitor candidates, such as low potency, solubility, stability and Gram-negative membrane permeability problems, cumbersome synthesis and purification,^{69,109,145,147} we designed a new series of phosphonic acid-based molecules (**Figure 3.1**). They share structural features that make them easy to synthesise and that are expected to make them chemically stable, balance their water solubility and Gram-negative membrane permeability and have binding affinity to metallo- β -lactamases.

It has been proven difficult so far to develop broad spectrum inhibitors mainly due to the diversity and active site flexibility of B1 MBLs.^{83,133} Designing inhibitors with dynamic chirality could confer advantages in adaptively binding to various MBLs or potentially to mutated variants. This dynamic adaptation could enhance the binding affinity and efficacy of the inhibitors against diverse enzyme targets, contributing to their effectiveness in combating antibiotic resistance. To adapt to the differences in the target enzyme's active sites and to potentially withstand rapid resistance development via single point mutations, dynamic chirality²⁰⁰ was introduced by adding a stereocenter in a benzylic position next to an amide and the phosphonic acid moiety. This position is ought to be easily deprotonable, enabling the dynamic interconversion of both stereoisomers. A phenyl group adjacent to the α -proton of an amino acid has been reported to decrease the activation barrier of racemization by ~ 8 kcal/mol leading to increased racemization by a factor of 40 000.²⁰¹

The design was also inspired by existing β -lactam antibiotic (e.g. the monobactam nocardicin A or the cephalosporin cephalothin) and both serine-(vaborbactam) and metallo- β -lactamase inhibitor (taniborbactam) structures (**Figure 3.1**).^{202 203} To improve binding affinity, our inhibitors incorporate a benzene ring with a phenolic hydroxy group, similar to nocardicin A, to facilitate π - π stacking and hydrogen bonding in the catalytic site.

Our design balances aqueous solubility and lipophilicity, having the phosphonic acid hydrophilic core and lipophilic moieties (e.g., thiophenes, benzothiofenes, phenyl and benzyl groups) attached via an amide bond.

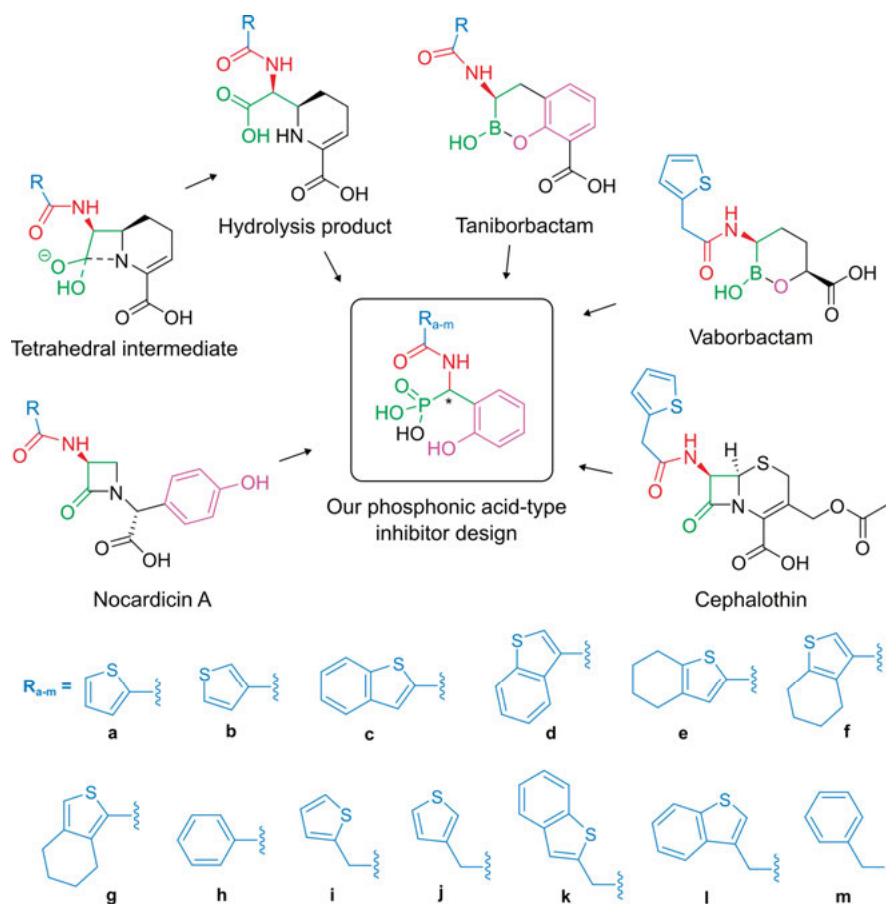


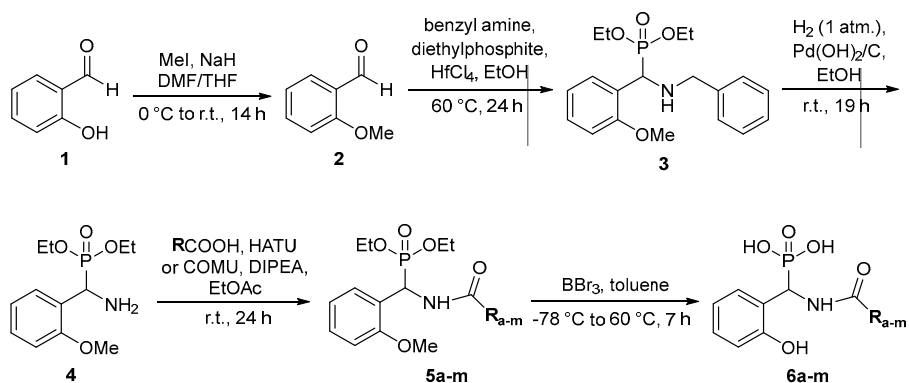
Figure 3.1. The design of dynamically chiral phosphonic acid inhibitors (circled) is based on the β -lactam hydrolysis mechanism by MBLs and existing β -lactam antibiotic or β -lactamase inhibitor structures.

3.2 Synthesis of phosphonic acids

13 new compounds were synthesized by a facile and straightforward synthetic route (**Scheme 3.1**). It starts with the key Kabachnik-Fields reaction to obtain the α -aminophosphonate core scaffold followed by the deprotection of the amine. The free amine enables the amide coupling of a variety of carboxylic acids which provides the final inhibitor structure. The last

step is the simultaneous cleavage of the methyl ether together with the phosphonic ester hydrolysis.

The commercially available 2-methoxybenzaldehyde **2** which is the starting material of the Kabachnik-Fields reaction can also be synthesised from the cheaper salicylaldehyde **1**. Salicylaldehyde **1** was O-methylated with methyl iodide in the presence of sodium hydride in a mixture of DMF and THF as solvent. The reaction gave the product 2-methoxybenzaldehyde **2** in excellent yield (94 %) in 14 hours. The Kabachnik-Fields reaction allowed to create the crucial phosphonate motif and an amino functionality in a single step, the latter enabling the subsequent synthesis of a series of amides. 2-Methoxybenzaldehyde **2**, diethyl phosphite as the phosphorous-containing reagent and hafnium-chloride as the catalyst in absolute ethanol at 60 °C were found to give the desired product **3** in the Kabachnik-Fields reaction in good yield (73 %) in 24 hours. The benzyl deprotection of the secondary amine of **3** was achieved by catalytic hydrogenation reaction using H₂ at atmospheric pressure and Pd(OH)₂/C (Pearlman's catalyst) in ethanol giving the common intermediate primary amine **4** after 19 hours with near quantitative yields. Compound **4** enabled the divergent synthetic strategy of the amides **5a-m**. The amide coupling reactions were performed using either coupling agents HATU or COMU both showing similar success to activate the 13 carboxylic acids. DIPEA was used as a base and ethyl acetate as a solvent being a greener alternative to DMF.²⁰⁴ The amides **5a-m** were obtained in 24 hours at room temperature in moderate to good yields (61-95 %) depending on the carboxylic acid employed. In the last step, the ethyl esters of **5** were hydrolysed together with the methyl ether cleavage with the use of boron tribromide in toluene within 7 hours. The final compounds **6a-m** were acquired after preparative reversed-phase HPLC purification in yields of 46-86 %.



Scheme 3.1. The optimized synthetic route towards the phosphonic acid-type metallo-β-lactamase inhibitors **6a-m**. Figure is reproduced from Paper I.

3.3 Assessment of the phosphonic acids as metallo- β -lactamase inhibitors

The initial evaluation step of the designed compounds' activity was to test their half-maximal inhibitory concentration (IC_{50}) on purified metallo- β -lactamases, namely on VIM-2, NDM-1 and GIM-1 (**Figure 3.2**). The measurements were carried out by Daniel Salamonsen at UiT. VIM-2 and NDM-1 were selected due to their high clinical relevance. GIM-1 was selected to assess the compounds' ability of becoming broad spectrum inhibitors as GIM-1 is a member of the B1 family with the most different active site.¹⁰⁷ All compounds showed low micromolar activity *in vitro* at least on one of the selected enzymes. Some compounds were able to inhibit two or even all of the three target enzymes with comparable potency, showing promise for the development of a broad spectrum inhibitor. To overcome the challenges of assessing potency of the inhibitors resulting only from a single IC_{50} measurement, and to enable comparison with following series of inhibitors, the IC_{50} values were also measured with the fluorescence protocol by a different group in Oxford.¹⁵² The overall conclusions were consistent, the most potent inhibitors were determined to be the same compounds with both methods, however the GIM-1 data is incomparable. (**Figure 3.2**) The best inhibitors all contained non-flexible and bulky groups attached to the amide group. The mechanism of inhibition was also determined to be competitive using Michaelis-Menten kinetics described in **Chapter 2.1**.

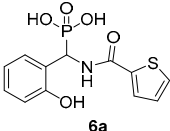
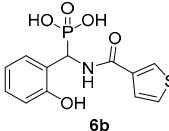
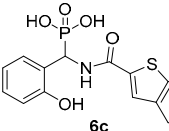
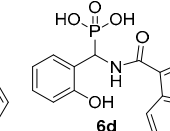
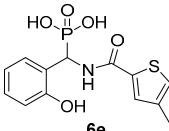
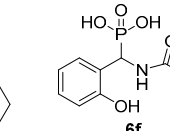
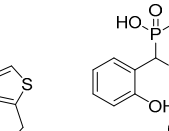
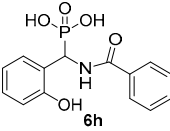
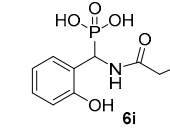
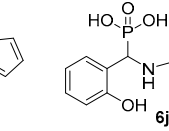
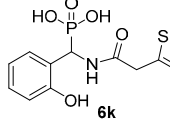
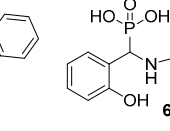
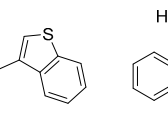
| | | | | |
|-----------|--|--|--|--|
| |  |  |  |  |
| IC_{50} | VIM-2: 71 (>100) μ M | 124 (>100) μ M | 103 (\geq 100) μ M | 21 (47) μ M |
| | NDM-1: 217 (>100) μ M | 97 (>100) μ M | - (25) μ M | - (7) μ M |
| | GIM-1: 20 (>100) μ M | 236 (>100) μ M | 101 (>100) μ M | 10 (>100) μ M |
| <hr/> | | | | |
| |  |  |  | |
| IC_{50} | VIM-2: 79 (>100) μ M | 48 (\geq 100) μ M | 12 (46) μ M | |
| | NDM-1: - (51) μ M | 30 (6) μ M | - (2) μ M | |
| | GIM-1: 53 (>100) μ M | 52 (>100) μ M | 21 (>100) μ M | |
| <hr/> | | | | |
| |  |  |  | |
| IC_{50} | VIM-2: 55 (>100) μ M | 38 (\geq 100) μ M | 37 (>100) μ M | |
| | NDM-1: 85 (>100) μ M | 87 (24) μ M | 232 (69) μ M | |
| | GIM-1: 35 (>100) μ M | 189 (>100) μ M | 103 (>100) μ M | |
| <hr/> | | | | |
| |  |  |  | |
| IC_{50} | VIM-2: 51 (>100) μ M | 26 (>100) μ M | 74 (>100) μ M | |
| | NDM-1: 65 (22) μ M | 67 (29) μ M | - (>100) μ M | |
| | GIM-1: 80 (>100) μ M | 51 (>100) μ M | 121 (>100) μ M | |

Figure 3.2. The IC_{50} values of phosphonic acids **6a-m** indicate good inhibitory activity against all three target MBLs, measured by Daniel Salamonsen at UiT. The values in parenthesis were measured with the fluorescence method by Gurleen Kaur in Oxford.

After confirming the activity of the inhibitors, we aimed to understand and characterize their binding mode. We utilized both experimental (solution NMR spectroscopy and X-ray crystallography) and computational (molecular docking and dynamics simulations) studies to better understand the binding event of this new series of phosphonic acid inhibitors. The most potent inhibitors were titrated to VIM-2 and NDM-1 and their binding pocket was determined by solution NMR. Titrations were carried out using ^{15}N -labelled enzymes up to 10.0 equivalents of the inhibitors over 10 titration steps. NMR

revealed that for both enzymes, the compounds bind in the same binding pocket with β -sheet 3, the hydrophobic loop 3 as well as flexible loops 5, -10 and residues around the zinc binding sites (from loops 7, -9 and -12) are oriented towards the ligands (**Figure 3.3**).

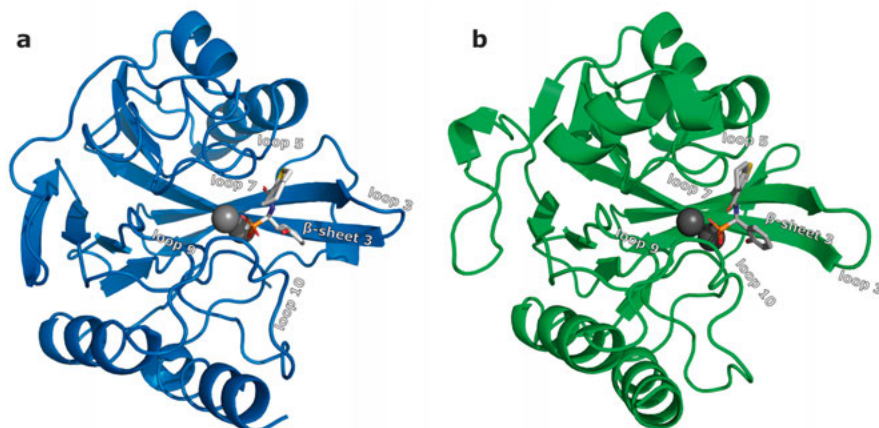


Figure 3.3. The loops oriented towards the bound ligand according to NMR titration experiments. (a) VIM-2 in complex with compound **6g**. (b) NDM-1 in complex with compound **6f**.

The NMR titration data indicates reversible inhibition, no removal of the zinc ions and similar binding mode for the different inhibitors according to the comparable chemical shift perturbations (**Figure 3.4**).^{109,149}

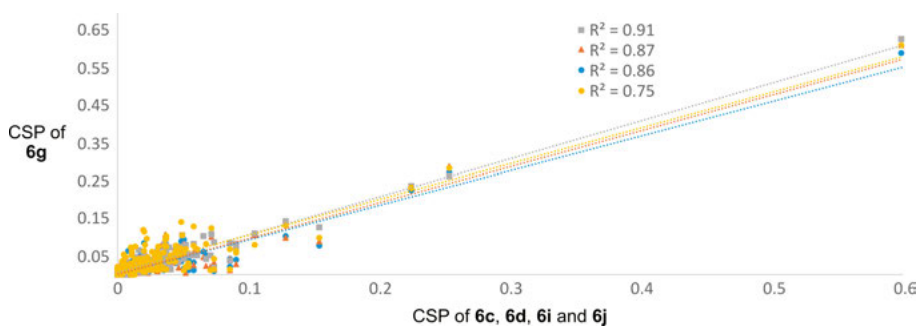


Figure 3.4. Linear regression of the chemical shift perturbations (CSP) of the most potent compound **6g** against VIM-2 as a function of the CSPs of compounds **6c** (yellow circle), **6d** (grey square), **6i** (red triangle) and **6j** (blue circle) for VIM-2. The graph shows that the same residues had comparable CSPs for each ligand, indicating binding in the same active site with comparable binding modes.

Four inhibitors (compounds **6c** PDB ID: 9F0P, **6d** PDB ID: 9F0Q, **6g** PDB ID: 9F0R and **6j** PDB ID: 9F0S) were co-crystallized with VIM-2 by the group of Eike C. Schulz in Hamburg. The structures showed that both of their stereoisomers bind to the enzyme with 180 ° flipped binding mode. Furthermore, as it was observed by NMR, the different inhibitors bind in the same binding pocket with similar binding mode (**Figure 3.5**). The X-ray diffraction corroborated that the key interaction is the expected binding of the phosphonic acid core to the zinc ions. As it was unrealistic to get X-ray data on all inhibitor-enzyme complexes and NDM-1 is known to be less stable than VIM-2, furthermore there is no experimental data available on GIM-1 binding modes, we developed and validated computational methods to analyse the binding of all the inhibitors against all the three target enzymes. First, the four compounds, where we had the co-crystals available, were docked to VIM-2 and subsequently molecular dynamics simulations were run. Importantly, the binding modes obtained by docking simulations were comparable to those detected by X-ray and NMR experiments. For all compounds, both enantiomers had a docking score around -8 kcal/mol, which suggests similar binding affinity. The two isomers were bound in the same binding pocket with a binding mode flipped by ~180 ° (**Figure 3.5**). Molecular dynamics simulations, run by Liping Zhou at SIMM, indicated that the docked enzyme-inhibitor complexes are stable over the simulation time.

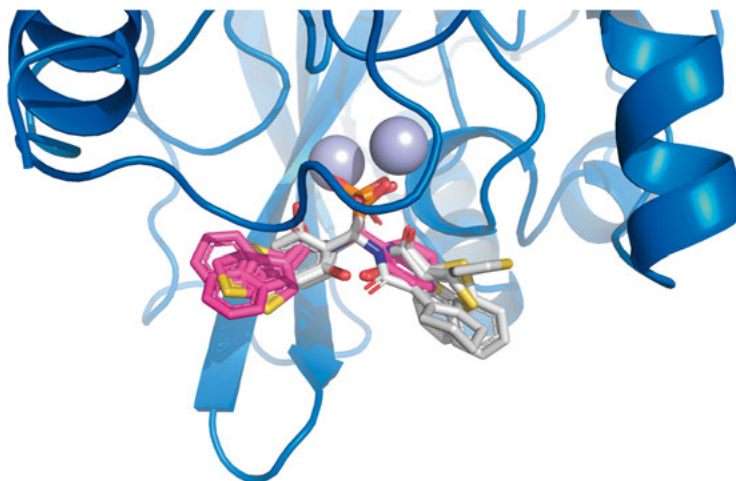


Figure 3.5. The docked binding modes of compounds **6c**, **6d**, **6g** and **6j** (*R*)-isomers (grey) and (*S*)-isomers (magenta) to VIM-2. The orientation of the two isomers is flipped by 180 °.

Following the validation, docking was also performed for the 13 inhibitors to all three enzymes using the validated protocol. Docking of the most potent

compound **6f** to NDM-1 indicated interactions that are in agreement with the outcome of the corresponding NMR titration experiment. Both methods showed that amino acid residues around the zinc ions are involved in the binding (e.g. His122, Asp124, Gly188, Thr190 and Ser191), furthermore residues in β -sheet 3 as well as in loops 3, -5, and -10 are oriented towards the bound ligand, similarly as it was seen for VIM-2. Common binding pocket and binding mode was observed for all the inhibitors with all three enzymes. The key interaction stays between the phosphonic acid and the zinc ions in the active site of the enzymes. Both stereoisomers of the inhibitors showed comparable affinity (docking scores around -8 kcal/mol) to all three target enzymes.

We also aimed to predict the possibility of single point mutations weakening the binding of both stereoisomers simultaneously. Jintian Li at SIMM conducted computational saturation mutagenesis screening on the amino acids located in the binding pocket followed by docking of both stereoisomers of the inhibitors to the mutated enzymes. The results show, that only in maximum 10 % of the possible mutations are both enantiomers losing their binding ability (**Table 3.1**). In at least 90 % of the cases, either one or both of the isomers remain bound to the enzyme's active site suggesting the possibility to withstand resistance development by single point mutations.

Table 3.1. Mutation combinations simultaneously weakening the binding of both stereoisomers of compounds **6c,d,g,j** to VIM-2, NDM-1 and GIM-1. Results of Jintian Li at SIMM.

| | VIM-2 | NDM-1 | GIM-1 |
|-----------------------|-------|-------|-------|
| Mutation combinations | 380 | 342 | 342 |
| (R+S)- 6c | 21 | 34 | 1 |
| (R+S)- 6d | 19 | 26 | 2 |
| (R+S)- 6g | 19 | 26 | 1 |
| (R+S)- 6j | 10 | 20 | 3 |

As metallo- β -lactamases are prevalent in the periplasm of Gram-negative bacteria, they need to be able to cross the Gram-negative outer membrane to reach their targets. Therefore, Gram-negative outer membrane permeability was measured by Johannes Thoma in Gothenburg, on outer membrane vesicles (OMV) carrying the target enzymes in their lumen.²⁰⁵⁻²⁰⁷ These OMVs can be used for modelling transmembrane uptake as they maintain the host bacteria's protein and lipid composition.²⁰⁷ The activity of VIM-2, NDM-1 and GIM-1 in the OMVs was reduced in the presence of the 13 inhibitors, which indicates

that these phosphonic acids are able to cross the Gram-negative outer membrane.

This was further confirmed on VIM-2 expressing clinical isolates where we observed up to 30 % zone inhibition compared with the wild-type *E. coli* without inhibitors. These measurements were carried out by Holger Rohde in Hamburg.

The lack of cytotoxicity is also important for successful clinical applicability. Therefore, the compounds cytotoxicity was assessed on human hepatocellular carcinoma (HepG2) cells by Viola Tamási in Hungary. The compounds proved to be non-cytotoxic, having at least 1000 μM cytotoxic concentration (CC_{50}). The selectivity index (SI, **Equation 3.1**) for the inhibitors with IC_{50} values below 100 μM were at least 12, but in 16 out of the 25 cases it was even over 50, highlighting the difference between their effective and toxic concentrations.

$$SI = \frac{\text{toxic concentration, e. g. } CC_{50}}{\text{effective concentration, e. g. } IC_{50}}$$

Equation 3.1. The formula for calculating the selectivity index (SI) used to describe the toxicity of a therapeutic.

3.4 Phosphonic acid inhibitors with favourable ADME properties

The ADME properties of the designed phosphonic acids were predicted and evaluated. The estimated values suggest generally good aqueous solubility that is also in accordance with our experimental observations. The predictions also show overall favourable lipophilicity, no BBB penetration, possibly no P-glycoprotein and CYP-enzymes inhibition. The compounds are predicted to have very low cell permeability (predicted for Caco-2 and MDCK cell permeability models), however this might not be a problem for MBL inhibitors as their targets are located in the periplasm of Gram-negative bacteria, thus, high cell permeability is not an essential requirement. High plasma protein binding is also expected for these compounds, which is in general undesirable. Nevertheless, literature data indicates that plasma protein binding has only limited impact on the *in vivo* efficacy of a drug candidate therefore it is generally not recommended to optimize a drug candidate on plasma protein binding.^{208,209} The last value predicted was human intestinal absorption, for 9 compounds categorized as “well absorbed“ and only the 4 thiophene-containing compounds being “moderately absorbed“. The drug-likeness of the compounds were also evaluated. All compounds fulfil the criteria that has been

used to describe compounds being potentially good drug candidates, including the Lipinski's Rule of Five¹⁹⁵, the CMC-like rule¹⁹⁶ or the Muegge filter¹⁹⁷. Overall the structures balance well aqueous solubility and lipophilicity, have favourable ADME properties and are predicted to be drug-like molecules showing promise for successful clinical development.

4. The effect of structural modifications on inhibitory activity (Paper II and III)

4.1 Design of the new core scaffolds

To investigate the influence of the aryl-phosphonic acid core structure on MBL binding, the ortho-hydroxyphenyl group from the inhibitor series discussed in **Chapter 3** was exchanged to a pyridine ring, a thiazole-4-carboxylate or a non-aromatic carboxylic acid (**Figure 4.1**).

Pyridine is a commonly used moiety in drug design and can be found also in antimicrobials, such as isoniazid or ozenoxacin.^{210,211} The pyridine ring can provide a different conformational constraint as compared to an ortho-hydroxyphenyl ring, which might influence the binding to the target enzymes, however, could still engage in π - π stacking or π -cation interactions similar to the original ortho-hydroxyphenyl core. For MBL inhibition, the nitrogen atom might contribute to the coordination of the zinc ions and to hydrogen bonding within the enzyme's binding pocket.^{212,213} Pyridine can improve aqueous solubility and is expected to increase metabolic stability of the drug candidates as compared to phenolic hydroxy groups, which are often subject to metabolic modifications, such as glucuronidation or sulfation.²¹⁴⁻²¹⁶ Pyridine has also different electronics compared to hydroxyphenyl. While the hydroxy group on the aromatic ring is mainly electron-donating via resonance and thus this aromatic moiety is electron rich and acidic, pyridine is an electron-poor aromatic heterocycle and is weakly basic. The most potent compounds of the first phosphonic acid-type inhibitor series in **Chapter 3** contained non-flexible thiophene/benzothiophene moieties, therefore four of them were kept (**a-d**) and used with the new pyridine core for comparison.

In our second design, we used thiazole as the new core (**Figure 4.1**), which is also often used in pharmaceuticals. It is a heteroaromatic moiety that has both electron-donating (-S-) and electron-accepting (C=N) groups. Several molecules containing a thiazole have biological activity, including many cephalosporin β -lactam antibiotics e.g. cefiderocol²¹⁷, ceftazidime, cefotaxime, ceftriaxone^{218,219} and the monobactams tigemonam^{220,221} and carumonam²²². Furthermore, the only non-bicyclic boronate-type metallo- β -lactamase inhibitor in clinical trials (ANT2681) also contains a thiazole ring.^{138,139} In

ANT2681, the thiazole group is equipped with a carboxylate functionality, which introduces more H-bonding possibilities and has been proven important for binding to MBLs.^{68,223} Therefore, we were motivated to put a carboxylate to position 4 of the ring. Our thiazole-4-carboxylate-containing phosphonic acid inhibitor also mimics the hydrolysed form of penem antibiotics.²²⁴ The thiazole-4-carboxylate ring is electron-poor as opposed to the hydroxyphenyl ring and similar to the pyridine ring. Similar to the pyridine core, the thiazole cannot act as H-bond donor, and is also metabolically more stable than the hydroxyphenyl group. We have also synthesized the free acid form, but it was unstable in aqueous solution and its more stable ethyl ester was therefore studied instead.

Lastly, a carboxylic acid was chosen as a non-aromatic core alternative (**Figure 4.1**). It can act as a second strongly zinc coordinating moiety in addition to the phosphonic acid.^{133,148} It increases polarity and is not capable of any π -interaction in the enzymes' binding pocket. It is also strongly electron withdrawing, is a much stronger acid than a phenol, and is largely ionized at physiological pH. The negatively charged carboxylate anion can potentially strengthen binding to metal ions or basic residues (Lys, Arg) near the binding pocket. Furthermore, carboxylic acids are a promising class of MBLIs as discussed in **Chapter 1.5**.

The thiophene attached to the core via an amide moiety was kept in all our inhibitor designs for comparison, while for the thiazole and carboxylic acid containing inhibitors, a non-aromatic aminocyclohexyl moiety (**Figure 4.1**) was also utilized to see whether the lack of aromaticity decreases the binding potency. The aminocyclohexyl moiety was inspired by taniborbactam, the most successful metallo- β -lactamase inhibitor that is currently in clinical trials.²⁰ To engage in hydrogen-bonding, π - π stacking or cation- π interactions in the metallo- β -lactamase binding pocket, natural amino acids were also attached to the amide moiety of the carboxylic acid-type inhibitor core. Sequences of natural amino acids can be easily made by solid-phase peptide synthesis and coupled to the free amine of the molecule. The peptide sequence was designed and optimized via computational methods. All tripeptide combinations were generated, the resulting inhibitor structures were docked to VIM-2 and the best sequence Trp-Tyr-Phe- was chosen.

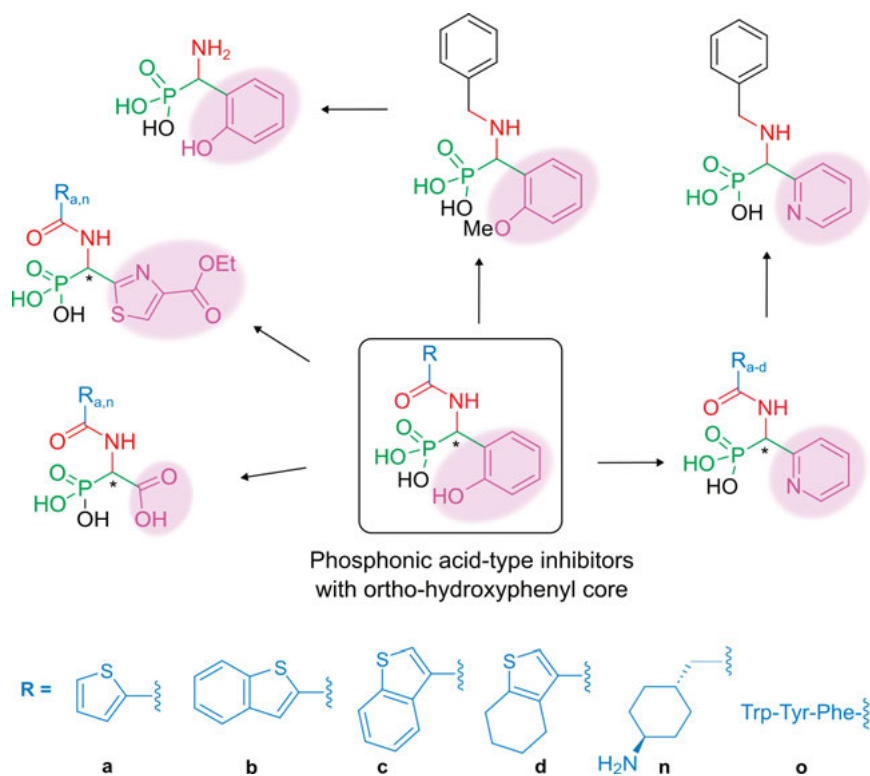
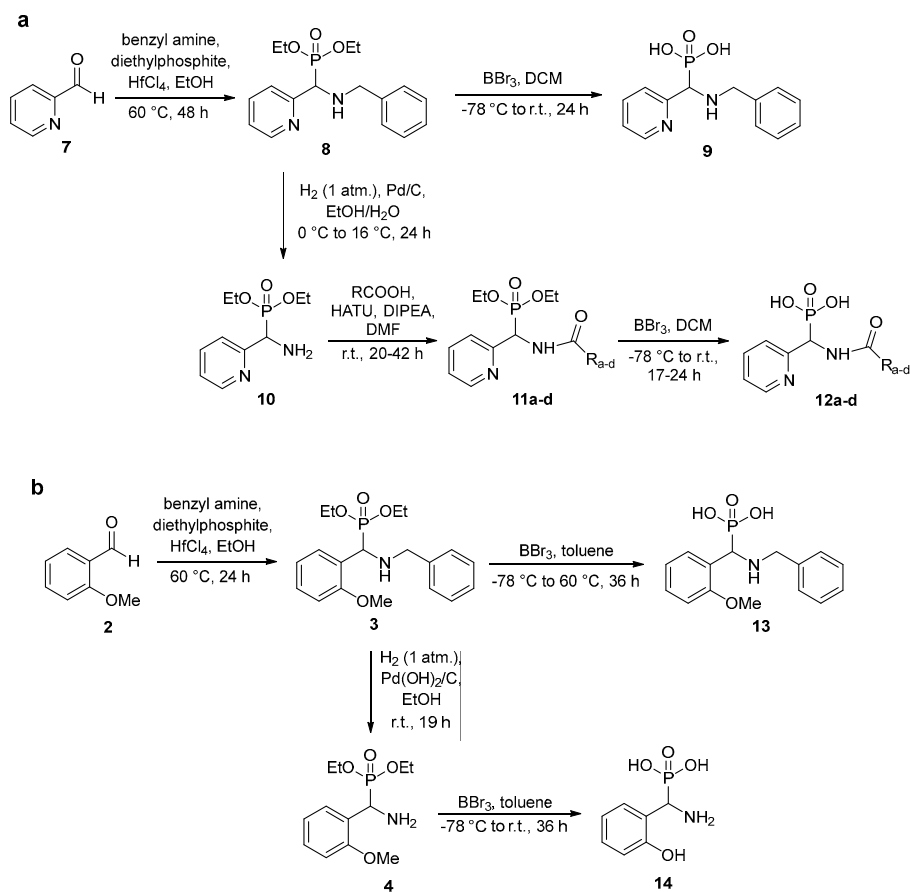


Figure 4.1. The design of the second series of phosphonic acid-type inhibitors is based on the previous series of compounds possessing the ortho-hydroxyphenyl core (circled).

4.2 Synthesis of the pyridinyl compounds

The synthetic route of the pyridine-containing inhibitors **12a-d** (Scheme 4.1) was based on the previous hydroxyphenyl phosphonic acid-inhibitor synthesis (Chapter 3). The 4-step synthetic pathway started from the commercially available 2-pyridinecarbaldehyde with the Kabachnik-Fields reaction. The reaction conditions previously optimized for 2-methoxybenzaldehyde **2** were applicable for 2-pyridinecarbaldehyde **7**, however the reaction was slower and gave lower yield (65 %). The amine of compound **8** was subsequently debenzylated by catalytic hydrogenation. This reaction needed to be optimized in order to avoid the reduction of the pyridine ring to piperidine. The best conditions were found to be Pd/C as catalyst, the 1:1 mixture of EtOH and water as solvent and low reaction temperature. The free amine of **10** was then coupled to various carboxylic acids via peptide coupling reactions. The coupling reaction also turned out to be slower and lower yielding than for the earlier substrates, therefore the solvent was switched from EtOAc to DMF. Lastly, the

phosphonic esters of **11** were hydrolysed with BBr_3 at room temperature, proving to be easier than for the hydroxyphenyl analogues. The Kabachnik-Fields product α -aminophosphonate **8** was alternatively hydrolysed with BBr_3 to afford the corresponding α -aminophosphonic acid **9**. Compound **9** was tested for MBL inhibition to compare the effect of a secondary amine to the amide moieties previously used. For comparison, the analogue of compound **9** bearing an ortho-methoxyphenyl core (compound **13**) was also synthesised through the equivalent synthetic pathway starting from 2-methoxybenzaldehyde **2**. The ortho-methoxyphenyl core is used for comparison instead of the ortho-hydroxyphenyl as the BBr_3 hydrolysis of the α -aminophosphonate ethyl ester intermediate **3** surprisingly did not cleave the methyl ether bond. In addition, the primary amine containing compound **14**, another readily accessible intermediate from the synthetic sequence that retains the essential phosphonic acid motif, was included in the MBL inhibition studies. This primary amine containing molecule allows evaluation of the importance of the second aromatic structural element in our phosphonic acid inhibitors. All final compounds were purified with preparative RP-HPLC that has been more cumbersome than for the previous series, and resulted in 29-46 % yields.



Scheme 4.1. The synthetic route towards (a) the pyridinylmethyl-phosphonic acid-type inhibitors and (b) the α -aminophosphonic acids with ortho-methoxyphenyl or ortho-hydroxyphenyl core.

4.3 Evaluation of the impact of core-changes on bioactivity

To investigate the capability of phosphonic acids for even broad spectrum inhibition, two additional enzymes, VIM-1 and IMP-1, were included in the evaluation of the potency of the second series of compounds. Our aim was to understand how scaffold changes contribute to the binding to VIM, NDM, IMP and GIM enzymes to help rationally advance phosphonic acid-type inhibitors toward clinically applicable medicines. The IC_{50} values of these compounds were measured by Gurleen Kaur at the University of Oxford (**Figure 4.2**).

Among the amide-linker containing molecules, no significant activity was observed against VIM-1. Only compound **15a** showed high μ M activity,

suggesting that both the core structure and the amide attached moiety simultaneously have a significant role in inhibitor binding to VIM-1. When changing the core from the thiazole-carboxylate to another scaffold, the activity was lost, as well as when changing the thiophene moiety to the non-aromatic aminocyclohexyl ring. The best inhibition of VIM-1 was achieved by the α -aminophosphonic acid compound **13** with IC_{50} value of 35.5 μ M. This activity was completely lost when the aromatic core was changed to pyridine (compound **9**) as well as when the amine attached benzyl group was removed (compound **14**).

Most of the compounds however showed some inhibitory activity against VIM-2, suggesting that the key structural element for VIM-2 binding is the common phosphonic acid core. Although VIM-1 and VIM-2 share 93 % sequence identity, our results highlight the difficulty of inhibiting more members of the VIM family. A decrease in VIM-2 activity was observed for the non-aromatic carboxylic acid-containing compounds. The lack of activity of compounds **16a,n,o** indicates that having two zinc-coordinating functionalities in close proximity in the inhibitor structure has an adverse effect on VIM-2 binding, rather than giving stronger coordination to both zinc ions in the active site. Alteration of the core structures while keeping the smaller thiophene moiety on the amide was well-tolerated. However, when the bigger aromatic benzothiophenes were used in the amide side of the molecules, the pyridine derivatives performed worse as compared to the hydroxyphenyl-containing inhibitors. We note that the orientation of the amide attached moiety matters for VIM-2 activity which has been previously observed for the ortho-hydroxyphenyl phosphonic acid inhibitors in **Chapter 3**. Compound **15n** with the non-aromatic, more flexible aminocyclohexyl amide moiety still kept VIM-2 activity, which suggests that VIM-2 tolerates the exchange of a possible aromatic interaction to a non-aromatic, e.g. hydrogen-bonding with the amine of the aminocyclohexyl ring. The most potent VIM-2 inhibitor was compound **13**, suggesting that this structure may be a lead for the development of inhibitors against multiple VIM-variants. The lack of the amine attached benzyl group (compound **14**) and the core change from ortho-methoxyphenyl to pyridine ring (compound **9**) show 17 to 25-fold activity drop compared to **13**, respectively. This highlights possible important interactions of the ortho-methoxy group and the amine attached benzyl moiety with the VIM-2 active site, however, the effect of the structural alteration is not as drastic as for VIM-1 inhibition. The importance of the benzyl group suggests possible π - π or cation- π interactions. The low inhibitory potency of **9** against VIM-1 and VIM-2 may be rationalized by loss of interaction to Asn210 when compared to analogue **13**, which allows hydrogen bonding through its methoxy group.

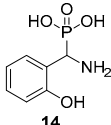
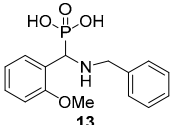
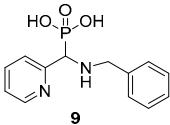
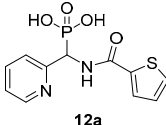
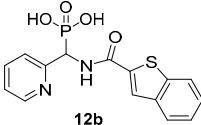
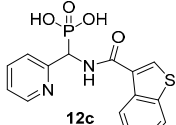
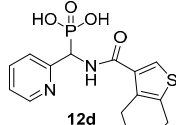
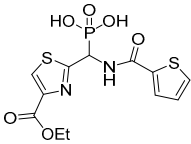
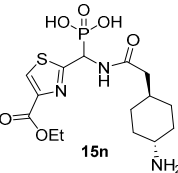
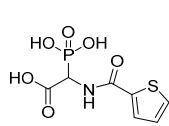
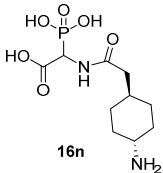
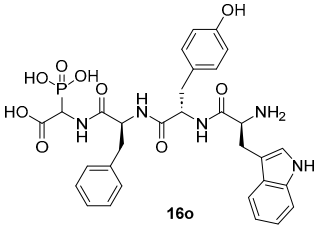
| | | | | |
|------------------|---|---|--|--|
| |  |  |  | |
| IC ₅₀ | VIM-1: >1000 μM | 35 μM | >1000 μM | |
| | VIM-2: 145 μM | 8.6 μM | 214 μM | |
| | NDM-1: >1000 μM | >1000 μM | >1000 μM | |
| | IMP-1: >1000 μM | 537 μM | 676 μM | |
| | GIM-1: >100 μM | >100 μM | >100 μM | |
| <hr/> | | | | |
| |  |  |  |  |
| IC ₅₀ | VIM-1: >1000 μM | >1000 μM | >1000 μM | >1000 μM |
| | VIM-2: 59 μM | 794 μM | 110 μM | 63 μM |
| | NDM-1: >1000 μM | >1000 μM | >1000 μM | >1000 μM |
| | IMP-1: >1000 μM | 166 μM | >1000 μM | >1000 μM |
| | GIM-1: >100 μM | >100 μM | >100 μM | >100 μM |
| <hr/> | | | | |
| |  |  |  |  |
| IC ₅₀ | VIM-1: 186 μM | >1000 μM | >1000 μM | >1000 μM |
| | VIM-2: 16.6 μM | 51 μM | 324 μM | >1000 μM |
| | NDM-1: 302 μM | 91 μM | 91 μM | >1000 μM |
| | IMP-1: >1000 μM | 191 μM | 46 μM | >1000 μM |
| | GIM-1: >100 μM | >100 μM | >100 μM | >100 μM |
| <hr/> | | | | |
| |  | | | |
| IC ₅₀ | VIM-1: >1000 μM | >1000 μM | >1000 μM | |
| | VIM-2: >1000 μM | >1000 μM | >1000 μM | |
| | NDM-1: 110 μM | >1000 μM | >1000 μM | |
| | IMP-1: >1000 μM | >1000 μM | >1000 μM | |
| | GIM-1: ≥100 μM | >1000 μM | >1000 μM | |

Figure 4.2. Inhibitory activities of phosphonic acids possessing different core structures, measured using a fluorogenic substrate by Gurleen Kaur at the University of Oxford. IC₅₀ values below 100 μM are highlighted in bold. Compounds **15a,n** and **16a,n,o** were synthesised by Bo Li (CAS SIMM).

Relative VIM-2 activity was also assessed in the presence of the inhibitors at a fixed concentration of 100 μM on purified enzyme and on the enzyme within

OMVs (without and with membrane permeabilization) (**Figure 4.3**). The carboxylic acid derivatives **16a,n,o** were the least active compounds whereas the best performing inhibitors were **13** and **15a**, in accordance with our IC_{50} measurements. The permeability data highlights that all compounds penetrate the Gram-negative outer membrane.

Generally, we achieved weaker inhibition for all inhibitors against NDM-1 as compared to VIM-2, which was not observed for the compounds having a hydroxyphenyl core. Dramatic activity loss was observed when pyridine was used as a core, but overall all core changes from the hydroxyphenyl had an adverse effect on NDM-1 activity, regardless of aromaticity. It suggests that an electron rich system is needed for binding, and that the hydroxy functionality has an observable positive effect on NDM-1 binding. When comparing the influence of the amide attached moieties for compounds with the same core, we observed that the amide attached moiety does not play a significant role and NDM-1 tolerates changing this part of the molecule even better than VIM-2, for instance. None of the α -aminophosphonic acids lacking the amide moiety were suitable inhibitors of NDM-1. This indicates that for NDM-1 inhibition, either the aromatic ring needs to have a free hydroxy group, an amide moiety, or the protonated quaternary amine has an adverse effect on the interaction with the NDM-1 binding pocket.

Assessing the GIM-1 activity data, the tripeptide analogue **16o** was the only possible lead candidate, which highlights that interaction with the binding pocket was lost by modification of the hydroxyphenyl core. The aromatic thiophenes or the aminocyclohexyl scaffold are unable to engage in interactions in the GIM-1 binding pocket, and the loss of binding by the core-change could only be partially compensated by attaching several aromatic amino acid residues to the amide linker. The measurable activity of the tripeptide analogue **16o** shows that GIM-1 as well as NDM-1 tolerate bulkier inhibitors in their binding pocket. However, the data measured on OMVs suggest that all compounds with different core than hydroxyphenyl behave similarly, and act as very weak inhibitors of GIM-1. Interestingly, the bulky tripeptide attached phosphonic acid **16o** crosses the Gram-negative outer membrane (**Figure 4.3**), despite its size and polarity.

Promising inhibitory activities against IMP-1 were observed for **16a**, and measurable activity for **15n**. This suggests that possible phosphonic acid inhibitors of IMP-1 need to be generally smaller, which corresponds to the reported findings of the IMP binding pocket being slightly narrower and more rigid. In those structures, only one aromatic moiety is tolerated on either side of the molecule. Interestingly, compound **12b** also shows IMP-1 activity,

which indicates that the orientation of the amide attached moiety is also important for IMP-1 binding, similar to that observed for VIM-2. However, the opposite effect appears for the two enzymes, namely the amide sidechain orientation that is favorable for VIM-2 is unfavorable for IMP-1 inhibition. The α -aminophosphonic acids proved to be only very weakly active against IMP-1 in the cases of both the ortho-methoxyphenyl- and pyridine-core, indicating that there is probably no additional interaction between the methoxy group and any IMP-1 amino acid residue in the binding pocket. The α -aminophosphonic acid structures may be possible to optimize for successful IMP-inhibition.

Comparing the different cores of the amide type compounds in general, the ortho-hydroxyphenyl and the thiazole-4-carboxylate phosphonic acids may have a potential to become VIM-1 inhibitors upon structure optimization, but successful VIM-1 inhibition might be easier achieved starting from the amine-type phosphonic acids. VIM-2 is a potentially good target for phosphonic acid inhibitors, as several of the structures including those possessing different core structures, amide-sidechains and the amide or amine-type compounds showed good inhibitory activity against this enzyme. NDM-1 was best inhibited by the ortho-hydroxyphenyl phosphonic acids, however also compounds possessing different core structures showed potential for NDM-1 inhibition, after structure optimization. The amine-type compounds were less successful against NDM-1. Lastly, IMP-1 was only inhibited by the smaller phosphonic acid structures, likely because of its binding pocket size. It might be inhibited by phosphonic acids, however, only after a careful structure optimization on the amide attached scaffold.

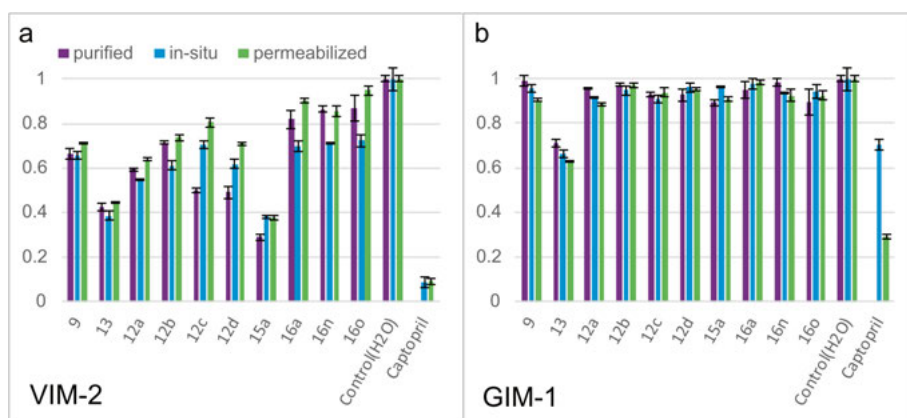


Figure 4.3. Normalized relative activities of (a) VIM-2 and (b) GIM-1. Purple bars represent the purified enzyme activity, blue bars represent the enzyme activity within OMVs and green bars represent the enzyme activity within the OMVs where the membrane was permeabilized with Triton-X.

Similar to the first set of phosphonic acids, none of the compounds possessing a modified core structure showed significant cytotoxicity on HepG2 cells (CC_{50} values are ranging between 0.8 mM for compound **15a** and 7.5 mM for compound **13**).

The binding of the most potent inhibitors of VIM-2 were evaluated with solution NMR. The pyridine-core bearing compound **12a** and the α -amino-phosphonic acid **13** were titrated to VIM-2 and the amino acid residues affected by their binding were identified (**Figure 4.4**). According to the NMR studies, these compounds bind in the same binding pocket of VIM-2, close to the zinc ions, as the phosphonic acids in **Chapter 3**. The α -aminophosphonic acid **13** showed shifted binding mode when compared to the previous compounds **6a-m** possessing a hydroxyphenyl-core and amide-linker. β -Sheet-3 (residues 67Y-72L) was much more affected by the binding of compound **13** than by the binding of inhibitors **6a-m**, highlighting the location of **13** being closer to this β -sheet and to the Zn2 site (Asp/Cys-site). This appears to be a difference in binding mode when compared to compounds **6a-m** that were bound between the two zinc ions accommodated by multiple of the active site flexible loops. Significant chemical shift perturbations were more pronounced along loop-10 (196G-216L) for compound **13**, whereas the other active site flexible loops were much less affected. Several residues surrounding the Zn2 coordination site (237I-242G) were influenced upon titration of VIM-2 with compound **13**, while only residues His240 and Gly241 showed changes for inhibitors **6a-m**, further suggesting that compound **13** is located closer to Zn2 of the active site. Compounds **6a-m** and the α -aminophosphonic acid **13** showed similar intensity decrease, line broadening (intermediate exchange) and disappearance (slow exchange) of several backbone resonances, indicating high flexibility and/or several binding modes with slower interconversion between states. To the contrary, throughout the titration, compound **12a** showed mostly fast exchange, well-defined, averaged backbone cross peaks suggesting a single dominant binding pose and confirming its moderate affinity. While the residues showing slow exchange were similar for **6a-m** and for **13** and **12a**, intermediate exchange was not observed for compound **12a**. The overall CSPs of compound **12a** can be described as a mixture of CSPs observed for compound **13** and for **6a-m**. Significant CSPs were observed upon titrating VIM-2 with **12a** in β -sheet 2 to β -sheet 3, loop-9, loop-10 and loop-12. Loop-3, connecting β -sheet 2 and 3, was affected similar to that observed upon titration with inhibitors **6a-m**, but CSPs were expanded also along the entire β -sheet 3, as observed upon titration with compound **13**. Although the most influenced region was loop-10 for the three inhibitors (**6a-m**, **13** and **12a**), in the case of compound **12a**, the affected residues all showed significant

CSPs, while the cross peaks mostly disappeared or showed intensity decrease and/or line broadening upon titration with the α -aminophosphonic acid **13**, and for **6a-m**. The affected residues in loop-12 were His240-Leu242 when VIM-2 was titrated with compound **12a**, showing detectable significant CSP and no cross peak disappearance. The results from the titrations of compound **12a** suggest a single, dominant, less flexible binding mode located close to the Zn2 site.

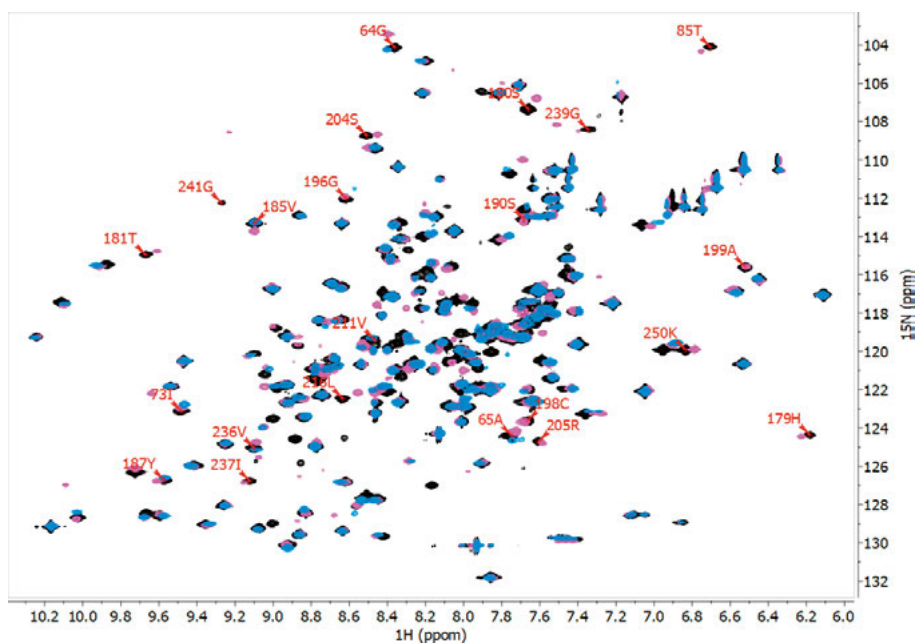


Figure 4.4. Superimposition of the ^1H , ^{15}N HSQC spectra of free VIM-2 (black) and VIM-2 in the presence of 10 molar equivalent inhibitor **12a** (magenta) and **13** (blue). Residues labeled with red showing differences in the binding of the two ligands.

Compound **13** was also co-crystallized with VIM-2 to further confirm its binding mode and to identify specific interactions with amino acid residues of the active site. The crystal structure corroborates the findings from the NMR titrations studies, highlighting the binding of the ligand closer to the Zn2 site, accommodated by residues in β -Sheet-3 and loop-10.

4.4 ADME predictions

The pharmacokinetic properties and drug-likeness of the inhibitors were evaluated computationally. According to the expectations, the introduction of a

pyridine ring was predicted to further increase the aqueous solubility, as compared to the hydroxyphenyl ring-substituted analogues. However, this simultaneously lead to slightly decreased lipophilicity, which might be undesirable. The topological polar surface area (TPSA) slightly decreased, which made these compounds comply even better with druglikeness-rules¹⁹⁵⁻¹⁹⁸ than the hydroxyphenyl core based series (**Table 4.1**). With the pyridine ring, but also with the amine linker-containing compounds, we removed a hydrogen-bond donor from the inhibitors as compared to the hydroxyphenyl based-compounds. This did not necessarily indicate the removal of interactions with the binding pocket, as no trend of decreasing activity was observed upon the removal of HBDs. A remarkable improvement was observed in the predicted gastrointestinal absorption of the compounds having pyridine core as compared to the hydroxyphenyl-ring containing compounds (**Table 4.1**).

Introduction of a thiazole-4-carboxylate ester increased the number of hydrogen-bond acceptors and rotatable bonds and lead to a higher TPSA as compared to the ortho-hydroxyphenyl inhibitors (**Table 4.1**). A favorable change was observed in the decreased plasma-protein binding (**Table 4.1**).

The carboxylic acid-type inhibitors showed similarities with the thiazole-containing compounds in ADME properties, yet with even more pronounced differences when compared to the original hydroxyphenyl-compounds. Upon changing to the carboxylic acid core, the number of hydrogen-bond acceptors and TPSA increased, contributing to a significantly decreased logP and the plasma-protein binding of these compounds is predicted to be even lower than of the previously discussed compounds (**Table 4.1**).

Comparing the ADME properties of the α -aminophosphonic acids to the amide-linker containing molecules, the primary amine encompassing compound **14** is not suitable as a drug candidate due to its limited activity and highly polar nature, the α -aminophosphonic acids **13** and **14** confer promising overall drug-like properties. They are predicted to have similarly favorable ADME features as the amide-type phosphonic acids **6a-m** (**Chapter 3**). These α -aminophosphonic acids showed however increased water solubility, decreased plasma protein binding and increased gastrointestinal absorption.

There are no other significant changes in the predicted pharmacokinetic properties of these compounds as compared to the previous series shown in **Chapter 3**, and thus they similarly comply with most criteria for oral bioavailability (e.g. Lipinski's Rule of Five¹⁹⁵, the CMC-like rule¹⁹⁶, Muegge filter¹⁹⁷ or the Veber filter¹⁹⁸).

Table 4.1. Predicted properties of compounds 6a, 12a, 15a, 16a, 13.

| Physicochemical properties | 6a | 12a | 15a | 16a | 13 |
|-----------------------------|---------|--------------------------|--------------------------------|--------------------------|-------------------------------------|
| MW [g/mol] | 313 | 298 | 376 | 265 | 307 |
| Nr. of heavy atoms | 20 | 19 | 23 | 16 | 21 |
| Nr. of aromatic heavy atoms | 11 | 11 | 10 | 5 | 12 |
| Nr. of H-bond acceptors | 5 | 5 | 7 | 6 | 5 |
| Nr. of H-bond donors | 4 | 3 | 3 | 4 | 3 |
| Molar refractivity | 75 | 71 | 85 | 55 | 81 |
| Nr. of rotatable bonds | 5 | 5 | 8 | 5 | 6 |
| TPSA [\AA^2] | 145 | 138 | 192 | 162 | 89 |
| SwissADME predictions | 6a | 12a | 15a | 16a | 13 |
| Consensus Log $P_{o/w}$ | 0.89 | 0.59 | 1.01 | -0.56 | 0.94 |
| Water solubility | Soluble | Very soluble/ Soluble | Soluble/ Moderately soluble | Very soluble/ Soluble | Very soluble/ Moderately soluble |
| BBB permeant | No | No | No | No | No |
| P-gp substrate | No | No | No | No | No |
| CYP3A4 inhibitor | No | No | No | No | No |
| CYP2D6 inhibitor | No | No | No | No | No |
| CYP2C19 inhibitor | No | No | Yes | No | No |
| CYP2C9 inhibitor | No | No | No | No | No |
| CYP1A2 inhibitor | No | No | No | No | No |
| GI absorption | Low | High | Low | Low | High |
| PreADME predictions | 6a | 12a | 15a | 16a | 13 |
| Water solubility [mg/L] | 17552 | 81657 | 14064 | 7715 | 8888 |
| logP | 1.69 | 0.94 | 1.53 | -0.02 | 2.17 |
| BBB penetration | 0.15 | 0.11 | 0.06 | 0.13 | 0.51 |
| HIA [%] | 60.0 | 65.4 | 33.1 | 17.7 | 91.9 |
| Pgp inhibition | No | No | No | No | No |
| CYP3A4 inhibition | No | No | No | No | Non |
| CYP2D6 inhibition | No | No | No | No | Yes |
| CYP2C19 inhibition | No | No | No | No | No |
| CYP2C9 inhibition | Yes | Yes | Yes | No | Yes |
| Caco-2 permeability | 0.37 | 0.38 | 0.44 | 0.36 | 0.83 |
| MDCK permeability | 4.4 | 8.4 | 2.0 | 0.7 | 232.9 |
| PPB [%] | 94.4 | 89.8 | 86.1 | 33.5 | 82.7 |

5. α -Aminophosphonic acids for improved inhibitory potency (Paper IV)

5.1 Design and predicted properties of α -aminophosphonic acids

((Benzylamino)(2-methoxyphenyl)methyl)phosphonic acid **13** was identified as a potent VIM-2 inhibitor. We designed derivatives of **13** to explore the impact of structural changes on its VIM-2 binding potency. Compound **13** was seen as an attractive starting point for further development due to its synthetic accessibility that facilitates easy structural modifications, its good inhibitory activity and ADME predicted properties.

Among phosphorous-compounds, α -aminophosphonic acids represent a so far underexplored compound class for targeting metallo- β -lactamases.²²⁵ These compounds are bioisosters of α -amino acids, offering easy modification for versatile substituent patterns and favorable aqueous solubility.²²⁶⁻²²⁸ α -Aminophosphonates might even possess antimicrobial activity.²²⁹⁻²³⁶ Despite their polarity, small α -aminophosphonic acids cross the Gram-negative outer membrane through porin channels.^{237,238} However, there is no comprehensive analyses of this scaffold so far. Understanding how structural modifications influence binding affinity, binding mode and enzyme selectivity is expected to facilitate their rational development into MBL inhibitors.

Halogenation was introduced as a central modification strategy, targeting both the hydroxyphenyl ring and the benzyl moiety attached to the amine (**Figure 5.1** and **Scheme 5.1**). Halogens are widely employed in medicinal chemistry to increase binding affinity, influence molecular properties, as they can enhance hydrophobic interactions, introduce steric bulk, and modulate electronic effects.²³⁹⁻²⁴⁹ For MBL inhibition, such modifications may improve complementarity with hydrophobic regions close to the zinc ions or with the hydrophobic active site loop 3, important for substrate binding.⁸³ Accordingly, different halogens (F, Cl, Br), substitution patterns, and substitution numbers were explored on the aromatic rings to probe pocket size, shape, and van der Waals contacts. In addition, fluorination can enhance metabolic stability by blocking labile sites.²⁴⁷⁻²⁴⁹

Hydrophobicity and conformational flexibility were further adjusted by incorporation of methyl groups either to the benzyl ring or to the secondary amine of **13**. Alternatively, the linker between the amine and the unsubstituted phenyl ring was elongated by one methylene unit. Increased flexibility may enable adaptation to isoenzymes that differ in loop conformations or residue compositions, whereas methylation of the amine decreases hydrogen-bond donor capacity and adds steric bulk that may alter binding orientation. Methyl substitution on the benzylamino ring increases hydrophobic surface area and can subtly influence aromatic ring orientation and electronic properties, thereby adjusting binding affinity and selectivity without significantly compromising solubility. As the phosphonic acid moiety confers good aqueous solubility, small hydrophobic substituents can improve lipophilicity, aiding Gram-negative outer membrane penetration.

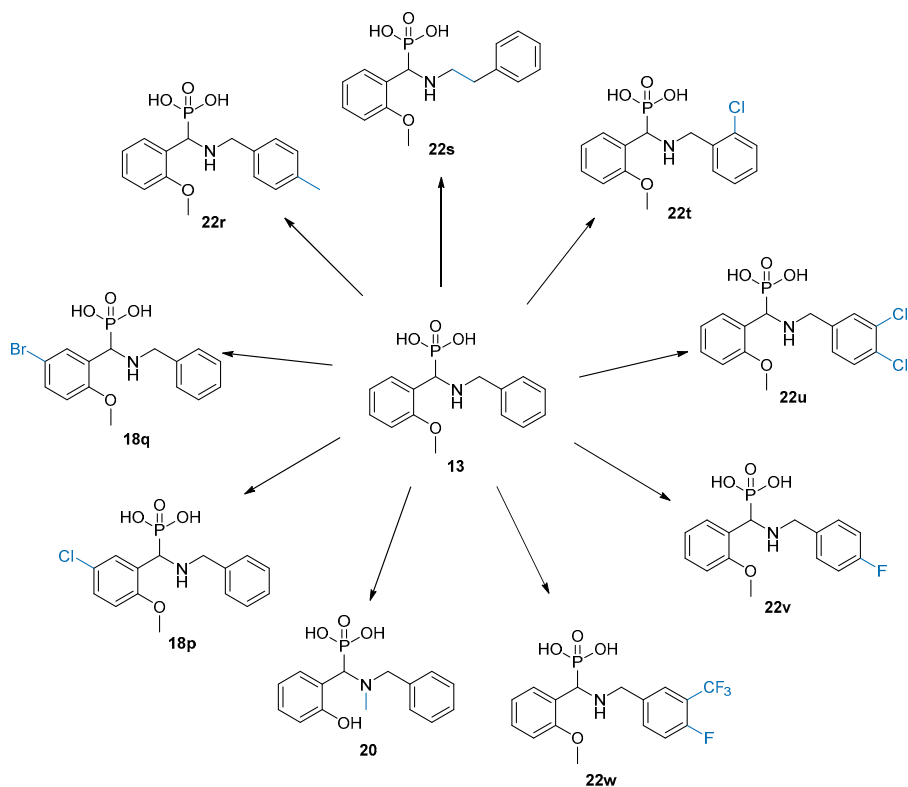


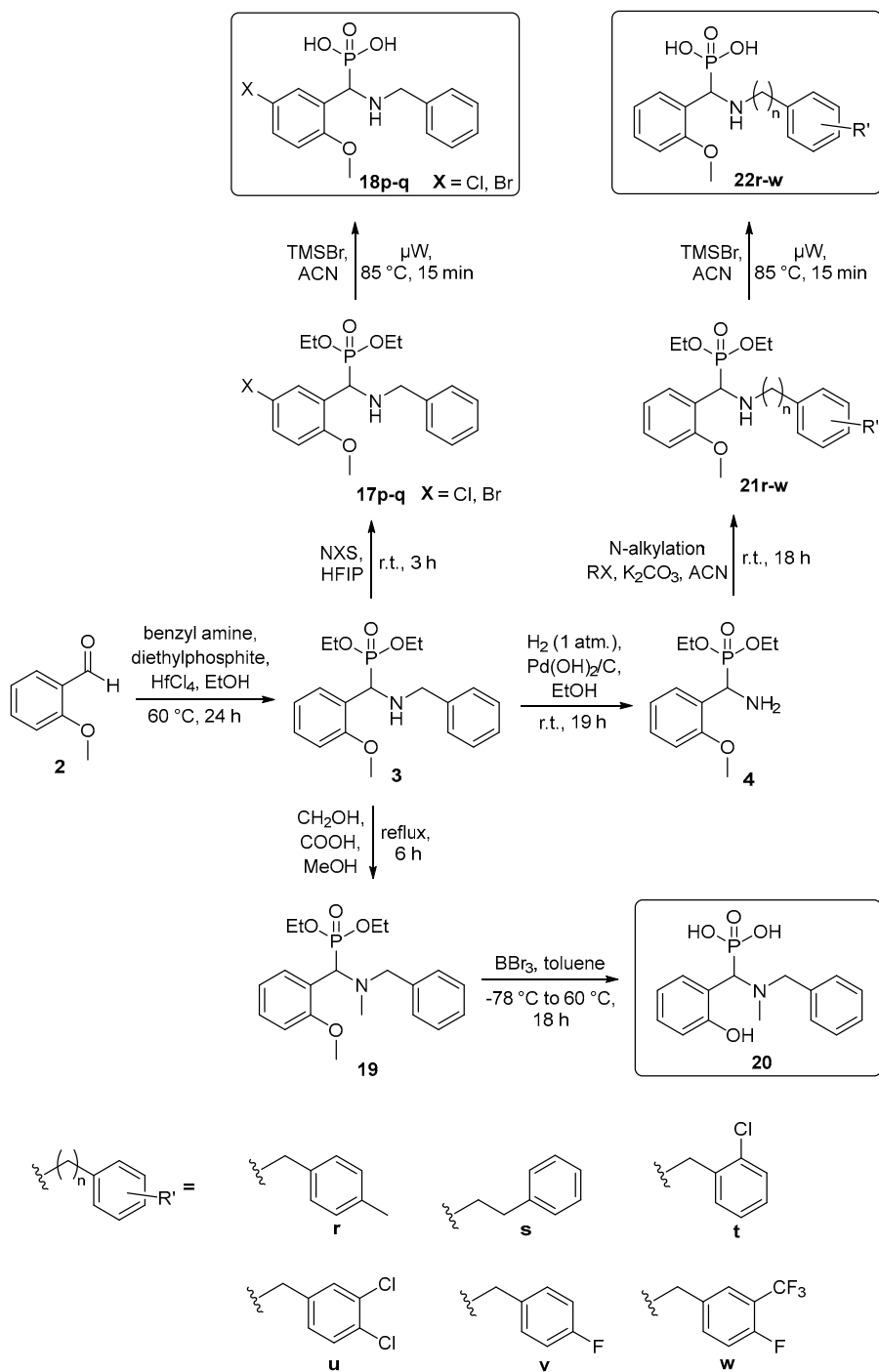
Figure 5.1. The structurally modified α -aminophosphonic acid inhibitors. Modifications highlighted with blue.

These compounds were designed to balance pharmacokinetic properties and to comply with the most common drug-likeness rules. All of the designed α -

aminophosphonic acids fulfil the criteria of most commonly used filters (e.g. Lipinski, CMC, Veber, Egan, Muegge, MDDR, WDI) meaning that the compounds' structure and physicochemical properties resemble those of typical orally bioavailable approved drugs. Their molecular weight is below 400 g/mol, they have 3 hydrogen bond donors, 5-6 hydrogen bond acceptors (except compound **22w** with 9 HBAs), 5-7 rotatable bonds, 88.6 Å² TPSA, show good aqueous solubility but also favourable lipophilicity, and are predicted to have high gastrointestinal absorption, no blood-brain barrier penetration, no CYP-enzyme inhibition and acceptable plasma protein binding (except compound **22w**).

5.2 α -Aminophosphonic acid synthesis

The synthetic route of the α -aminophosphonic acid inhibitors **18p-q**, **20** and **22r-w** is summarized on **Scheme 5.1**. α -Aminophosphonate **3**, the common structure for derivatization, was synthesized with the Kabachnik-Fields reaction as described in **Chapter 3**. Compound **3** was then modified with 1-3 synthetic steps to provide a variety of α -aminophosphonic acid inhibitors. Thus, the secondary amine of **3** was methylated with paraformaldehyde and formic acid in methanol within 6 hours to give compound **19**, or debenzylated with hydrogen gas and palladium catalyst in ethanol to obtain compound **4**. Alkylation of the primary amine of **4** with a variety of aryl halides in the presence of potassium carbonate as a base allowed the synthesis of α -aminophosphonate ethyl esters **21r-w**. Alternatively, compound **3** was selectively mono-halogenated on the para-position to the methoxy group on the methoxyphenyl ring with NBS or NCS in HFIP as solvent, at room temperature in 3 hours yielding compounds **17p-q**. The last step of hydrolysing the diethyl phosphonates was carried out with the McKenna reaction using TMSBr or TMSI under microwave (μ W) conditions at 85 °C in 15 min affording compounds **18p-q** and **22r-w** or with BBr₃ in toluene at 60 °C to obtain compound **20**. The final compounds were purified by preparative RP-HPLC resulting in 55-78 % yield. In total, 9 new α -aminophosphonic acids were synthesized and evaluated for MBL inhibition (**Figure 5.1**).



Scheme 5.1. The synthesis of the α -aminophosphonic acids.

5.3 Inhibition of VIM-2 and GIM-1

To assess the enzyme binding affinity of the 9 new α -aminophosphonic acids, their IC_{50} values were measured against VIM-2, NDM-1 and IMP-26 (**Table 5.1**). Corroborating our preliminary observation for molecule **13**, these α -aminophosphonic acids were most active against VIM-2, while only some were slightly active against NDM-1, and they were inactive against IMP-26. It has been reported difficult to develop potent inhibitors against IMP-type enzymes^{58,94,95,133,250} and so far, α -aminophosphonic acid-type compounds were not tested against them. All compounds showed good activity against VIM-2 with IC_{50} values ranging from high nanomolar to low micromolar. The compounds could be divided into three groups based on their potency. Compound **18q** bearing a bromide on the methoxyphenyl ring and compound **22t** with a chloride in the ortho position on the benzylamino ring, were the most active with 728 nM and 1.3 μ M IC_{50} , respectively. The second group included compounds **18p** and **22s** with a 5-10-fold activity decrease. Compound **18p** is equipped with a chloride on the methoxyphenyl ring (IC_{50} 7.0 μ M) and compound **22s** possesses the flexible phenethylamino ring (IC_{50} 7.5 μ M). The remaining compounds **20**, **22r**, **22u-w** belong to the least active group with ~22-52-fold increase in IC_{50} values as compared to **18q**. These compounds still showed moderate activity with IC_{50} values between 16-38 μ M against VIM-2. From our IC_{50} measurements, the halogenation on the methoxyphenyl group, together with increasing the flexibility on the second, amine-attached substituent was the most beneficial for increased VIM-2 potency. The modifications on the second, benzylamino ring were not advantageous when compared to the starting molecule **13**, but all the modified compounds remained active against VIM-2. This suggests, that the second aromatic ring is needed but its substitution pattern does not play a crucial role in VIM-2 binding. Similar conclusion can be drawn about the amine group of the molecule, where the methyl protection did not significantly influence the binding potency, indicating that any hydrogen bonding present must be weak. However, it is important to note that for the *N*-methylated compound **20**, the first ring has an unprotected hydroxy group capable of compensating with additional hydrogen bonding interactions.

The most potent inhibitors of NDM-1 were compounds **22u**, **22w** and **18q**. These α -aminophosphonic acids are certainly not suitable clinical inhibitors of NDM-1, however it is to note, that the original compound **13** was completely inactive against NDM-1, while with simple structural modifications, promising inhibitor candidates were achieved.

Table 5.1. The IC_{50} values of the α -aminophosphonic acid compounds suggest good inhibitory activity against VIM-2.

| Inhibitor | IC_{50} (μ M) | |
|------------|----------------------|-------|
| | VIM-2 | NDM-1 |
| 20 | 19 | 681 |
| 18p | 7.0 | 204 |
| 18q | 0.73 | 60 |
| 22r | 16 | 196 |
| 22s | 7.5 | 288 |
| 22t | 1.3 | 165 |
| 22u | 38 | 58 |
| 22v | 21 | 767 |
| 22w | 21 | 82 |

The Gram-negative membrane permeability of the inhibitors was addressed using outer membrane vesicles, which carry VIM-2 or GIM-1 in their lumen.²⁰⁵⁻²⁰⁷ Normalized relative activities of the enzymes were measured both on the purified enzymes and on the enzymes within OMV-s (without and with permeabilizing the membrane) (**Figure 5.2**). L-Captopril and water were used as positive and negative controls, respectively. All α -aminophosphonic acids showed decrease in VIM-2 activity within the OMV-s suggesting their ability to cross the Gram-negative outer membrane and successfully reaching their target in the periplasm. The most potent compounds **18p-q** and **22t** showed comparable potency to L-captopril, a known MBL inhibitor often used as a positive reference (IC_{50} 4.4 μ M²⁵¹). The compounds demonstrated activity against GIM-1 as well (**Figure 5.2b**). Whereas there was no clear trend in the substitution's influence on VIM-2 or NDM-1 potency, in the case of GIM-1 it is clear that halogenation on the 2-methoxyphenyl ring (**18p-q**) has a significant advantage compared to alterations on the amine attached scaffold. Importantly, compound **18p** and **18q** outcompeted L-Captopril. Both the VIM-2 and GIM-1 data demonstrate that despite the polarity of the α -aminophosphonic acids, the Gram-negative membrane permeability is not a limiting factor as the relative activities of the purified enzymes are almost the same as for the enzymes inside the OMVs (**Figure 5.2**).

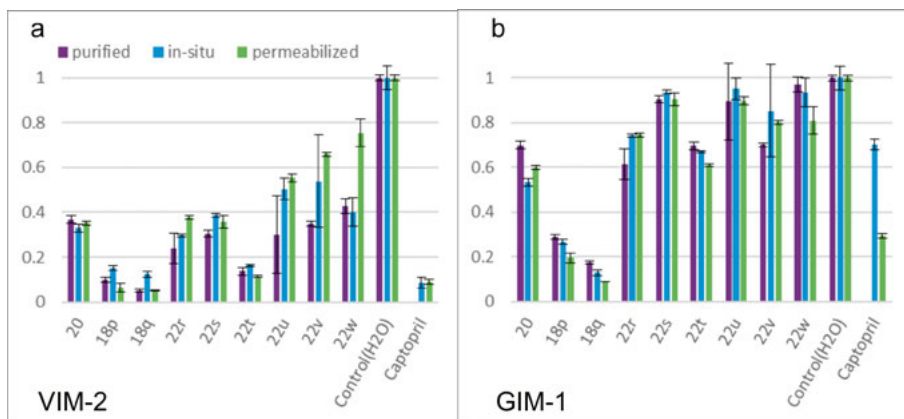


Figure 5.2. Relative activities of (a) VIM-2 and (b) GIM-1 in the presence of the α -aminophosphonic acid inhibitors.

As the compounds showed good activity against purified VIM-2 as well as for the VIM-2-containing OMVs, their efficacy was subsequently evaluated in whole bacterial cells. This was performed to assess whether in addition to their binding, they would be able to reach their target in the periplasm and exert a synergistic effect in combination with a β -lactam antibiotic. The minimal inhibitory concentration (MIC) of meropenem, a last-resort carbapenem antibiotic, was determined on VIM-2 expressing *E. coli* using 500 μ M of the α -aminophosphonic acid inhibitors (**Figure 5.3**). All the compounds decreased the MIC of meropenem from 1 mg/L to 0.06 mg/L indicating their ability of crossing the outer membrane, avoiding rapid efflux, reaching and binding VIM-2 in the periplasm and being stable under cellular conditions. The \sim 16-fold decrease in meropenem MIC might suggest the potential for these α -aminophosphonic acids to restore the susceptibility of VIM-2 expressing strains to meropenem.

The α -aminophosphonic acids had CC_{50} values ranging between 0.9 to 4.3 mM tested on HepG2 cells. This translates to selectivity index values between 13 and 1099, indicating that these compounds are non-cytotoxic.

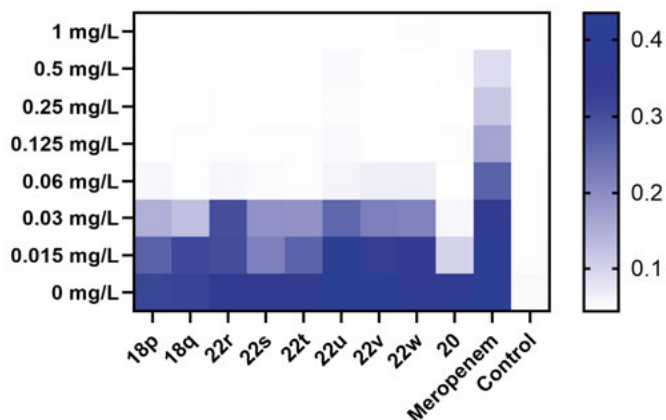


Figure 5.3. MIC heat map showing no bacterial growth when α -aminophosphonic acid inhibitors (500 μ M) were used in combination with 0.06 mg/L meropenem.

The most potent compound **18q** was titrated to VIM-2. The most affected VIM-2 residues were located loop-3, β -sheet 3, loop-10 and loop-12 (only the Zn²⁺ binding residue His240 and its neighbouring amino acid Gly241). The conserved active-site perturbations indicate a similar binding mode as that of analogue **13** and they occupy similar region of the active site (**Figure 5.4**). However, residues at the N-terminus (33Y-39I), β -sheet 1 (44V-47Y) and C-terminus (254N-262R) which are distant from the catalytic pocket, showed significant chemical shift perturbations when the brominated compound **18q** was titrated to VIM-2. The distal CSPs likely reflect subtle conformational or dynamic effects propagated through the protein scaffold. Bromine is bulky, polarizable and hydrophobic which may result in increased van der Waals contacts, improved hydrophobic packing and/or better shape complementarity in the binding pocket. The bromine may slightly alter how the ligand sits in the pocket. According to the NMR chemical shift perturbation results, compound **18q** locks VIM-2 into a more defined inhibited conformation, which is consistent with its increased affinity. The bromine does not alter the binding mode but it changes how strongly and how rigidly the compound binds. It significantly increases affinity by packing and polarizability effects, and the formation of a halogen bond cannot be excluded. The increased affinity probably results from thermodynamic strengthening of the interactions. It is not uncommon in drug development that a halogen substitution significantly enhances affinity while preserving the fundamental binding mode.²⁴⁰

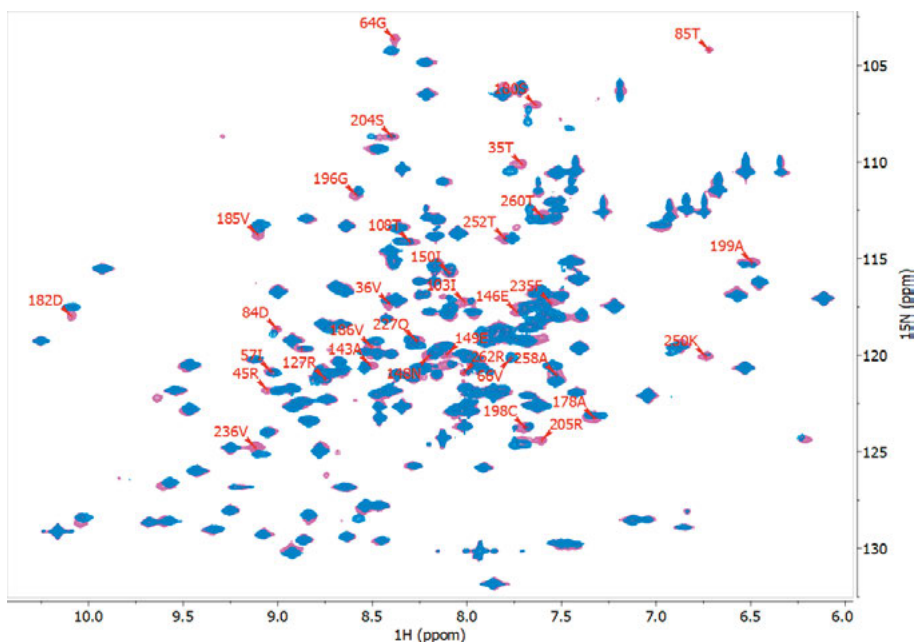


Figure 5.4. Superimposition of the ^1H , ^{15}N HSQC spectra of VIM-2 in the presence of 10 molar equivalent inhibitor **18q** (magenta) and **13** (blue). Residues labeled with red showing differences in the binding of the two ligands. Residues far from the active site were significantly affected by the titration of compound **18q**.

5.4 NMR backbone resonance assignment of German-imipenemase 1

GIM-1 represents an interesting target within the B1 MBL subclass as it has the most different binding site with more aromatic residues as compared to other B1 MBLs.^{107,108} Understanding the binding of the most different member of the MBL B1 subfamily might contribute to the design of broad spectrum inhibitors. Currently there is no co-crystal structure available of GIM-1 together with an inhibitor, and the NMR assignment of this enzyme is not known. No NMR studies were previously reported on GIM-1. The availability of resonance assignment will enable the solution NMR investigation of the binding of GIM-1 inhibitor candidates.

We expressed single ^{15}N - and double ^{15}N , ^{13}C -labeled GIM-1, consisting of 232 amino acid residues, and performed ^1H , ^{15}N HSQC experiments to address the stability of the enzyme. ^1H , ^{15}N HSQC spectra were recorded at 25 °C once per day on single labelled GIM-1, for 6 days, indicating that the enzyme was stable. No disappearance of cross peaks was observed. This was important as backbone resonance assignment needs several days' spectral acquisition. A

series of variable temperature ^1H , ^{15}N HSQC experiments were measured between 7–37 °C to find the ideal temperature for the backbone assignment (**Figure 5.5**). The best result, meaning largest number of well resolved peaks, was obtained at 30 °C. In order to identify the resonance frequencies (chemical shifts) of GIM-1's backbone nuclei (N, C_α , C_β , H_α , C=O), the 3D HNCA, HNCACB, HNcoCA, HNcoCACB, HNCO and HNcaCO experiments were measured on 250 μM GIM-1 at 30 °C and pH 7.0, in a solution containing 20 mM HEPES, 0.1 mM ZnCl_2 , in 90% H_2O /10% D_2O .

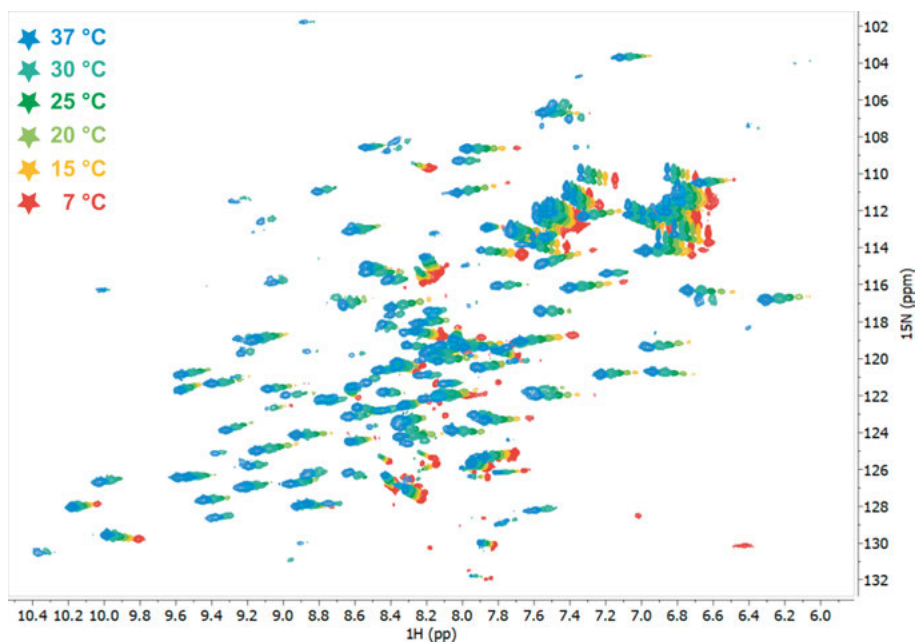


Figure 5.5. Superimposition of the ^1H , ^{15}N HSQC spectra of GIM-1 at 7–37 °C.

During the data analysis, first specific amino acids that have typical C_α and C_β chemical shifts (δ) were identified. For instance, glycines only have C_α and no C_β cross peaks, whereas threonines and serines have their δC_β at higher chemical shifts than their δC_α and this δC_β is also at a much higher chemical shift than the usual amino acid C_β chemical shift range. Furthermore, alanines have their δC_β at a much lower chemical shift than all the other amino acids. These were easily recognizable diagnostic features, providing suitable starting points for the assignment. Each ^1H , ^{15}N HSQC cross peak represented an amino acid residue's δH and δN (in case of no overlap) and had a corresponding δC_α , δC_β (except glycines) and carbonyl δC . Connectivity was established by finding neighbouring residues as e.g. in the HNCA spectrum one could see the δC_α of

amino acid residue (i) and in the HNcoCA one could see the δC_α of the neighbouring amino acid residue (i-1). This latter δC_α (i-1) from the HNcoCA should be found then in the HNCA as the chemical shift of another amino acid residue (j) and one could go on to the neighbour of this amino acid residue in the HNcoCA where one could find then the δC_α (j-1) (**Figure 5.6a**). The process was similar when examining the HNCO and HNcaCO spectra. Here however, one could identify the carbonyl δC of amino acid residue (i) from the HNcaCO experiment, and the δC of the neighbouring amino acid residue (i-1) from the HNCO experiment (**Figure 5.6b**). This process provided valuable information about the sequential connectivity of amino acids in the protein backbone. Furthermore, the HNCACB and HNcoCACB experiments gave us C_β cross peaks and information about the δC_β of amino acid residue (i) and (i-1).

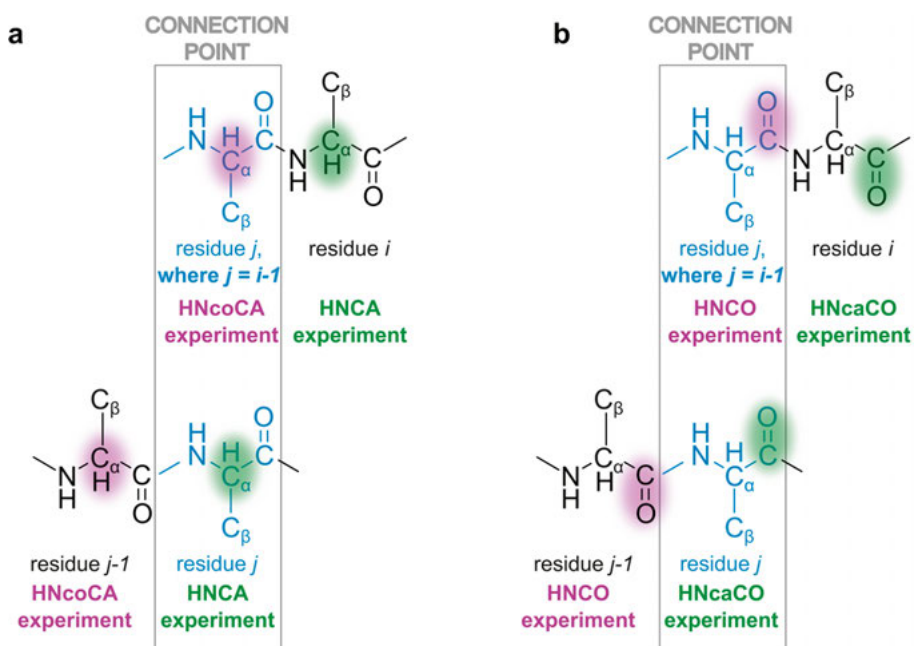


Figure 5.6. NMR backbone resonance assignment connection points using the (a) C_α - or the (b) carbonyl C cross peaks.

Backbone assignment is a prerequisite for determining the three-dimensional structure of proteins, understanding their dynamics, and studying their interactions with ligands or other molecules by solution NMR spectroscopy. Similar to all metallo- β -lactamases in the B1 family, GIM-1 is a highly flexible enzyme. Accordingly, 21 % of the cross peaks are not visible in the spectra most probably due to intermediate exchange regime dynamics and/or the long helical regions. In the GIM-1 sequence, ten amino acids are prolines that lack the backbone NH

6. Peptidic phosphonic acids for IMP-1 inhibition

6.1 Design introducing natural amino acids

The binding studies of the first series (**Chapter 3**) of phosphonic acid-based inhibitors revealed that there is an empty space in the binding pocket surrounded with acidic amino acid residues offering H-bonding sites. Therefore, we decided to change the amide attached aromatic phenyl, thiophene and benzothiophenes moieties, which did not interact strongly with the binding pocket and were mostly solvent exposed, to natural amino acids encompassing sidechains capable of H-bonding to the amino acids of the binding site (**Figure 6.1**). Using natural amino acids in drug design has a series of advantages.^{252,253} They offer a diverse range of functional groups capable of interacting with biological targets, thereby improving binding affinity and specificity. Thereto, they are readily available and cheap, are usually recognized and processed by biological systems, enhancing bioavailability and metabolic compatibility. Being the building blocks of proteins, natural amino acids are well-tolerated and unlikely to cause adverse reactions, making them a safe choice in drug development.²⁵³ The primary goal with the introduction of amino acids was to optimize the interactions within the enzyme's binding pocket. This might decrease oral bioavailability and membrane permeability, however, these properties can subsequently be adjusted when the functional groups important for binding have been identified.

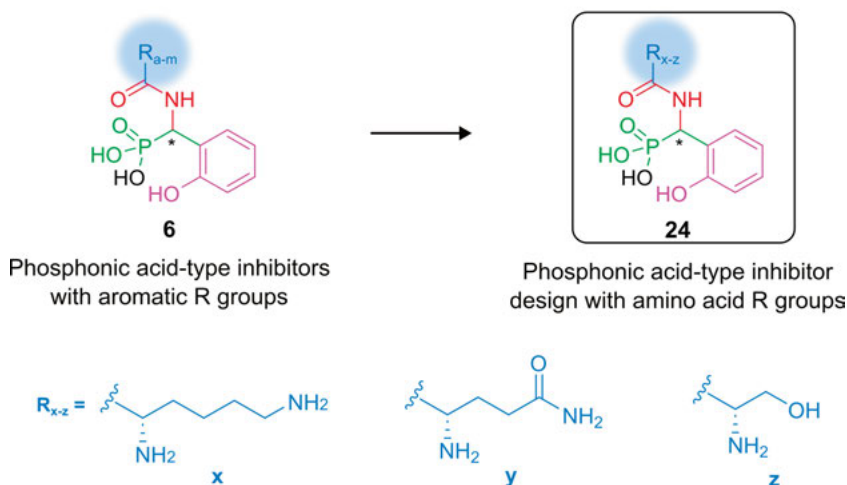


Figure 6.1. The amino acid substituted phosphonic acid inhibitors.

6.2 Docking simulations

To identify amino acids to be attached to the phosphonic acid core, the possible target compounds were docked to VIM-2 and NDM-1 and those having the best docking scores and the most possible interactions within the binding pocket were selected (Lys, Ser and Gln) for synthesis.

Computational docking of the lysine-containing molecule **24x** (**Figure 6.1**) predicted that the two stereoisomers have similar binding mode and orientation (**Figure 6.2a**), both showing comparable affinity to VIM-2 (docking scores (DS) of -9.1 kcal/mol (*RS*)- and -9.2 kcal/mol (*SS*)-isomer). Both of the amino groups of lysine were predicted to possess H-bonding and salt bridges with Asp117, Asp213 and Glu146 for both stereoisomers. In contrast, these stereoisomers docked to NDM-1 were bound with 180 ° flipped orientation (**Figure 6.2b**) and with slightly worse their docking scores (DS of -8.9 kcal/mol (*RS*)- and -8.5 kcal/mol (*SS*)-isomer) than those for VIM-2. The lysine amino group was predicted to interact with Asn220, Phe70, His250 or to Glu152 and Asp223 of NDM-1.

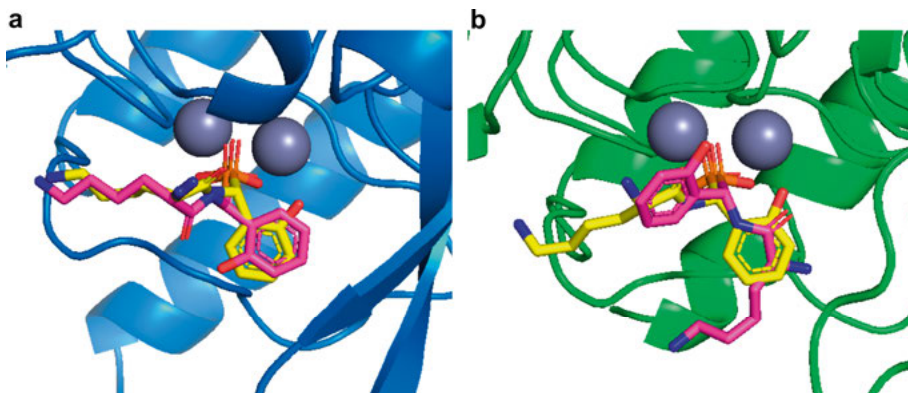


Figure 6.2. The binding poses of *(RS)*-24x (yellow) and *(SS)*-24x (magenta) when binding to (a) VIM-2 and (b) NDM-1.

The *(RS)*-diastereomer of compound **24y**, which possesses a glutamine moiety (**Figure 6.1**), was predicted to bind VIM-2 with higher affinity, with docking score of -9.4 kcal/mol, while its *(SS)*-diastereomer had a docking score of -7.9 kcal/mol, yet still fitted into the binding pocket. This difference is attributed to the different binding interactions of the two isomers. While for the *(RS)*-isomer, both the amide NH₂ and the carboxylic O was predicted to bind along with the amino group, for the *(SS)*-isomer the amide NH₂ was solvent exposed. However, the orientation of the core structure of the two stereoisomers remained unaltered, despite the amino acid moiety having a different placement in the binding pocket (**Figure 6.3a**). The two stereoisomer of compound **24y** docked to NDM-1 were flipped by 180 ° (**Figure 6.3b**), with docking scores of -9.0 kcal/mol for *(RS)*-isomer) and -8.4 kcal/mol for *(SS)*-isomer. The primary amino group of glutamine was predicted to not have any interactions to the binding pocket of NDM-1.

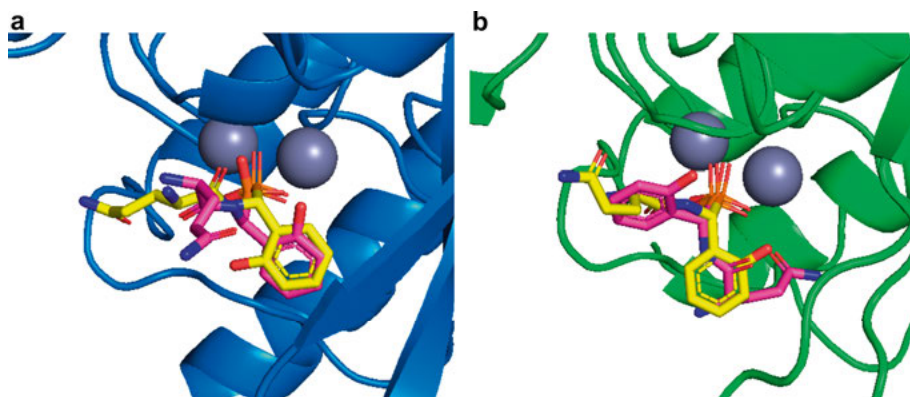


Figure 6.3. The binding poses of compound (RS)-24y (yellow) and (SS)-24y (magenta) docked to (a) VIM-2 and (b) NDM-1.

Compound **24z** functionalized with a serine moiety (**Figure 6.1**) had comparable docking scores to the above analogues (DS_{VIM-2} of -9.1 kcal/mol (RS)- and -8.6 kcal/mol (SS)-isomer). When docked to VIM-2, the (SS)-isomer showed the same orientation as the (RS)-isomer, with only the serine moiety being placed differently in the pocket whereas the arylphosphonic acid core remaining oriented identically for the diastereomers (**Figure 6.4a**). The amino group of the serine moiety was predicted to interact with Asp117, whereas its hydroxy functionality to H-bond to Trp87. The two stereoisomers of compound **24z** in the NDM-1 pocket were flipped by 180° (**Figure 6.4b**), with slightly worse docking scores than the previous amino acid substituted analogues (DS of -8.3 kcal/mol (RS)- and -7.9 kcal/mol (SS)-isomer).

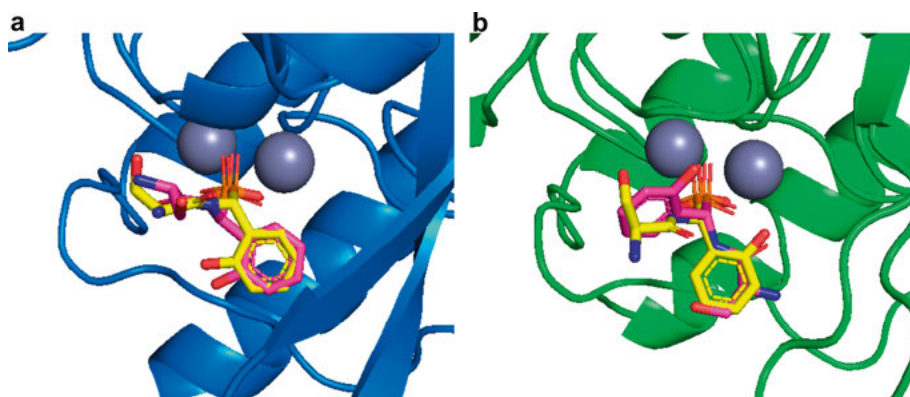


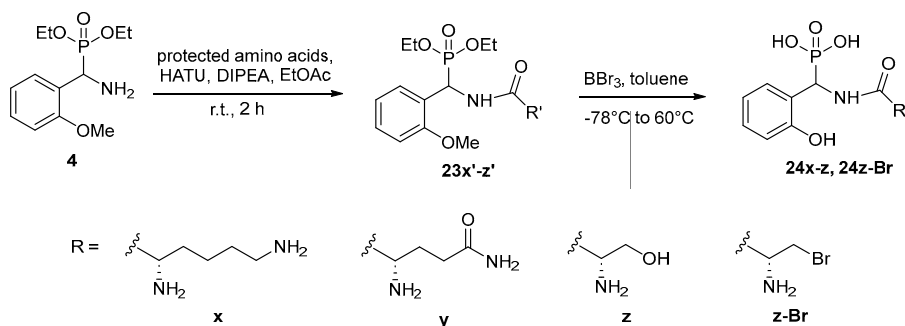
Figure 6.4. The docked binding poses of compound (RS)-24z (yellow) and (SS)-24z (magenta) to (a) VIM-2 and (b) NDM-1.

Bigger differences between the docking scores of the members of this inhibitor series was observed than for the previous series of phosphonic acids, most probably because of the additional and more specific interactions the amino acid moieties were predicted to possess within the enzymes' binding pocket. Comparison of the ligand efficiencies (LE) of these compounds rather than their docking scores may therefore be more informative. The ligand efficiency of a compound describes its binding free energy value normalized by its number of heavy atoms.²⁵⁴ Comparing ligand efficiencies is advised when the sizes of the compounds to be compared are different, as this provides a measure of how efficiently each atom contributes to binding. This can be important because larger molecules often have higher docking scores simply due to having more atoms, which does not necessarily reflect that they would be better binders. Judging solely from the ligand efficiencies, the (*RS*)-isomer of the serine-substituted inhibitor (LE = -0.48 kcal/mol for VIM-2 and -0.44 kcal/mol for NDM-1) was the most promising among the candidates. However, the differences were not significant and in general, it is rarely a good idea to base a drug development decision on docking or on ligand efficiency score only.

Overall, the amino acid moieties in this series of compounds are predicted to form H-bonding and salt bridges with the aspartic acid and glutamic acid residues, and some π -cation interactions with tyrosine in the MBL binding pocket. The key interaction between the phosphonic acid core and the zinc ions of the enzymes remains the most important for binding.

6.3 Synthesis of the peptidic inhibitors

The synthetic route (**Scheme 6.1**) was adapted from the first series (**Chapter 3**), and compound **4** was prepared accordingly. The amide coupling reaction time could be reduced to 2 hours retaining good yields (64-88 %), using protected amino acids (Boc, Fmoc, Trt) for the reaction. The deprotection step was done using boron tribromide which effectively removed the amine protecting groups along with cleaving the ether and hydrolysing the phosphonic ester in one step. Using natural amino acids, a second stereocenter was introduced, yielding a pair of diastereomer products. The final compounds were purified with preparative RP-HPLC accomplishing the separation of the diastereomers of compounds **24y-z**. Reacting compound **23z'** with boron tribromide additionally resulted in the brominated analogue **24z-Br** that was separated on HPLC and also tested against metallo- β -lactamases.



Scheme 6.1. The synthesis of the amino acid substituted phosphonic acid-type inhibitors.

6.4 Enzyme inhibitory activities

The half-maximal inhibitory activities were measured with the fluorescence method on VIM-1, VIM-2, NDM-1 IMP-1 and GIM-1 (**Table 6.1**). While some of these compounds showed measurable activity against VIM-1, VIM-2 and NDM-1, they were not suitable inhibitors for these enzymes and generally performed worse than the aryl-substituted analogues **6a-m** in **Chapter 3**. This suggests that increasing the number of HBDs and HBAs is not a viable strategy for improving potency against these enzymes or that these highly polar molecules were disrupting the H-bonding network of the enzymes' active site. Interesting to note is that NDM-1 is less sensitive to the alteration of the amide attached moiety than to the change of the aryl core, indicated by the generally better inhibitory activities for the amino acid substituted compounds keeping the 2-hydroxyphenyl core (**24x-z-Br**) than for the compounds with altered core structures described in **Chapter 4**. However, these compounds showed promising activity against IMP-1. This observation is consistent with our findings in **Chapter 4**, indicating that improved inhibition of IMP-1 is achieved when only one aromatic moiety is present. This is likely due to the slightly narrower active site of IMP-1 compared to other B1 MBLs. In most cases, we observed differences in the binding potency of the two stereoisomers of the compounds presented in this chapter, as predicted by molecular docking. This suggests that specific interactions with the amide attached amino acids occur within the binding pocket. This is further corroborated with the observation that these differences decreased when the serine-containing compound **24z** was changed to the brominated analogue **24z-Br**.

Table 6.1. The activities of the amino acid substituted phosphonic acids on purified metallo- β -lactamases measured by Gurleen Kaur at the University of Oxford. Promising activities are highlighted with green.

| Compound | IC_{50} (μM) | | | | | Stereochemistry |
|-----------------|-----------------------|-------|-------|-----------|-------|-----------------|
| | VIM-1 | VIM-2 | NDM-1 | IMP-1 | GIM-1 | |
| 24x | 389 | 102 | >1000 | 282 | >100 | mixture |
| 24y-1 | 135 | 74 | 62 | 26 | >100 | diastereomer 1 |
| 24y-2 | >1000 | 141 | >1000 | 112 | >100 | diastereomer 2 |
| 24z-1 | >1000 | 389 | 178 | 87 | >100 | diastereomer 1 |
| 24z-2 | >1000 | 200 | 54 | 23 | >100 | diastereomer 2 |
| 24z-Br-1 | >1000 | 195 | 65 | 28 | >100 | diastereomer 1 |
| 24z-Br-2 | >1000 | 117 | 72 | 38 | >100 | diastereomer 2 |

This was the only series in this work designed partially relying on docking to VIM-2 and NDM-1. However, the compounds showed worse inhibitory activity than the first series shown in **Chapter 3**, the crystal structure of which were used as a starting point for the docking. This highlights the difficulties of computational simulation for successful MBL inhibitor design, as discussed in **Chapter 2.4**. However, the activity against IMP-1 matches with our conclusions from the core-changed derivatives shown in **Chapter 4**. Hence, for successful IMP-inhibition, only one aromatic moiety is preferred. IMP-1's slightly narrower binding site accommodates the more flexible and aliphatic natural amino acid sidechains better than the previous, bulkier aromatic thiophenes and benzothiophenes. It has been proven very difficult to obtain inhibitors of IMP-1. Potential IMP-inhibitory structures are therefore highly valuable given the high clinical relevance of this enzyme. There are very few co-crystal structures of IMP-1 and its NMR backbone assignment is not available. Accordingly, experimental binding information of ligands to IMP-1 is very limited making inhibitor design extremely difficult. It is very common in literature that the transition state analogue and zinc-targeting inhibitor strategies still do not work on IMP-1 despite these being common features of the B1 MBL family.

6.5 ADME property predictions

The ADME properties of this series were computationally evaluated. Attachment of amino acids to the phosphonic acid core, replacing aromatic moieties, resulted in a significant decrease in logP and an improvement in aqueous solubility. The lipophilicity decrease is undesirable and is expected to signifi-

cantly reduce the Gram-negative bacterial membrane permeability. To overcome this issue, at least partially, the phosphonic ester moiety may be mono-hydrolysed, instead of hydrolysing it completely (**Figure 6.5**). The mono-ethyl ester analogue of the compounds is predicted to still fit into the binding pocket and keep the key interaction between the phosphonic acid moiety and the zinc ions, and their synthesis is also achievable.⁶⁹ Another option could be to incorporate fluorine atom(s) into the molecule, a common strategy in medicinal chemistry to alter the ADME properties without significantly effecting activity.^{249,255} In our case, a fluorine atom could be added to the aromatic ring. (**Figure 6.5**) The gastrointestinal absorption was predicted to be low thanks to the hydroxyphenyl core. The change of the aryl moieties to amino acids increased the topological polar surface area, which violates most drug-likeness rules. However, upon this substitution, an improvement was observed with significantly decreased plasma protein binding. This is desirable, as only the free, non-bound molecules are able to act as MBL inhibitors. The CYP2C9 inhibition is attributed to the aromatic moiety attached to the amide side, as inhibition was predicted for both the hydroxyphenyl- and pyridine-based series but not for the amino acid functionalized series. A potential CYP2D6 and CYP3A4 inhibition is, however, predicted for compounds containing amino acids with a sidechain amide motif, such as glutamine and asparagine.

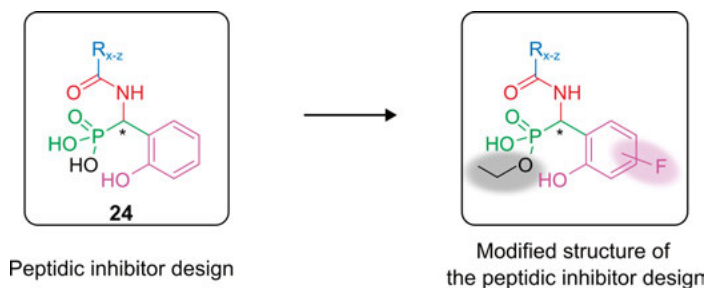


Figure 6.5. Modification of the peptidic inhibitor design to optimize ADME properties.

7. Halogenated arylphosphonic acids inhibit VIM-2

7.1 Design of the inhibitors

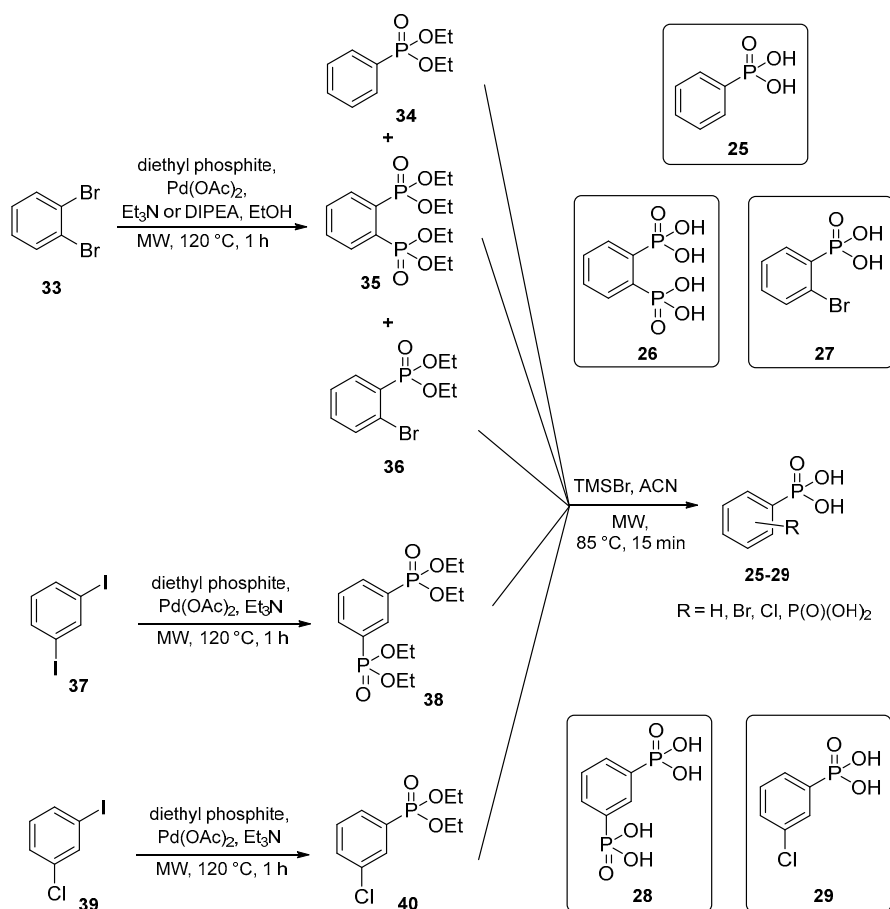
The phosphonic acid moiety played the most important role for binding of all our previous inhibitors designed in this thesis. Furthermore, halogenation has proved its ability to significantly enhance inhibitory potency. To further evaluate the potential of halogenation and of introducing a second phosphonic acid moiety for improving MBL inhibition potency, a series of halogenated aryl phosphonic acids as well as aliphatic and aromatic bisphosphonic acids were synthesised (**Schemes 7.1** and **7.2**).

Bisphosphonic acids are used to treat osteoporosis and other bone diseases.²⁵⁶⁻²⁵⁸ Their two phosphonic acid groups may interact with both zinc ions of the B1 MBL active site. To investigate the optimal distance between the two phosphonic acid groups, 1,2- and 1,3-bisphosphonatedbenzene and aliphatic bisphosphonic acids with different linker lengths were synthesised. The flexible aliphatic bisphosphonic acids were expected to allow the adaptation to different zinc distances across isoenzymes. In contrast, the aromatic bisphosphonic acids introduced rigidity, and a well-defined spatial orientation between the two phosphonic acid groups. Halogenated arylphosphonic acids may alter binding affinity, as it was observed for the α -aminophosphonic acid inhibitors in **Chapter 5** and alter physicochemical properties. Overall, this compound set was designed to explore metal coordination, scaffold flexibility, hydrophilic versus hydrophobic and electronic effects. A few examples of bisphosphonic acids were tested for MBL inhibition and they were identified as promising candidates.²⁵⁹⁻²⁶¹ However, the binding was not experimentally explored so it is not known whether those compounds coordinate to the zinc ions with both of their phosphonic acid groups.

7.2 Microwave synthesis

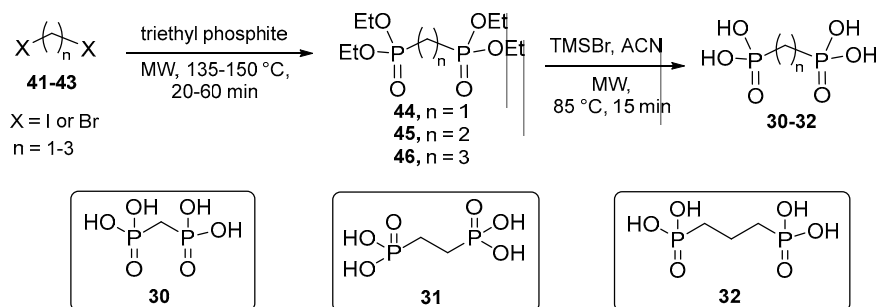
The target aliphatic and aryl phosphonic acids were synthesized using microwave-assisted phosphorous chemistry (**Schemes 7.1** and **7.2**). These reactions use microwave irradiation instead of conventional heating that enables a more

uniform and controlled temperature profile. Microwaves heating allows significantly shorter reaction times,²⁶² offering energy efficiency, cost-effectiveness, and often milder reaction conditions, higher yields and higher purity, providing improved sustainability.²⁶²⁻²⁶⁵ The target compounds were synthesised from a dihalogenated starting material in two synthetic steps. To obtain the aryl phosphonic acid, the dihalogenated starting materials 1,2-dibromobenzene, 1,3-diiodobenzene or 1-chloro-3-iodobenzene were reacted with diethyl phosphite in the presence of palladium acetate catalyst and the amine base triethyl amine or DIPEA in a Hirao-coupling reaction. Hirao-coupling is the palladium-catalysed cross-coupling reaction of vinyl- or aryl halides or triflates and a phosphorous reagent with at least one P-H bond, to form a phosphorous-carbon bond.^{266,267} For the synthesis of 1,3-substituted phosphonate **38**, 1,3-diiodobenzene **37** was reacted with diethylphosphite (neat) for 1 hour using triethyl amine as the base. (3-Chlorophenyl)phosphonate **40** was obtained under the same reaction conditions starting from 1-chloro-3-iodobenzene **39**. These reaction conditions, however, did not work for the synthesis of 1,2-phenylenebis(phosphonate) **35** but delivered instead mono-phosphonated compound as the main product (**Table 7.1**). Changing to a polar and protic solvent and the less reactive dibromobenzene as starting material yielded the bisphosphonate **35**. The sterically hindered, non-nucleophilic DIPEA was utilized instead of triethyl amine as a base to suppress the formation of the mono-halogenated **36** and non-halogenated **34**. 1,2-Phenylenebis(phosphonate) **35**, phenylphosphonate **34** and (2-bromophenyl)phosphonate **36** were obtained after preparative RP-HPLC separation.



Scheme 7.1. Hiraou-coupling followed by the McKenna reaction to synthesise arylphosphonic acids. The final compounds are circled.

To create the alkyl (sp^3) carbon-phosphorous bond, the Michaelis-Arbuzov (or just Arbuzov) reaction was used. In this reaction, an alkyl halide was reacted with a trivalent phosphorous ester to create a pentavalent phosphorous species.²⁶⁸ The aliphatic tetraethyl methylenebisphosphonate **44** was synthesised in the microwave-assisted Arbuzov reaction of 1,2-diiodomethane and triethyl phosphite at 135 °C in 20 min. The same reaction of 1,2-diiodoethane, however, did not give the corresponding bisphosphonate **45**. Therefore, 1,2-dibromoethane was reacted with triethyl phosphite at 140 °C for 30 min to give tetraethyl ethylenebisphosphonate **45**. Lastly, tetraethyl(1,3-propylene)bisphosphonate **46** was obtained from the reaction of 1,3-dibromopropane and triethylphosphite at 150 °C for 60 min. The aliphatic bisphosphonates were purified on silica gel. All phosphonates were finally hydrolysed with TMSBr in acetonitrile at 85 °C within a 15 min microwave McKenna reaction.



Scheme 7.2. Arbuzov reaction followed by the McKenna reaction to synthesise aliphatic bisphosphonic. The final compounds are circled.

Table 7.1. Reaction conditions for the 1,2-phenylenebis(phosphonic acid) synthesis.

| Starting material | Solvent | Base (+ligand) | Products |
|-------------------|---------|-------------------|--|
| | EtOH | Et ₃ N | 34 (main) + 36 + 35 (minor) |
| | neat | Et ₃ N | 36 (only) no 34 , no 35 |
| | ACN | Et ₃ N | 36 (main) + 34 no 35 |
| | neat | Et ₃ N | 36-I* (main) + 34 no 35 |
| | ACN | DIPEA + dppf | 36-I* (only) no 34 , no 35 |
| | EtOH | DIPEA | 34 (main) + 35 (traces) no 36-I* |
| | EtOH | DIPEA | 35 (main) + 34 (~4:1) no 36 |

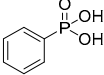
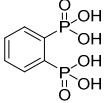
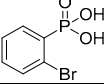
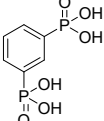
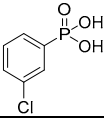
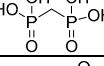
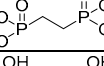
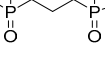
* **36-I** is the corresponding (2-iodophenyl)phosphonic acid due to the use of 1,2-diiodobenzene instead of 1,2-dibromobenzene as the starting material.

7.3 Activity and binding studies

The inhibitory activity of the aliphatic- and aryl phosphonic acids was determined on purified VIM-2, NDM-1 and IMP-26 (**Table 7.2**). The aliphatic compounds were inactive against all three MBLs. Hence, flexibility increase resulted in decreased affinity to MBLs. Only compound **30**, with the least rotatable bonds showed measurable VIM-2 activity. Out of the aromatic compounds, the halogenated ones were more potent against VIM-2 as compared

to the compounds with two or one phosphonic acid groups lacking a halogen. Significant increase in potency was observed upon halogenation, resulting in the most potent compound **27** of this series with 25 μM IC_{50} against VIM-2. Halogenation did not increase affinity for NDM-1. The chlorinated compound **29** was inactive, while the brominated **27** showed measurable activity, but with a worse IC_{50} value than the non-halogenated monophosphonic acid **25**. While the 1,3-substituted bisphosphonic acid **28** was completely inactive against all studied enzymes, the 1,2-substituted analogue **26** showed comparable, but high μM activity against VIM-2 and NDM-1. Similarly, the phenylphosphonic acid **25** had the same activity on VIM-2 and NDM-1, yet with high IC_{50} values. However, bisphosphonic acid **26** was the most active of all studied compounds in this chapter against NDM-1. In addition, the bisphosphonates were among the least cytotoxic compounds (HepG2 cells) of the phosphonic acids developed and evaluated in this thesis (Table 7.2).

Table 7.2. Inhibitory activities against selected metallo- β -lactamases and cytotoxicities against HepG2 cells of the aliphatic and aryl phosphonic acids.

| Compound | IC_{50} (μM) | | | CC_{50} (mM) |
|---|-----------------------------|----------|----------|----------------|
| | VIM-2 | NDM-1 | IMP-26 | HepG2 |
| 25  | 308 | 303 | >1500 | 2.5 |
| 26  | 212 | 195 | >1500 | 9.1 |
| 27  | 25 | 490 | >1000 | 1.3 |
| 28  | >1500 | inactive | inactive | 2.7 |
| 29  | 57 | >1000 | >1000 | 2.4 |
| 30  | 649 | inactive | inactive | 6.6 |
| 31  | >1500 | inactive | inactive | 2.9 |
| 32  | inactive | inactive | inactive | 8.8 |

The similar relative enzyme activity decrease on purified enzymes as well as on enzymes within the OMVs suggest that these compounds, despite their highly polar nature, were still able to go through the Gram-negative outer membrane (**Figure 7.1**). This, along with our previous data, suggests that phosphonic acids reach MBLs through the Gram-negative outer membrane and stay soluble and accumulate in the periplasm.

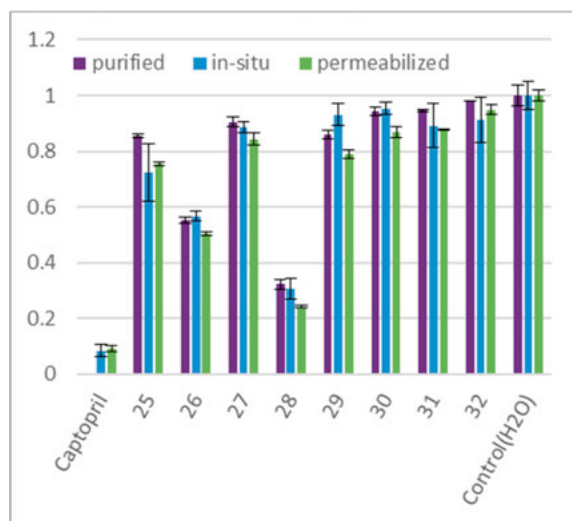


Figure 7.1. Normalized relative activities of VIM-2 in the presence of aliphatic- and aryl phosphonic acids. Purple bars represent the purified enzyme activity, blue bars represent the enzyme activity within OMVs and green bars represent the enzyme activity within the OMVs where the membrane was permeabilized with Triton-X.

To understand the binding of the most potent inhibitor **27** to VIM-2, solution NMR was used. The binding of **27** induced significant chemical shift perturbations at the end of loop 3 and in β -sheet 3 (64G-71G), in loop 10 (206T-214T), for the zinc binding residues 179H, 240H and its neighbouring residue 241G. This indicates that compound **27** binds with its phosphonic acid group close to the zinc ions of the enzyme active site. The significant CSPs of 179H and 240H suggest that there is direct interaction with the dinuclear zinc center. Perturbation in loop 3 and β -sheet 3 indicate that the aryl ring is positioned towards the substrate-binding hydrophobic wall formed by those structural elements of the enzyme. CSPs in loop 10 demonstrates that the ligand extends toward the Zn²⁺ site. The phosphonic acid group is likely located between the two zinc ions while the rest of the molecule is oriented towards the hydrophobic pocket formed by loop 10 and loop 3 towards the Zn²⁺ site. All CSPs could be followed and no significant broadening was observed in contrast to the titrations with the previous inhibitors described in this thesis. The data suggests

that compound **27** induced local structural perturbations only, without large conformational changes of the enzyme. The data also indicates stable binding and that the complex did not exhibit dynamic behaviour. The bromine substituent most likely enhances hydrophobic contacts, van der Waals interactions and polarizability therefore strengthening packing interactions within the pocket. However, this is not proven by the NMR data. The weaker activity of compound **27** against NDM-1 most probably originates from the differences in the amino acid sequence mainly in loop-3 between VIM-2 and NDM-1 (**Table 7.3**). As the NMR data indicates that the aromatic ring of **27** is shifted towards the Zn²⁺ site, there might be π - π stacking between this ring and Tyr67 of VIM-2. There is also a possibility for halogen- π interactions or halogen bonding between the bromine and the phenolic oxygen of tyrosine and for hydrophobic and van der Waals interactions. At the same position, NDM-1 has a valine instead of a tyrosine, which may form non-specific, weak hydrophobic interactions.

Table 7.3. Amino acid residues of VIM-2 loop 3, β -sheet 3 and loop 10 that showed significant CSP when binding compound **27**, and the corresponding residues of NDM-1 in the same position. Differences highlighted in bold.

| CSP for VIM-2 | VIM-2 | NDM-1 |
|---------------|---------------|---------------|
| 0.08 | Gly64 | Phe70 |
| 0.10 | Val66 | Ala72 |
| 0.11 | Tyr67 | Val73 |
| 0.14 | Ser69 | Ser75 |
| 0.09 | Gly71 | Gly77 |
| 0.09 | Thr206 | Lys216 |
| 0.18 | Ala208 | Leu218 |
| 0.13 | Gly209 | Gly219 |
| 0.12 | Asp213 | Asp223 |
| 0.09 | Ala214 | Ala224 |

8. Concluding remarks

Antibiotic resistance is a critical global health issue exacerbated by the emergence of metallo- β -lactamase enzymes that degrade our precious, worldwide most-used β -lactam antibiotics. Combination therapy using β -lactam antibiotics with enzyme inhibitors offers a potential solution for resistance against β -lactams. However, no metallo- β -lactamase inhibitors are currently available on the market. This research focuses on the investigation of phosphonic acids, which have recently emerged as promising metallo- β -lactamase inhibitor candidates.

We developed phosphonic acid-based transition state analogue inhibitor candidates of the bacterial enzymes. Following synthesis, they were evaluated against purified metallo- β -lactamase enzymes, several of them showing inhibitory activities. The compounds were predicted to have favourable ADME properties, fulfil the criteria used for describing drug-likeness, they were non-cytotoxic to human cells and were able to cross the Gram-negative outer membrane. The binding mode of the inhibitor candidates was confirmed by NMR spectroscopic, X-ray crystallographic and computational methods indicating that the key interaction is between the phosphonic acid core and the zinc ions in the active site of the enzymes. This is conserved and is essential for all metallo- β -lactamases in the clinically most relevant B1 family. To evaluate and understand the structural features needed for broad-spectrum alternatively for selective MBL inhibition, the phosphonic acid-type molecules were structurally modified.

In the first project, dynamically chiral phosphonic acids containing an ortho-hydroxyphenyl core and an amide-linked aromatic thiophene or benzothiophene moiety were developed. These showed comparable inhibition of VIM-2, NDM-1, and GIM-1, demonstrating potential as broad-spectrum inhibitors. The stereodynamic adaptability of the inhibitors was demonstrated to allow adaptation of alternative binding orientations, with both stereoisomers binding VIM-2 yet with a 180 ° flipped binding mode, and acting as competitive transition-state analogues.

In the second project, the ortho-hydroxyphenyl core was changed to pyridine-, thiazole-4-carboxylate or a carboxylic acid scaffold, and the effect of

the modifications on metallo- β -lactamase inhibition were evaluated. Changing the core scaffold reduced activity on NDM-1 and GIM-1, whereas VIM-2 remained tolerant to core alterations.

The third project explored α -aminophosphonic acids, where replacement of an amide with an amine linker improved potency against VIM-2 and GIM-1. Halogenation of the aromatic ring further enhanced inhibitory activity for these enzymes, although this strategy did not translate to NDM-1 or IMP-1 inhibition. Importantly, these compounds were able to reduce the meropenem MIC in VIM-2-expressing *E. coli* and were shown to act as time-independent inhibitors.

In the fourth project, we developed IMP-1 and NDM-1 inhibitors by altering the amide-attached scaffold from aromatic moieties to natural amino acids. Lastly, we evaluated aliphatic and aromatic bisphosphonic acids and halogenated aryl phosphonic acids. Bromination was shown to significantly enhance VIM-2 potency.

This thesis work explored several phosphonic acid compound classes and proved the possibility of successfully targeting a variety of clinically relevant metallo- β -lactamases with phosphorous-scaffold. We demonstrated that phosphonic acid-based molecules represent a versatile platform for the development of metallo- β -lactamase inhibitors and that they have potential to become lead compounds for combating antibiotic resistance mediated by these enzymes.

9. Sammanfattning på svenska

Antibiotikaresistens utgör ett allvarligt globalt hälsoproblem. Resistens mot β -laktamantibiotika orsakas ofta av bakteriella metallo- β -laktamaser (MBL) som hydrolyserar och därmed gör β -laktamer ineffektiva. En möjlig strategi för att motverka sådan resistens är kombinationsbehandling där β -laktamantibiotika kombineras med enzymhämmare. Trots omfattande forskningsinsatser finns i dagsläget inga kliniskt godkända hämmare av metallo- β -laktamaser. Denna avhandling fokuserar på utveckling och syntes av fosfonsyrabaserade hämmare. Dessa har identifierats som lovande kandidater för MBL-hämning på sistone.

Jag utvecklade flera serier av fosfonsyrabaserade molekyler som efterliknar övergångstillståndet i den enzymatiska reaktion som bryter ner β -laktamer. Efter syntes utvärderades de med isolerade metallo- β -laktamasenzymer, där flera av molekylerna visade hämmande aktivitet. Föreningarna förutsågs ha gynnsamma ADME-egenskaper, uppfyllde kriterier för läkemedelslikhet, var icke-cytotoxiska för humana celler samt kunna passera det gramnegativa yttermembranet. Bindningssätten undersöktes med en kombination av NMR-spektroskopi samt röntgenkristallografiska och beräkningsbaserade metoder, vilka visade att interaktionen mellan fosfonsyrgruppen och de katalytiska zinkjonerna i enzymets aktiva centrum var viktigast för binding. Denna interaktion är avgörande för aktivitet mot den kliniskt mest relevanta B1-familjen av metallo- β -laktamaser. För att utvärdera och förstå de strukturella egenskaperna som krävs för bredspektrum- respektive selektiv metallo- β -laktamas hämning varierades fosfonsyrornas struktur systematiskt.

I det första projektet utvecklades dynamiskt kirala fosfonsyrhämmare innehållande en orto-hydroxifenylkärna och en amidbunden aromatisk tiofen- eller bensotiofendel. Dessa föreningar visade jämförbar aktivitet mot VIM-2, NDM-1 och GIM-1 och uppvisade därmed potential som bredspektrumhämmare. Hämmarnas stereodynamiska flexibilitet möjliggjorde att båda stereoisomererna band till VIM-2 med ett liknande men 180° -vridet bindningssätt. Båda stereoisomererna agerade som kompetitiva övergångstillståndsanaloga hämmare.

I det andra projektet modifierades orto-hydroxifenylkärnan till pyridin-, tiazol-4-karboxylat- eller karboxylsyra-derivat för att utvärdera effekten av strukturella förändringar på metallo- β -laktamase-hämning. Dessa modifieringar påverkade bindningen till NDM-1 och GIM-1 negativt, medan VIM-2 visade större tolerans för förändringar i kärnstrukturen.

Det tredje projektet utvärderade α -aminofosfonsyror som potenta hämmare av VIM-2 och GIM-1. När amidgruppen i den ursprungliga designen byttes mot en amin resulterade det i förbättrad hämningspotential mot dessa enzymer. Halogenering av orto-metoxifenylringen förstärkte den hämmande aktiviteten mot VIM-2 och GIM-1, medan motsvarande effekt var inte observerad för NDM-1 eller IMP-1 hämning. α -Aminofosfonsyrorna kunde dock sänka MIC-värdet för meropenem i VIM-2-uttryckande *Escherichia coli* och visade sig fungera som tidsberoende hämmare.

I det fjärde projektet utvecklade vi hämmare av IMP-1 och NDM-1 genom att ersätta den amidbundna aromatiska strukturen med naturliga aminosyror.

Slutligen, jag undersökte alifatiska och aromatiska bisfosfonsyror samt halogenerade arylfosfonsyror, där bromering ökade den hämmande aktiviteten mot VIM-2 avsevärt.

Detta avhandlingsarbete utforskade flera klasser av fosfonsyra-föreningar som enzyminhibitorer. Resultaten visar att fosfonsyra-föreningar utgör en mångsidig och lovande plattform för utveckling av metallo- β -laktamashämmare. Arbetet bidrar till en fördjupad förståelse av de strukturella faktorer som styr metallo- β -laktamas hämning och demonstrerar att fosfonsyror är potentiella kandidater i utvecklingen av nya läkemedel för att bekämpa antibiotikaresistens.

10. Acknowledgement

I would like to thank and express my appreciation to everyone involved in my PhD journey:

My supervisor Máté Erdélyi, for giving me the most interesting project I fell in love with, for trusting me and supporting me throughout my PhD and for all the help and knowledge.

Ruisheng Xiong, for always helping with literally everything at work.

To Farshid, Gunnar, Daniel and Johanna A., for sending my compounds to the collaborators, solving HPLC issues, answering questions about teaching, for always helping, always being nice and always smiling. To Helena G., for guiding me through this PhD journey.

To the Uppsala Antibiotic Center and all its members for the good friendships, courses, conferences, retreats, events and mainly all the amazing opportunities I got through the center. I am extremely grateful for being part of such a great organization. Ottilia, Eva, Valeriia, Carla, Xiguo, Adrián, Chris, Jacob, Filip, thank you for the talks, I am grateful for going through this journey from the very beginning till the end with all of you.

To all the collaborators who taught me all the new methods and helped my life during my PhD exchanges:

Dr Anna Andersson Rasmussen, for teaching me protein expression and purification in Lund.

Dr Weiliang Zhu and his group for welcoming me in Shanghai, and for giving me opportunities to improve as a scientist. Liping and Leyun, for teaching me docking and molecular dynamics simulations, for helping me so much in China and for becoming my friends.

Dr Christopher Fröhlich who taught me how to do the IC_{50} and MIC measurements. Thank you for the discussions about the enzymes, about my future and for welcoming me in the middle of the darkness in Tromsø. It is difficult to describe how grateful I am for the time I could spend there and for all the knowledge I got from you.

Dr Mikael Widersten, for kindly helping me with the enzyme kinetics.

To everyone involved in my projects and papers, measuring my samples, being open for collaborations, helping with discussions, and with improving my papers. To all my students: Rebekka, Máté, Vojta, Áron, Erik, Stasiak. You all did a great job and contributed to the metallo- β -lactamase projects.

To all the people I met during my PhD so far and can call friends. I am so grateful for all of you, you made my life in Uppsala so much better: Scott, Mariya, Kate K., Mauricio, Anna, Stefan, Chris, Dani, Michael, Sanne and Daniel, Marie and Fabio, Silvia, Karin, Fredrik, Philipp. You welcomed and included me in your lives and I am happy to share all those memories of coffee breaks, brunches, lunches and dinners, walks and talks, afterworks, gym and swimming sessions, parties, Midsommar trips, happy and sad moments and a lot more. To Manuel, Merve, Luca, Susanna, Susanne, Alessandro, Federico, Jan Luca, Ivan, Julia, Raffaella, Daniel U., Wouter, Andrew, Yang, Orsola, Duy and a lot more, for the talks and sharing all great moments at work.

To the best office mates I could just wish for, Hermina and Billy. I hope you both know, it would have been impossible for me to do this PhD if it wasn't you guys sitting next to me!

To the Hungarians, Petra, Eszter, Eszti, Gábor, Peti and Johan, for making it possible in Uppsala to feel just like at home with all the amazing feasts we had together and all the very needed Hungarian-style complaining.

To my long-lasting Erasmus friends, Irene, Kate and Julia, even though we are far apart, I know you are also there for me!

To Kim, Paul and Adam: the Uppsala Beasts or the Fantastic Four as I would call us. Thank you for helping me through the most difficult year of my PhD, thank you for the deep and the silly conversations, for always smiling and making me smile as well, for making me become the best of myself when I was feeling the worst.

To my best ones at home, Kitti, Nati, Imi és Gábor. Kitti, együtt vészeltük át az összes létező sulit, végül is csak 24 évünkbe telt. Ahogy magunkat ismerem, a doktori még nem a vége volt. Nati, Imi és Gábor, köszönöm a sírósnévetős beszélgetéseket, videóhívásokat, nyaralásokat, és még annyi mindent amit túl hosszú lenne ide felsorolni. Nélkületek nem ment volna!

To the Uppsala Antibiotic Center, Vetenskapsrådet, Apotekarsocieteten, Liljewalch- and Anna Maria Lundins scholarships for the financial support.

And last but not least, I am thankful for all past and present members of the Erdélyi group and the Chemistry department of BMC for all the help, good atmosphere and work environment.

És a legfontosabbaknak, a családomnak, akiknek mindent köszönhetek!
Szeretlek Titeket!
Stubán Ferenc emlékére!

11. References

1. Adedeji, W.A. THE TREASURE CALLED ANTIBIOTICS. *Ann. Ibd. Pg. Med.* **14**, 56–57 (2016).
2. ReAct - Action on Antibiotic Resistance (www.reactgroup.org).
3. Subramaniam, G. & Girish, M. Antibiotic Resistance — A Cause for Reemergence of Infections. *Indian J Pediatr* **87**, 937–944 (2020).
4. World Health Organization. Antimicrobial resistance (<https://www.who.int/news-room/fact-sheets/detail/antimicrobial-resistance>). (2023).
5. Salam, M.A. et al. Antimicrobial Resistance: A Growing Serious Threat for Global Public Health. *Healthcare* **11**, 1946 (2023).
6. Antimicrobial Resistance Collaborators. Global burden of bacterial antimicrobial resistance in 2019: a systematic analysis. *Lancet* **399**, 629-655 (2022).
7. O’Neill, J. Tackling Drug-Resistant Infections Globally: final report and recommendations (amr-review.org). (2016).
8. Ju, L.-C., Cheng, Z., Fast, W., Bonomo, R.A. & Crowder, M.W. The Continuing Challenge of Metallo- β -Lactamase Inhibition: Mechanism Matters. *Trends Pharmacol Sci.* **39**, 635-647 (2018).
9. Mojica, M.F., Rossi, M.-A., Vila, A.J. & Bonomo, R.A. The urgent need for metallo- β -lactamase inhibitors: an unattended global threat. *Lancet Infect Dis.* **22**, e28–e34 (2022).
10. Li, X. et al. Drug development concerning metallo- β -lactamases in gram-negative bacteria. *Front. Microbiol.* **13:959107**(2022).
11. Asempe, T.E., Abdelraouf, K. & Nicolau, D.P. Activity of b-Lactam Antibiotics against Metallo-b-Lactamase Producing Enterobacterales in Animal Infection Models: a Current State of Affairs. *Antimicrob Agents Chemother.* **65**, e02271-20 (2021).
12. Morrill, H.J., Pogue, J.M., Kaye, K.S. & LaPlante, K.L. Treatment Options for Carbapenem-Resistant Enterobacteriaceae Infections. *Open Forum Infectious Diseases* **2**(2015).
13. Sheu, C.-C., Chang, Y.-T., Lin, S.-Y., Chen, Y.-H. & Hsueh, P.-R. Infections Caused by Carbapenem-Resistant Enterobacteriaceae: An Update on Therapeutic Options. *Front. Microbiol.* **10:80**, 1-13 (2019).
14. Doi, Y. Treatment Options for Carbapenem-resistant Gram-negative Bacterial Infections. *Clin. Infect. Dis.* **69**, S565-S575 (2019).

15. Zeng, M. et al. Guidelines for the diagnosis, treatment, prevention and control of infections caused by carbapenem-resistant gram-negative bacilli. *J. Microbiol. Immunol. Infect.* **56**, 653-671 (2023).
16. Palzkill, T. Metallo- β -lactamase structure and function. *Ann NY Acad Sci.* **1277**, 91–104 (2013).
17. Chaturvedi, P., Giri, B.S., Shukla, P. & Gupta, P. Recent advancement in remediation of synthetic organic antibiotics from environmental matrices: Challenges and perspective. *Bioresource Technology* **319**, 124161 (2021).
18. Bush, K. & Bradford, P.A. beta-Lactams and beta-Lactamase Inhibitors: An Overview. *Cold Spring Harb. Perspect. Med.* **6**(2016).
19. Buynak, J.D. Understanding the longevity of the β -lactam antibiotics and of antibiotic/ β -lactamase inhibitor combinations. *Biochemical Pharmacology* **71**, 930-940 (2006).
20. Liu, B. et al. Discovery of Taniborbactam (VNRX-5133): A Broad-Spectrum Serine- and Metallo- β -lactamase Inhibitor for Carbapenem-Resistant Bacterial Infections. *J. Med. Chem.* **63**, 2789–2801 (2020).
21. Årdal, C. et al. Antibiotic development — economic, regulatory and societal challenges. *Nat. Rev. Microbiol.* **18**, 267–274 (2020).
22. Monnet, D.L. Antibiotic development and the changing role of the pharmaceutical industry. *International Journal of Risk & Safety in Medicine* **17**, 133–145 (2005).
23. Power, E. Impact of antibiotic restrictions: the pharmaceutical perspective. *Clinical Microbiology and Infection* **12**, 25-34 (2006).
24. Keenan, K., Corrêa, J.S., Sringeriyuang, L., Nayiga, S. & Chandler, C.I.R. The social burden of antimicrobial resistance: what is it, how can we measure it, and why does it matter? *JAC-AMR* **7**, dlac208 (2025).
25. Bassetti, M. & Giacobbe, D.R. A look at the clinical, economic, and societal impact of antimicrobial resistance in 2020. *Expert Opin. Pharmacother.* **21**, 2067-2071 (2020).
26. Dadgostar, P. Antimicrobial Resistance: Implications and Costs. *Infection and Drug Resistance* **12**, 3903-3910 (2019).
27. Sipahi, O.R. Economics of antibiotic resistance. *Expert Review of Anti-Infective Therapy* **6**, 523-539 (2008).
28. Niederman, M. Impact of antibiotic resistance on clinical outcomes and the cost of care. *Crit Care Med* **29**, N114-N120 (2001).
29. Nwobodo, D.C. et al. Antibiotic resistance: The challenges and some emerging strategies for tackling a global menace. *J Clin Lab Anal.* **36**, e24655 (2022).
30. Nguyen, L., Garcia, J., Gruenberg, K. & MacDougall, C. Multidrug-Resistant Pseudomonas Infections: Hard to Treat, But Hope on the Horizon? *Curr Infect Dis Rep* **20**, 1 -10 (2018).
31. Frieri, M., Kumar, K. & Boutin, A. Antibiotic resistance. *Journal of Infection and Public Health* **10**, 369-378 (2017).

32. Friedman, N.D., Temkin, E. & Carmeli, Y. The negative impact of antibiotic resistance. *Clin Microbiol Infect* **22**, 416-422 (2016).
33. Larsson, S., Svensson, M. & Ternhag, A. Production loss and sick leave caused by antibiotic resistance: a register-based cohort study. *BMC Public Health* **22**(2022).
34. Ahmad, M. & Khan, A.U. Global economic impact of antibiotic resistance: A review. *Journal of Global Antimicrobial Resistance* **19**, 313-316 (2019).
35. Mendelson, M. Review: Role of antibiotic stewardship in extending the age of modern medicine. *South African Medical Journal* **105**, 414-419 (2015).
36. Teillant, A., Gandra, S., Barter, D., Morgan, D.J. & Laxminarayan, R. Potential burden of antibiotic resistance on surgery and cancer chemotherapy antibiotic prophylaxis in the USA: a literature review and modelling study. *Lancet Infect Dis.* **15**, 1429-1437 (2015).
37. Sulis, G., Sayood, S. & Gandra, S. Antimicrobial resistance in low- and middle-income countries: current status and future directions. *Expert Review of Anti-Infective Therapy* **20**, 147–160 (2021).
38. Pokharel, S., Raut, S. & Adhikari, B. Tackling antimicrobial resistance in low-income and middle-income countries. *BMJ Global Health* **4**(2019).
39. Barlam, T.F. & Gupta, K. Antibiotic Resistance Spreads Internationally Across Borders. *J Law Med Ethics.* **43**, 12-16 (2015).
40. Stavropoulou, E., Tsigalou, C. & Bezirtzoglou, E. Spreading of Antimicrobial Resistance Across Clinical Borders. *Erciyes Med J.* **41**, 238–243 (2019).
41. Chatterjee, A. et al. Quantifying drivers of antibiotic resistance in humans: a systematic review. *Lancet Infect Dis.* **18**, E368-E378 (2018).
42. Vikesland, P. et al. Differential Drivers of Antimicrobial Resistance across the World. *Acc. Chem. Res.* **52**, 916–924 (2019).
43. Larsson, D.G.J. & Flach, C.-F. Antibiotic resistance in the environment. *Nat Rev Microbiol* **20**, 257–269 (2021).
44. Aminov, R.I. The role of antibiotics and antibiotic resistance in nature. *Environmental Microbiology* **11**, 2970–2988 (2009).
45. Dickey, S.W., Cheung, G.Y.C. & Otto, M. Different drugs for bad bugs: antivirulence strategies in the age of antibiotic resistance. *Nat Rev Drug Discov.* **16**, pages457–471 (2017).
46. Watkins, R.R., Smith, T.C. & Bonomo, R.A. On the path to untreatable infections: colistin use in agriculture and the end of ‘last resort’ antibiotics. *Expert Review of Anti-Infective Therapy* **14**, 785-788 (2016).
47. Mohapatra, S.S., Dwibedy, S.K. & Padhy, I. Polymyxins, the last-resort antibiotics: Mode of action, resistance emergence, and potential solutions. *J Biosci.* **46**(2021).

48. Daulaire, N., Bang, A., Tomson, G., Kalyango, J.N. & Cars, O. Universal Access to Effective Antibiotics is Essential for Tackling Antibiotic Resistance. *Journal of Law, Medicine & Ethics* **43**, 17 - 21 (2015).
49. Rossi, M., Olkkola, S., Roasto, M., Kivistö, R. & Hänninen, M.-L. Chapter 4. - *Antimicrobial Resistance and Campylobacter jejuni and C. coli*, (Academic Press, Antimicrobial Resistance and Food Safety, 2015).
50. Thakuria, B. & Lahon, K. The Beta Lactam Antibiotics as an Empirical Therapy in a Developing Country: An Update on Their Current Status and Recommendations to Counter the Resistance against Them. *J. Clin. Diagn. Res.* **7**, 1207-14. (2013).
51. Coates, A.R.M., Halls, G. & Hu, Y. Novel classes of antibiotics or more of the same? *British Journal of Pharmacology* **163**, 184-194 (2011).
52. Maffioli, S.I. *Antibiotics: Targets, Mechanisms and Resistance - A Chemist's Survey of Different Antibiotic Classes*, (Wiley-VCH, 2014).
53. Hutchings, M.I., Truman, A.W. & Wilkinson, B. Antibiotics: past, present and future. *Current Opinion in Microbiology* **51**, 72–80 (2019).
54. Theuretzbacher, U., Outterson, K., Engel, A. & Karlén, A. The global preclinical antibacterial pipeline. *Nat Rev Microbiol.* **18**, 275–285 (2020).
55. Kapoor, G., Saigal, S. & Elongavan, A. Action and resistance mechanisms of antibiotics: A guide for clinicians. *J Anaesthesiol Clin Pharmacol.* **33**, 300–305 (2017).
56. Page, M.G.P. et al. *Antibiotic Discovery and Development - Marketed Major Classes of Compounds*, (Springer, 2012).
57. Worthington, R.J. & Melander, C. Overcoming Resistance to beta-Lactam Antibiotics. *Journal of Organic Chemistry* **78**, 4207-4213 (2013).
58. Ikeda, A. et al. A new selective inhibitor for IMP-1 metallo- β -lactamase, 3Z,5E-octa-3,5-diene-1,3,4-tricarboxylic acid-3,4-anhydride. *Bioorg. Med. Chem.* **78**, 117109 (2023).
59. Nordmann, P., Dortet, L. & Poirel, L. Carbapenem resistance in Enterobacteriaceae: here is the storm! *Trends Mol. Med.* **18**, 263-272 (2012).
60. World Health Organization. The selection and use of essential medicines, 2025: WHO Model List of Essential Medicines, 24th list. Geneva, 10-19 (2025).
61. World Health Organization. WHO Bacterial Priority Pathogens List, 2024: bacterial pathogens of public health importance to guide research, development and strategies to prevent and control antimicrobial resistance. . Geneva (2024).

62. Palacios, A.R., Rossi, M.-A., Mahler, G.S. & Vila, A.J. Metallo- β -Lactamase Inhibitors Inspired on Snapshots from the Catalytic Mechanism. *Biomolecules* **10**, 854 (2020).
63. Fleming, A. On the Antibacterial Action of Cultures of a Penicillium, with Special Reference to Their Use in the Isolation of B. influenzae. *Br. J. Exp. Pathol.* **10**, 226-236 (1929).
64. Kardos, N. & Demain, A.L. Penicillin: the medicine with the greatest impact on therapeutic outcomes. *Appl Microbiol Biotechnol.* **92**, 677–687 (2011).
65. Linciano, P., Cendron, L., Gianquinto, E., Spyrakis, F. & Tondi, D. Ten Years with New Delhi Metallo- β -lactamase-1 (NDM-1): From Structural Insights to Inhibitor Design. *ACS Infect. Dis.* **5**, 9–34 (2019).
66. Brem, J. et al. Rhodanine hydrolysis leads to potent thioenolate mediated metallo- β -lactamase inhibition. *Nature Chem.* **6**, 1084–1090 (2014).
67. Meletis, G. Carbapenem resistance: overview of the problem and future perspectives. *Ther Adv Infect Dis* **3**, 15-21 (2016).
68. Brem, J. et al. Imitation of β -lactam binding enables broad-spectrum metallo- β -lactamase inhibitors. *Nat. Chem.* **14**, 15-24 (2022).
69. Palica, K. et al. Metallo- β -Lactamase Inhibitor Phosphoramidate Monoesters. *ACS Omega* **7**, 4550–4562 (2022).
70. Tan, X. et al. Therapeutic Options for Metallo- β -Lactamase-Producing Enterobacterales. *Infection and Drug Resistance* **14**, 125-142 (2021).
71. Garau, J. Beta-lactamases: current situation and clinical importance. *Intensive Care Med.* **20**, S5–S9 (1994).
72. Tooke, C.L. et al. β -Lactamases and β -Lactamase Inhibitors in the 21st Century. *J Mol Biol.* **431**, 3472-3500 (2019).
73. Fisher, J.F., Meroueh, S.O. & Mobashery, S. Bacterial resistance to beta-lactam antibiotics: compelling opportunism, compelling opportunity. *Chem Rev.* **105**, 395-424 (2005).
74. Xu, D., Xie, D. & Guo, H. Catalytic Mechanism of Class B2 Metallo- β -lactamase. *The Journal of Biological Chemistry* **281**, 8740–8747 (2006).
75. Bush, K., Jacoby, G.A. & Medeiros, A.A. A functional classification scheme for beta-lactamases and its correlation with molecular structure. *Antimicrob Agents Chemother.* **39**, 1211-1233 (1995).
76. Oelschlaeger, P. β -Lactamases: Sequence, Structure, Function, and Inhibition. *Biomolecules* **11**, 986 (2021).
77. Boyd, S.E., Livermore, D.M., Hooper, D.C. & Hope, W.W. Metallo- β -Lactamases: Structure, Function, Epidemiology, Treatment Options, and the Development Pipeline. *Antimicrob Agents Chemother.*, e00397-20. (2020).

78. Brem, J. et al. Structural basis of metallo- β -lactamase, serine- β -lactamase and penicillin-binding protein inhibition by cyclic boronates. *Nat Commun* **7**, 12406 (2016).
79. Li, X., Zhao, D., Li, W., Sun, J. & Zhang, X. Enzyme Inhibitors: The Best Strategy to Tackle Superbug NDM-1 and Its Variants. *Int J Mol Sci.* **23**, 197 (2022).
80. Kareem, S.M., Hamzah, I.H. & Ali, M.G. Metallo Beta Lactamase Enzymes. *Indian J. Microbiol.* **65**, 890–897 (2025).
81. Huang, Y.-S. & Zhou, H. Breakthrough Advances in Beta-Lactamase Inhibitors: New Synthesized Compounds and Mechanisms of Action Against Drug-Resistant Bacteria. *Pharmaceuticals* **18**, 206 (2025).
82. Drusin, S.I. et al. Structural basis of metallo- β -lactamase resistance to taniborbactam. *Antimicrob Agents Chemother.* **68**, e01168-23 (2023).
83. Mojica, M.F., Bonomo, R.A. & Fast, W. B1-Metallo- β -Lactamases: Where Do We Stand? *Curr. Drug Targets* **17**, 1029-1050 (2016).
84. Bush, K. Metallo- β -Lactamases: A Class Apart. *Clin Infect Dis.* **27**, S48-53 (1998).
85. Yuan, Q., He, L. & Ke, H. A Potential Substrate Binding Conformation of β -Lactams and Insight into the Broad Spectrum of NDM-1 Activity. *Antimicrob. Agents Chemother.* **56**, 5157–5163 (2012).
86. Wang, Z., Fast, W., Valentine, A.M. & Benkovic, S.J. Metallo- β -lactamase: structure and mechanism. *Curr Opin Chem Biol.* **3**, 614-622 (1999).
87. Makena, A. et al. Comparison of Verona Integron-Borne Metallo- β -Lactamase (VIM) Variants Reveals Differences in Stability and Inhibition Profiles. *Antimicrob Agents Chemother.* **60**, 1377–1384 (2016).
88. Naas, T. et al. Beta-Lactamase DataBase (BLDB) – Structure and Function. *J. Enzyme Inhib. Med. Chem.* **32**, 917-919 (2017).
89. Yang, Y. et al. Metallo- β -lactamase-mediated antimicrobial resistance and progress in inhibitor discovery. *Trends in Microbiology* **31**, 735-748 (2023).
90. Osano, E. et al. Molecular characterization of an enterobacterial metallo beta-lactamase found in a clinical isolate of *Serratia marcescens* that shows imipenem resistance. *Antimicrob Agents Chemother.* **38**, 71-78 (1994).
91. Shibata, N. et al. PCR Typing of Genetic Determinants for Metallo- β -Lactamases and Integrases Carried by Gram-Negative Bacteria Isolated in Japan, with Focus on the Class 3 Integron. *J. Clin. Microbiol.* **41**(2003).
92. Cornaglia, G. et al. Appearance of IMP-1 metallo- β -lactamase in Europe. *The Lancet* **353**, 899-900 (1999).

93. Yamamoto, K. et al. Structural insights into the substrate specificity of IMP-6 and IMP-1 metallo- β -lactamases. *J. Biochem.* **173**, 21–30 (2023).
94. Le Terrier, C. et al. Relative inhibitory activities of the broad-spectrum β -lactamase inhibitor xeruborbactam in comparison with taniborbactam against metallo- β -lactamases produced in *Escherichia coli* and *Pseudomonas aeruginosa*. *Anti* **68**, e01570-23 (2024).
95. McGeary, R.P., Tan, D.T.C. & Schenk, G. Progress toward inhibitors of metallo- β -lactamases. *Future Med. Chem.* **9**, 673-691 (2017).
96. Lomovskaya, O. et al. In vitro potency of xeruborbactam in combination with multiple β -lactam antibiotics in comparison with other β -lactam/ β -lactamase inhibitor (BLI) combinations against carbapenem-resistant and extended-spectrum β -lactamase-producing Enterobacterales. *Antimicrob Agents Chemother.* **67**, e0044023 (2023).
97. Poirel, L. et al. Characterization of VIM-2, a Carbapenem-Hydrolyzing Metallo- β -Lactamase and Its Plasmid- and Integron-Borne Gene from a *Pseudomonas aeruginosa* Clinical Isolate in France. *Antimicrob Agents Chemother.* **44**(2000).
98. Loucif, L. et al. First Detection of VIM-2 Metallo- β -Lactamase-Producing *Pseudomonas putida* in *Blattella germanica* Cockroaches in an Algerian Hospital. *Antimicrob Agents Chemother.* **61**, e00357-17 (2017).
99. Fraenkel, C.-J., Starlander, G., Tano, E., Sütterlin, S. & Melhus, Å. The First Swedish Outbreak with VIM-2-Producing *Pseudomonas aeruginosa*, Occurring between 2006 and 2007, Was Probably Due to Contaminated Hospital Sinks. *Microorganisms* **11**, 974-984 (2023).
100. Docquier, J.-D. et al. On functional and structural heterogeneity of VIM-type metallo- β -lactamases. *JAC* **51**, 257–266 (2003).
101. Lauretti, L. et al. Cloning and Characterization of *bla*_{VIM}, a New Integron-Borne Metallo- β -Lactamase Gene from a *Pseudomonas aeruginosa* Clinical Isolate. *Antimicrob. Agents Chemother.* **43**, 1584-1590 (1999).
102. Yong, D. et al. Characterization of a New Metallo- β -Lactamase Gene, *bla*_{NDM-1}, and a Novel Erythromycin Esterase Gene Carried on a Unique Genetic Structure in *Klebsiella pneumoniae* Sequence Type 14 from India. *Antimicrob Agents Chemother.* **53**, 5046-5054 (2009).
103. Venkata, K.C.N., Ellebrecht, M. & Tripathi, S.K. Efforts towards the inhibitor design for New Delhi metallo-beta-lactamase (NDM-1). *European Journal of Medicinal Chemistry* **225**, 113747 (2021).
104. Bayoumi, M.A. & Hamid, O.M. The Emergence of Carbapenem Resistant *Enterobacteriaceae* Producing GIM-1 and SIM-1 Clinical Isolates in Khartoum-Sudan. *Infect. Drug Resist.* **15**, 2679–2684 (2022).

105. Kaase, M. et al. Description of the metallo- β -lactamase GIM-1 in *Acinetobacter pittii*. *J. Antimicrob. Chemother.* **69**, 81–84 (2014).
106. Wendel, A.F. et al. Protracted Regional Dissemination of GIM-1-Producing *Serratia marcescens* in Western Germany. *Antimicrob Agents Chemother.* **61**, e01880-16 (2017).
107. Borra, P.S. et al. Crystal Structures of *Pseudomonas aeruginosa* GIM-1: Active-Site Plasticity in Metallo- β -Lactamases. *Antimicrobial Agents and Chemotherapy* **57**, 848–854 (2013).
108. Castanheira, M., Toleman, M.A., Jones, R.N., Schmidt, F.J. & Walsh, T.R. Molecular Characterization of a β -Lactamase Gene, *bla*_{GIM-1}, Encoding a New Subclass of Metallo- β -Lactamase. *Antimicrobial Agents and Chemotherapy* **48**(2004).
109. Palica, K. et al. α -Aminophosphonate inhibitors of metallo- β -lactamases NDM-1 and VIM-2. *RSC. Med. Chem.* **14**, 2277-2300 (2023).
110. Skagseth, S. et al. Metallo-beta-lactamase inhibitors by bioisosteric replacement: Preparation, activity and binding. *Eur. J. Med. Chem.* **135**, 159-173 (2017).
111. Wieske, L.H.E. et al. NMR Backbone Assignment of VIM-2 and Identification of the Active Enantiomer of a Potential Inhibitor. *ACS Medicinal Chemistry Letters* **13**, 257-261 (2022).
112. Bebrone, C. Metallo- β -lactamases (classification, activity, genetic organization, structure, zinc coordination) and their superfamily. *Biochem. Pharmacol.* **74**, 1686-1701 (2007).
113. Lewis, K. The Science of Antibiotic Discovery. *Cell* **181**, 29-45 (2020).
114. Angst, D.C., Tepekule, B., Sun, L., Bogos, B. & Bonhoeffer, S. Comparing treatment strategies to reduce antibiotic resistance in an in vitro epidemiological setting. *PNAS* **118**, e2023467118 (2021).
115. Lee, N., Yuen, K.-Y. & Kumana, C.R. Clinical Role of β -Lactam/ β -Lactamase Inhibitor Combinations. *Drugs* **63**, 1511-1524 (2003).
116. Leigh, D.A., Bradnock, K. & Marriner, J.M. Augmentin (amoxycillin and clavulanic acid) therapy in complicated infections due to β -Lactamase producing bacteria. *Journal of Antimicrobial Chemotherapy* **7**, 229–236 (1981).
117. Bortone, B. et al. High global consumption of potentially inappropriate fixed dose combination antibiotics: Analysis of data from 75 countries. *PLoS ONE* **16**, e0241899 (2021).
118. Definitive Healthcare LLC. What were the most prescribed antibiotics of 2023? (<https://www.definitivehc.com/resources/healthcare-insights/most-prescribed-antibiotics>, Published Feb 27th, 2024).
119. Shi, C. et al. Approaches for the discovery of metallo- β -lactamase inhibitors: A review. *Chem Biol Drug Des.* **94**, 1427–1440 (2019).

120. Kondratieva, A. et al. Fluorinated captopril analogues inhibit metallo- β -lactamases and facilitate structure determination of NDM-1 binding pose. *European Journal of Medicinal Chemistry* **266**, 116140 (2024).
121. Bush, K. & Bradford, P.A. Interplay between β -lactamases and new β -lactamase inhibitors. *Rev Microbiol.* **17**, 295–306 (2019).
122. Suay-Garcia, B. & Perez-Gracia, M.T. Present and Future of Carbapenem-resistant Enterobacteriaceae (CRE) Infections. *Antibiotics* **8**, 16 (2019).
123. Meini, M.-R., Llarrull, L.I. & Vila, A.J. Evolution of Metallo- β -lactamases: Trends Revealed by Natural Diversity and in vitro Evolution. *Antibiotics* **3**, 285-316 (2014).
124. Tao, S., Chen, H., Li, N., Wang, T. & Liang, W. The Spread of Antibiotic Resistance Genes In Vivo Model. *Can. J. Infect. Dis. Med. Microbiol.* **2022**, 3348695 (2022).
125. Nasrollahian, S., Graham, J.P. & Halaji, M. A review of the mechanisms that confer antibiotic resistance in pathotypes of *E. coli*. *Front. Cell. Infect. Microbiol.* **14**, 1387497 (2024).
126. Nusrat, S., Aliyu, M. & Zohora, F.T. Mechanisms of antimicrobial resistance: From genetic evolution to clinical manifestations. *AIMS Microbiol.* **11**, 1007–1034 (2025).
127. Partridge, S.R., Kwong, S.M., Firth, N. & Jensen, S.O. Mobile Genetic Elements Associated with Antimicrobial Resistance. *Clin. Microbiol. Rev.* **31**, e00088-17 (2018).
128. Reddy, N. et al. Navigating the complexities of drug development for metallo- β -lactamase inhibitors. *RSC Med. Chem.* **16**, 3393-3415 (2025).
129. Docquier, J.-D. & Mangani, S. An update on β -lactamase inhibitor discovery and development. *Drug Resist Updat.* **36**, 13–29 (2018).
130. King, A.M. et al. Aspergillomarasmine A overcomes metallo- β -lactamase antibiotic resistance. *Nature* **510**, 503–506 (2014).
131. Bahr, G., González, L.J. & Vila, A.J. Metallo- β -lactamases and a tug-of-war for the available zinc at the host–pathogen interface. *Curr. Opin. Chem. Biol.* **66**, 102103 (2022).
132. Samuelsen, Ø. et al. ZN148 Is a Modular Synthetic Metallo- β -Lactamase Inhibitor That Reverses Carbapenem Resistance in Gram-Negative Pathogens *In Vivo*. *Antimicrob. Agents Chemother.* **64**, 10.1128/aac.02415-19 (2020).
133. De Falco, A., Alfano, A.I., Cutarella, L., Mori, M. & Brindisi, M. Harder than Metal: Challenging Antimicrobial Resistance with Metallo- β -lactamase Inhibitors. *J. Med. Chem.* **68**, 10556–10576 (2025).
134. Cheng, Y. & Chen, H. Aberrance of Zinc Metalloenzymes-Induced Human Diseases and Its Potential Mechanisms. *Nutrients* **13**, 4456 (2021).

135. Natesh, R., Schwager, S.L.U., Evans, H.R., Sturrock, E.D. & Acharya, K.R. Structural Details on the Binding of Antihypertensive Drugs Captopril and Enalaprilat to Human Testicular Angiotensin I-Converting Enzyme. *Biochemistry* **43**, 8718–8724 (2004).
136. Wade, N. et al. Mechanistic Investigations of Metallo- β -lactamase Inhibitors: Strong Zinc Binding Is Not Required for Potent Enzyme Inhibition. *ChemMedChem* **16**, 1651 – 1659 (2021).
137. Ma, G. et al. Structure-guided optimization of D-captopril for discovery of potent NDM-1 inhibitors. *Bioorg. Med. Chem.* **29**, 115902. (2021).
138. Zalacain, M. et al. Novel Specific Metallo- β -Lactamase Inhibitor ANT2681 Restores Meropenem Activity to Clinically Effective Levels against NDM-Positive Enterobacterales. *Antimicrob. Agents Chemother.* **65**, e00203-21 (2021).
139. Davies, D.T. et al. ANT2681: SAR Studies Leading to the Identification of a Metallo- β -lactamase Inhibitor with Potential for Clinical Use in Combination with Meropenem for the Treatment of Infections Caused by NDM-Producing Enterobacteriaceae. *ACS Infect. Dis.* **6**, 2419–2430 (2020).
140. Li, H. & Sun, H. A hydroxide lock for metallo- β -lactamases. *Nat. Chem.* **14**, 6–8 (2022).
141. Le Terrier, C. et al. Wide dissemination of Gram-negative bacteria producing the taniborbactam-resistant NDM-9 variant: a One Health concern. *J Antimicrob Chemother* **78**, 2382–2384 (2023).
142. Abbott, C., Satola, S.W. & Weiss, D.S. Heteroresistance to cefepime–taniborbactam in metallo- β -lactamase-encoding Enterobacterales. *The Lancet Infectious Diseases* **23**, E277-E278 (2023).
143. Krečmerová, M., Majer, P., Rais, R. & Slusher, B.S. Phosphonates and Phosphonate Prodrugs in Medicinal Chemistry: Past Successes and Future Prospects. *Front. Chem.* **10**, 889737 (2022).
144. Rodriguez, J.B. & Gallo-Rodriguez, C. The Role of the Phosphorus Atom in Drug Design. *ChemMedChem* **14**, 190 – 216 (2019).
145. Yang, K.-W. et al. New β -phospholactam as a carbapenem transition state analog: Synthesis of a broad-spectrum inhibitor of metallo- β -lactamases. *Bioorg. Med. Chem. Lett.* **23**, 5855–5859 (2013).
146. Hinchliffe, P. et al. Structural and Kinetic Studies of the Potent Inhibition of Metallo- β -lactamases by 6-Phosphonomethylpyridine-2-carboxylates. *Biochem.* **57**, 1880–1892 (2018).
147. Pemberton, O.A. et al. Heteroaryl Phosphonates as Noncovalent Inhibitors of Both Serine- and Metallo-carbapenemases. *Journal of Medicinal Chemistry* **62**, 8480-8496 (2019).
148. Tehrani, K.H.M.E. et al. Small Molecule Carboxylates Inhibit Metallo- β -lactamases and Resensitize Carbapenem-Resistant Bacteria to Meropenem. *ACS Infect. Dis.* **6**, 1366–1371 (2020).

149. Rivière, G. et al. NMR Characterization of the Influence of Zinc(II) Ions on the Structural and Dynamic Behavior of the New Delhi Metallo- β -Lactamase-1 and on the Binding with Flavonols as Inhibitors. *ACS Omega* **5**, 10466-10480 (2020).
150. Lienhard, G.E. Transition State Analogs as Enzyme Inhibitors. *Annu. Rep. Med. Chem.* **7**, 249-258 (1972).
151. Cheng, Y.-C. & Prusoff, W.H. Relationship between the inhibition constant (K_I) and the concentration of inhibitor which causes 50 per cent inhibition (I_{50}) of an enzymatic reaction. *Biochem. Pharmacol.* **22**, 3099-3108 (1973).
152. van Berkel, S.S. et al. Assay Platform for Clinically Relevant Metallo- β -lactamases. *J. Med. Chem.* **56**, 6945–6953 (2013).
153. Fröhlich, C., Sørum, V., Tokuriki, N., Johnsen, P.J. & Samuelsen, Ø. Evolution of β -lactamase-mediated cefiderocol resistance. *JAC* **77**, 2429–2436 (2022).
154. Kondratieva, A. et al. Fluorinated captopril analogues inhibit metallo- β -lactamases and facilitate structure determination of NDM-1 binding pose. *Eur. J. Med. Chem.* **266**, 116140 (2024).
155. Lorentzen, Ø.M., Haukefer, A.S.B., Johnsen, P.J. & Fröhlich, C. The Biofilm Lifestyle Shapes the Evolution of β -Lactamases. *Genome Biol. Evol.* **16**, evae030 (2024).
156. Kadeřábková, N., Mahmood, A.J.S. & Mavridou, D.A.I. Antibiotic susceptibility testing using minimum inhibitory concentration (MIC) assays. *npj Antimicrob. Resist.* **2**, 37 (2024).
157. Kowalska-Krochmal, B. & Dudek-Wicher, R. The Minimum Inhibitory Concentration of Antibiotics: Methods, Interpretation, Clinical Relevance. *Pathogens* **10**, 165 (2021).
158. European Committee for Antimicrobial Susceptibility Testing of the European Society of Clinical Microbiology and Infectious Diseases. Determination of minimum inhibitory concentrations (MICs) of antibacterial agents by broth dilution. *Clinical Microbiology and Infection* **9**, ix-xv (2003).
159. Dias, D.M. & Ciulli, A. NMR approaches in structure-based lead discovery: Recent developments and new frontiers for targeting multi-protein complexes. *Prog. Biophys. Mol. Biol.* **116**, 101-112 (2014).
160. Li, Q. & Kang, C. A Practical Perspective on the Roles of Solution NMR Spectroscopy in Drug Discovery. *Molecules* **25**, 2974 (2020).
161. Harner, M.J., Mueller, L., Robbins, K.J. & Reily, M.D. NMR in drug design. *Arch. Biochem. Biophys.* **628**, 132–147 (2017).
162. Teilum, K., Kunze, M.B.A., Erlendsson, S. & Kragelund, B.B. (S)Pinning down protein interactions by NMR. *Protein Sci.* **26**, 436-451 (2017).

163. Furukawa, A., Konuma, T., Yanaka, S. & Sugase, K. Quantitative analysis of protein-ligand interactions by NMR. *Prog. Nucl. Magn. Reson. Spectrosc.* **96**, 47-57 (2016).
164. Latham, M.P., Zimmermann, G.R. & Pardi, A. NMR Chemical Exchange as a Probe for Ligand-Binding Kinetics in a Theophylline-Binding RNA Aptamer. *J. Am. Chem. Soc.* **131**, 5052–5053 (2009).
165. Kaplan, J.I. & Fraenkel, G. *NMR of Chemically Exchanging Systems.*, (Academic Press, New York, 1980).
166. Mulder, F.A.A., Schipper, D., Bott, R. & Boelens, R. Altered flexibility in the substrate-binding site of related native and engineered high-alkaline *Bacillus subtilis*ins. *J. Mol. Biol.* **292**, 111-123 (1999).
167. Williamson, M.P. Using chemical shift perturbation to characterise ligand binding. *Prog. Nucl. Magn. Reson. Spectrosc.* **73**, 1-16 (2013).
168. Andersson, H., Jarvoll, P., Yang, S.-K., Yang, K.-W. & Erdélyi, M. Binding of 2-(Triazolylthio)acetamides to Metallo- β -lactamase CcrA Determined with NMR. *ACS Omega* **5**, 21570-21578 (2020).
169. Christopheit, T., Carlsen, T.J.O., Helland, R. & Leiros, H.-K.S. Discovery of Novel Inhibitor Scaffolds against the Metallo- β -lactamase VIM-2 by Surface Plasmon Resonance (SPR) Based Fragment Screening. *J. Med. Chem.* **58**, 8671–8682 (2015).
170. Rosano, G.L. & Ceccarelli, E.A. Recombinant protein expression in *Escherichia coli*: advances and challenges. *Front. Microbiol.* **5**, 172 (2014).
171. Kitchen, D.B., Decornez, H., Furr, J.R. & Bajorath, J. Docking and scoring in virtual screening for drug discovery: methods and applications. *Nat. Rev. Drug Discov.* **3**, 935-949 (2004).
172. Pagadala, N.S., Syed, K. & Tuszynski, J. Software for molecular docking: a review. *Biophys. Rev.* **9**, 91–102 (2017).
173. Dwivedi, M. et al. Chapter 23 - *In silico* techniques for screening of key secondary metabolites of medicinal plants. in *Nanotechnology and In Silico Tools* (ed. Mital Kaneria, K.R., Chukwuebuka Egbuna) 331-347 (Elsevier, 2024).
174. Meng, X.-Y., Zhang, H.-X., Mezei, M. & Cui, M. Molecular Docking: A powerful approach for structure-based drug discovery. *Curr. Comput. Aided Drug Des.* **7**, 146–157 (2011).
175. Zoete, V., Grosdidier, A. & Michielin, O. Docking, virtual high throughput screening and in silico fragment-based drug design. *J. Cell. Mol. Med.* **13**, 238-248 (2009).
176. Gervasoni, S. et al. A multiscale approach to predict the binding mode of metallo beta-lactamase inhibitors: Binding mode prediction for IMP-1 inhibitors. *Proteins* **90**, 372–384 (2022).
177. Rauh, D., Klebe, G. & Stubbs, M.T. Understanding protein-ligand interactions: the price of protein flexibility. *J. Mol. Biol.* **335**, 1325-1341 (2004).

178. Warren, G.L. et al. A Critical Assessment of Docking Programs and Scoring Functions. *J. Med. Chem.* **49**, 5912–5931 (2006).
179. Bajorath, J. Integration of virtual and high-throughput screening. *Nat. Rev. Drug Discov.* **1**, 882-894 (2002).
180. Sun, D., Gao, W., Hu, H. & Zhou, S. Why 90% of clinical drug development fails and how to improve it? *Acta Pharm. Sin. B.* **12**, 3049–3062 (2022).
181. Dowden, H. & Munro, J. Trends in clinical success rates and therapeutic focus. *Nat. Rev. Drug Discov.* **18**, 495-496 (2019).
182. Harrison, R.K. Phase II and phase III failures: 2013–2015. *Nat Rev Drug Discov.* **15**, 817–818 (2016).
183. Li, A.P. Screening for human ADME/Tox drug properties in drug discovery. *Drug Discov. Today* **6**, 357-366 (2001).
184. Kerns, E.H. & Li, D. Pharmaceutical profiling in drug discovery. *Drug Disc. Today* **8**, 316-323 (2003).
185. Roberts, S.A. Drug metabolism and pharmacokinetics in drug discovery. *Curr. Opin. Drug Discov. Devel.* **6**, 66-80 (2003).
186. Davies, A.M. & Riley, R.J. Predictive ADMET studies, the challenges and the opportunities. *Curr Opin Chem Biol.* **8**, 378-386 (2004).
187. Dulsat, J., López-Nieto, B., Estrada-Tejedor, R. & Borrell, J.I. Evaluation of Free Online ADMET Tools for Academic or Small Biotech Environments. *Molecules* **28**, 776 (2023).
188. Kar, S. & Leszczynski, J. Open access in silico tools to predict the ADMET profiling of drug candidates. *Expert Opin. Drug Discov.* **15**, 1473-1487 (2020).
189. Hsiao, Y., Su, B.-H. & Tseng, Y.J. Current development of integrated web servers for preclinical safety and pharmacokinetics assessments in drug development. *Brief. Bioinform.* **22**, bbaa160 (2021).
190. Lee, S.K. et al. The PreADME: PC-BASED PROGRAM FOR BATCH PREDICTION OF ADME PROPERTIES. (EuroQSAR 2004, 9.5-10, Istanbul, Turkey, 2004).
191. Lee, S.K. et al. The PreADME Approach: Web-based program for rapid prediction of physico-chemical, drug absorption and drug-like properties. in *EuroQSAR 2002 Designing Drugs and Crop Protectants: processes, problems and solutions* 418-420 (Blackwell Publishing, Massachusetts, USA, 2003).
192. Daina, A., Michielin, O. & Zoete, V. SwissADME: a free web tool to evaluate pharmacokinetics, drug-likeness and medicinal chemistry friendliness of small molecules. *Sci. Rep.* **7**:42717(2017).
193. Ferreira, L.L.G. & Andricopulo, A.D. ADMET modeling approaches in drug discovery. *Drug Discov. Today* **24**, 1157-1165 (2019).
194. Teo, Y.L., Ho, H.K. & Chan, A. Metabolism-related pharmacokinetic drug–drug interactions with tyrosine kinase inhibitors: current understanding, challenges and recommendations. *Br J Clin Pharmacol.* **79**, 241–253 (2015).

195. Lipinski, C.A., Lombardo, F., Dominy, B.W. & Feeney, P.J. Experimental and computational approaches to estimate solubility and permeability in drug discovery and development settings. *Adv. Drug. Deliv. Rev.* **23**, 3-25 (1997).
196. Ghose, A.K., Viswanadhan, V.N. & Wendoloski, J.J. A Knowledge-Based Approach in Designing Combinatorial or Medicinal Chemistry Libraries for Drug Discovery. 1. A Qualitative and Quantitative Characterization of Known Drug Databases. *J. Comb. Chem.* **1**, 55-68 (1999).
197. Muegge, I., Heald, S.L. & Brittelli, D. Simple Selection Criteria for Drug-like Chemical Matter. *J. Med. Chem.* **44**, 1841-1846 (2001).
198. Veber, D.F. et al. Molecular Properties That Influence the Oral Bioavailability of Drug Candidates. *J. Med. Chem.* **45**, 2615-2623 (2002).
199. Egan, W.J., Merz, K.M. & Baldwin, J.J. Prediction of Drug Absorption Using Multivariate Statistics. *J. Med. Chem.* **43**, 3867-3877 (2000).
200. Danelius, E. et al. Dynamic Chirality in the Mechanism of Action of Allosteric CD36 Modulators of Macrophage-Driven Inflammation. *J. Med. Chem.* **62**, 11071-11079 (2019).
201. Smith, G.G. & Sivakua, T. Mechanism of the Racemization of Amino-Acids - Kinetics of Racemization of Arylglycines. *J. Org. Chem.* **48**, 627-634 (1983).
202. Hecker, S.J. et al. Discovery of a Cyclic Boronic Acid β -Lactamase Inhibitor (RPX7009) with Utility vs Class A Serine Carbapenemases. *J. Med. Chem.* **58**, 3682-3692 (2015).
203. Rojas, L.J. et al. Boronic Acid Transition State Inhibitors Active against KPC and Other Class A β -Lactamases: Structure-Activity Relationships as a Guide to Inhibitor Design. *Antimicrob Agents Chemother.* **60**, 1751-1759 (2016).
204. Scognamiglio, A. et al. Once Upon a Time Without DMF: Greener Paths in Peptide and Organic Synthesis. *Molecules* **31**, 536 (2026).
205. Gulyás, K.V. et al. Dynamically chiral phosphonic acid-type metallo- β -lactamase inhibitors. *Commun. Chem.* **8**, 119 (2025).
206. Thoma, J. & Burmann, B.M. Preparation of Bacterial Outer Membrane Vesicles for Characterisation of Periplasmic Proteins in Their Native Environment. *Bio Protoc.* **10**, e3853 (2020).
207. Schwechheimer, C. & Kuehn, M.J. Outer-membrane vesicles from Gram-negative bacteria: biogenesis and functions. *Nat. Rev. Microbiol.* **13**, 605-619 (2015).
208. Smith, D.A., Di, L. & Kerns, E.H. The effect of plasma protein binding on *in vivo* efficacy: misconceptions in drug discovery. *Nat. Rev. Drug Discov.* **9**, 929-939 (2010).

209. Liu, X., Wright, M. & Hop, C.E.C.A. Rational Use of Plasma Protein and Tissue Binding Data in Drug Design. *J. Med. Chem.* **57**, 8238–8248 (2014).
210. De, S. et al. Pyridine: the scaffolds with significant clinical diversity. *RSC Adv.* **12**, 15385-15406 (2022).
211. Marinescu, M. & Popa, C.-V. Pyridine Compounds with Antimicrobial and Antiviral Activities. *Int. J. Mol. Sci.* **23**, 5659 (2022).
212. Prathima, P., Sethy, S.P., Sameena, T. & Shailaja, K. Pyridine and Its Biological Activity: A Review. *Asian Journal of Research In Chemistry* **6**, 888-899 (2013).
213. Dixit, G. & Prabhu, A. Design, synthesis, metal chelation potential and biological evaluation of pyridine chalcones as multi-target-directed ligands against Alzheimer's disease. *Journal of Molecular Structure* **1294**, 136498 (2013).
214. Walle, T. Methylation of Dietary Flavones Increases Their Metabolic Stability and Chemopreventive Effects. *Int. J. Mol. Sci.* **11**, 5002-5019 (2009).
215. Hussain, M.B. et al. Bioavailability and Metabolic Pathway of Phenolic Compounds. in *Plant Physiological Aspects of Phenolic Compounds* (eds. Soto-Hernández, M., García-Mateos, R. & Palma-Tenango, M.) (IntechOpen, 2019).
216. Redan, B.W., Buhman, K.K., Novotny, J.A. & Ferruzzi, M.G. Altered Transport and Metabolism of Phenolic Compounds in Obesity and Diabetes: Implications for Functional Food Development and Assessment. *Adv Nutr.* **7**, 1090-1104 (2016).
217. Sato, T. & Yamawaki, K. Cefiderocol: Discovery, Chemistry, and In Vivo Profiles of a Novel Siderophore Cephalosporin. *CID* **69**, S538–S543 (2019).
218. Garzone, P., Lyon, J. & Yu, V.L. Third-Generation and Investigational Cephalosporins: I. Structure-Activity Relationships and Pharmacokinetic Review. *Drug Intell. Clin. Pharm.* **17**, 507-515 (1983).
219. Sader, H.S. & Jones, R.N. Historical overview of the cephalosporin spectrum: Four generations of structural evolution. *Antimicrobial Newsletter* **8**, 75-82 (1992).
220. Fuchs, P.C., Jones, R.N. & Barry, A.L. In vitro antimicrobial activity of tigemonam, a new orally administered monobactam. *Antimicrob Agents Chemother.* **32**, 346–349 (1988).
221. Chin, N.-X. & Neu, H.C. Tigemonam, an oral monobactam. *Antimicrob Agents Chemother.* **32**, 84–91 (1988).
222. Manchand, P.S. et al. A novel synthesis of the monobactam antibiotic carumonam. *J. Org. Chem.* **53**, 5507–5512 (1988).

223. Leiris, S. et al. SAR Studies Leading to the Identification of a Novel Series of Metallo- β -lactamase Inhibitors for the Treatment of Carbapenem-Resistant Enterobacteriaceae Infections That Display Efficacy in an Animal Infection Model. *ACS Infect. Dis.* **5**, 131–140 (2019).
224. Twidale, R.M., Hinchliffe, P., Spencer, J. & Mulholland, A.J. Crystallography and QM/MM Simulations Identify Preferential Binding of Hydrolyzed Carbapenem and Penem Antibiotics to the L1 Metallo- β -Lactamase in the Imine Form. *J. Chem. Inf. Model.* **61**, 5988–5999 (2021).
225. Mucha, A., Kafarski, P. & Berlicki, L. Remarkable Potential of the α -Aminophosphonate/Phosphinate Structural Motif in Medicinal Chemistry. *J. Med. Chem.* **54**, 5955–5980 (2011).
226. Maestro, A., Martinez de Marigorta, E., Palacios, F. & Vicario, J. α -Iminophosphonates: Useful Intermediates for Enantioselective Synthesis of α -Aminophosphonates. *Asian J. Org. Chem.* **9**, 538–548 (2020).
227. Lu, J., Yu, Y., Li, Z., Luo, J. & Deng, L. Practical Synthesis of Chiral α -Aminophosphonates with Weak Bonding Organocatalysis at ppm Loading. *J. Am. Chem. Soc.* **146**, 16706–16713 (2024).
228. Choi, I.H. et al. DNA-Compatible Synthesis of α -Aminophosphonate Scaffolds via Kabachnik-Fields Reaction. *Org. Lett.* **27**, 13374–13379 (2025).
229. Koszelewski, D. et al. Relationship between Structure and Antibacterial Activity of α -Aminophosphonate Derivatives Obtained via Lipase-Catalyzed Kabachnik-Fields Reaction. *Materials* **15**, 3846 (2022).
230. Sonar, S.S., Sadaphal, S.A., Labade, V.B., Shingate, B.B. & Shingare, M.S. An Efficient Synthesis and Antibacterial Screening of Novel Oxazepine α -Aminophosphonates by Ultrasound Approach. *Phosphorus Sulfur Silicon Relat. Elem.* **185**, 65–73 (2009).
231. Grib, I. et al. Efficient synthesis, crystallographic study, antimicrobial activity and in silico studies of novel bioactive α -aminophosphonates based on pyridine moiety *J. Mol. Struct.* **1309**, 138138 (2024).
232. Litim, B., Djahoudi, A., Meliani, S. & Boukhari, A. Synthesis and potential antimicrobial activity of novel α -aminophosphonates derivatives bearing substituted quinoline or quinolone and thiazole moieties. *Med. Chem. Res.* **31**, 60–74 (2021).
233. El Tantawy El Sayed, I., Fathy, G. & Ahmed, A.A.S. Synthesis and Antibacterial Activity of Novel Cyclic α -Aminophosphonates. *Biomed. J. Sci. Tech. Res.* **23**, 17609–17614 (2019).
234. Allen, J.G. et al. Phosphono-peptides, a new class of synthetic antibacterial agents. *Nature* **272**, 56–58 (1978).

235. Atherton, F.R., Hassall, C.H. & Lambert, R.W. Synthesis and structure-activity relationships of antibacterial phosphonopeptides incorporating (1-aminoethyl)phosphonic acid and (aminomethyl)phosphonic acid. *J. Med. Chem.* **29**, 29-40 (1986).
236. Atherton, F.R. et al. Phosphonopeptides as antibacterial agents: mechanism of action of alaphosphin. *Antimicrob. Agents Chemother.* **15**, 696-705 (1979).
237. Saxena, D. et al. Tackling the outer membrane: facilitating compound entry into Gram-negative bacterial pathogens. *npj Antimicrob. Resist.* **1**, 17 (2023).
238. Acosta-Gutiérrez, S. et al. Getting Drugs into Gram-Negative Bacteria: Rational Rules for Permeation through General Porins. *ACS Infect. Dis.* **4**, 1487–1498 (2018).
239. Zhang, J. et al. Unexpected effect of halogenation on the water solubility of small organic compounds. *Comput. Biol. Med.* **172**, 108209 (2024).
240. Wilcken, R., Zimmermann, M.O., Lange, A., Joerger, A.C. & Boeckler, F.M. Principles and Applications of Halogen Bonding in Medicinal Chemistry and Chemical Biology. *J. Med. Chem.* **56**, 1363–1388 (2013).
241. Wilcken, R. et al. Halogen-Enriched Fragment Libraries as Leads for Drug Rescue of Mutant p53. *J. Am. Chem. Soc.* **134**, 6810–6818 (2012).
242. Hardegger, L.A. et al. Systematic investigation of halogen bonding in protein-ligand interactions. *Angew. Chem. Int. Ed. Engl.* **50**, 314-318 (2011).
243. Bissantz, C., Kuhn, B. & Stahl, M. A Medicinal Chemist's Guide to Molecular Interactions. *J. Med. Chem.* **53**, 5061–5084 (2010).
244. Kortagere, S., Ekins, S. & Welsh, W.J. Halogenated ligands and their interactions with amino acids: implications for structure-activity and structure-toxicity relationships. *J. Mol. Graph. Model.* **27**, 170-177 (2008).
245. Lu, Y., Wang, Y. & Zhu, W. Nonbonding interactions of organic halogens in biological systems: implications for drug discovery and biomolecular design. *Phys. Chem. Chem. Phys.* **12**, 4543-4551 (2010).
246. Shinada, N.K., de Brevern, A.G. & Schmidtke, P. Halogens in Protein–Ligand Binding Mechanism: A Structural Perspective. *J. Med. Chem.* **62**, 9341–9356 (2019).
247. Müller, K., Faeh, C. & Diederich, F. Fluorine in Pharmaceuticals: Looking Beyond Intuition. *Science* **317**, 1881-1886 (2007).
248. Gillis, E.P., Eastman, K.J., Hill, M.D., Donnelly, D.J. & Meanwell, N.A. Applications of Fluorine in Medicinal Chemistry. *J. Med. Chem.* **58**, 8315–8359 (2015).

249. Böhm, H.-J. et al. Fluorine in Medicinal Chemistry. *Chembiochem* **5**, 637-643 (2004).
250. Le Terrier, C. et al. The emerging concern of IMP variants being resistant to the only IMP-type metallo- β -lactamase inhibitor, xeruborbactam. *Antimicrob. Agents Chemother.* **69**, e00297-25 (2025).
251. Brem, J. et al. Structural Basis of Metallo- β -Lactamase Inhibition by Captopril Stereoisomers. *Antimicrob. Agents Chemother.* **60**, 142-150 (2015).
252. Xu, Q., Deng, H., Li, X. & Quan, Z.-S. Application of Amino Acids in the Structural Modification of Natural Products: A Review. *Front. Chem.* **9**, 650569 (2021).
253. Bongioanni, A., Soledad Bueno, M., Mezzano, B.A., Longhi, M.R. & Garnerio, C. Amino acids and its pharmaceutical applications: A mini review. *Int. J. Pharm.* **613**, 121375 (2022).
254. Hopkins, A.L., Groom, C.R. & Alex, A. Ligand efficiency: a useful metric for lead selection. *Drug Discov. Today* **9**, 430-431 (2004).
255. Glyn, R.J. & Pattison, G. Effects of Replacing Oxygenated Functionality with Fluorine on Lipophilicity. *J. Med. Chem.* **64**, 10246–10259 (2021).
256. Ebetino, F.H. et al. Bisphosphonates: The role of chemistry in understanding their biological actions and structure-activity relationships, and new directions for their therapeutic use. *Bone* **156**, 116289 (2021).
257. Sparidans, R.W., Twiss, I.M. & Talbot, S. Bisphosphonates in bone diseases. *Pharm. World Sci.* **20**, 206-213 (1998).
258. Dunstan, C.R., Felsenberg, D. & Seibel, M.J. Therapy Insight: the risks and benefits of bisphosphonates for the treatment of tumor-induced bone disease. *Nat. Clin. Pract. Oncol.* **4**, 42–55 (2007).
259. Muteeb, G., Alsultan, A., Farhan, M. & Aatif, M. Risedronate and Methotrexate Are High-Affinity Inhibitors of New Delhi Metallo- β -Lactamase-1 (NDM-1): A Drug Repurposing Approach. *Molecules* **27**, 1283 (2022).
260. Zhang, C. et al. Rh(III)-Catalyzed directed C–H carbenoid coupling reveals aromatic bisphosphonates inhibiting metallo- and Serine- β -lactamases. *Org. Chem. Front.* **5**, 1288-1292 (2018).
261. Afinogenova, A.G., Voroshilova, T.M., Afinogenov, G.E. & Rodionov, G.G. Checkerboard Array» as a Test for Evaluation of Decrease in Gram-Negative Bacteria Resistance to Carbapenems in the Presence of Bisphosphonate. *Clin. Microbiol. Antimicrob. Chem.* **17**, 24-32 (2015).
262. Kitchen, H.J. et al. Modern Microwave Methods in Solid-State Inorganic Materials Chemistry: From Fundamentals to Manufacturing. *Chem. Rev.* **114**, 1170–1206 (2014).

263. Henary, M. et al. Benefits and applications of microwave-assisted synthesis of nitrogen containing heterocycles in medicinal chemistry. *RSC Adv.* **10**, 14170–14197 (2020).
264. Wagner, R.B. Microwave-assisted synthesis in the pharmaceutical industry - A current perspective and future prospects. *Drug Discovery World* **7**, 59-66 (2006).
265. Starvaggi, J. & Ettari, R. Microwave-Assisted Organic Synthesis: An Eco-Friendly Method of Green Chemistry. *Pharmaceuticals* **18**, 1692 (2025).
266. Belabassi, Y., Alzghari, S. & Montchamp, J.-L. Revisiting the Hirao Cross-coupling. Improved Synthesis of Aryl and Heteroaryl Phosponates. *J. Organomet. Chem.* **693**, 3171–3178 (2007).
267. Henyecz, R. & Keglevich, G. New Developments on the Hirao Reactions, Especially from “Green” Point of View. *Curr. Org. Synth.* **16**, 523–545 (2019).
268. Bhattacharya, A.K. & Thyagarajan, G. Michaelis-Arbuzov rearrangement. *Chem. Rev.* **81**, 415–430 (1981).

Acta Universitatis Upsaliensis

Digital Comprehensive Summaries of Uppsala Dissertations from the Faculty of Science and Technology 2650

Editor: The Dean of the Faculty of Science and Technology

A doctoral dissertation from the Faculty of Science and Technology, Uppsala University, is usually a summary of a number of papers. A few copies of the complete dissertation are kept at major Swedish research libraries, while the summary alone is distributed internationally through the series Digital Comprehensive Summaries of Uppsala Dissertations from the Faculty of Science and Technology. (Prior to January, 2005, the series was published under the title “Comprehensive Summaries of Uppsala Dissertations from the Faculty of Science and Technology”.)

Distribution: publications.uu.se
urn:nbn:se:uu:diva-582535



ACTA UNIVERSITATIS
UPSALIENSIS
2026